Synthesis and structure of bithiophene complexes

by

Mandy van Staden

Submitted in partial fulfillment of the requirements for the degree

Magister Scientiae

in the Faculty of Natural & Agricultural Science

University of Pretoria

Pretoria

July 2001

Acknowledgments

I would like to thank :

My supervisors, Professor P.H. van Rooyen and Professor S. Lotz, for their advice, support and patience;

Mr. Eric Palmer for assisting with the NMR spectra;

Mr. Robin Muir for the glassware;

The Foundation of Research and Development and the University of Pretoria for financial assistance;

My parents for making it all possible and for always believing in me;

My husband for all the cold winter nights in the lab and all the love and patience he showed me;

My brother, Grant, for his help with IT-related issues;

My parents-in-law for their support and assistance;

My friends Marile, Denise and Chantel, for all their patience and help throughout.

Thank you all very much!

Mandy

July 2001

Table of contents

Page

Chapter 1
Introduction

Chapter 2

Chromium carbene complexes of bithiophene

Page

Chapter 3
Tungsten carbene complexes of bithiophene

Chapter 4
Manganese carbene complexes of bithiophene

Chapter 5
Iron alkyl complexes of bithiophene

UNIVERSITEIT VAN PRETORIA
UNIVERSITY OF PRETORIA
YUNIBESITHI YA PRETORIA

Sintese en struktuur van bitiofeenkomplekse

Naam van student: Mandy Czernowalow
Studieleier: Prof. P.H. van Rooyen
Mede-studieleier: Prof. S. Lotz
Departement: Chemie
Graad: Magister Scientiae

Opsomming

Organometaalkomplekse van tiofeen en derivate daarvan het, weens hulle geskiktheid vir toepassings op die gebiede van geleidende polimere en nie-liniêre optika, al die basis waarop aantal studies geskoei was, gevorm,. Hierdie werk het gefokus op die studie van beide karbeen- en alkielkomplekse deur die gebruik van bitiofeeneenhede.

Mono- en biskarbeenkomplekse, [M{C(OEt)C_4H_2S-C_4H_3S}] en [M{C(OEt)C_4H_2S-C_4H_2SC(OEt)}M], met M = [Cr$(CO)_5$], [W$(CO)_5$] en [MnCpMe$(CO)_2$] is berei. Die klassieke Fischer metode van sintese is gebruik om oorgangsmetaalkarboniele aan bitiofeeneenhede te verbind. Die reaksie van die gevormde komplekse met suurstof het gelei tot addisionele produkte: [M{C(OEt)C_4H_2S-C_4H_2S(O)COEt}] en [EtOC(O)C_4H_2S-C_4H_2S(O)COEt] in die geval van M = [Cr$(CO)_5$] en [W$(CO)_5$], maar nie vir M = [MnCpMe$(CO)_2$] nie. Die rede hiervoor is dat die komplekse van mangaan meer stabiel is as dié van wolfram en chroom. Onverwagte nuwe organiese produk, [C_4H_3S-C_4H_2SC(O)C(O)C_4H_2S-C_4H_3S], is gevorm in die reaksie van die chroomkarboniel met bitiofeen, maar nie in die reaksies van die wolfram- en mangaankarboniele nie. Dit kan toegeskryf word aan die groter stabiliteite van die wolfram- en mangaankomplekse. Daar is onsekerheid oor die meganisme waardeur die organiese produk gevorm word. Verskeie moontlike meganismes is voorgestel en bespreek, ondermeer: vorming voor alkilering, deur die koppelling van twee asilaateenhede; vorming tydens alkilering, as

gevolg van die koppelling van asilaateenheid met monokarbeeneenheid; en vorming ná alkilering, deur die koppelling van twee monokarbeeneenhede.

Die invloed van die karbeeneenheid op die elektronverspreiding in die ringe is duidelik waarneembaar van die ^{1}H- en ^{13}C-KMR data wat versamel is. Bykans al die KMR seine is na laer veld verskuif as dié verkry van die vrye ligand, as gevolg van ontskerming deur die elektrofiele karbeeneenhede en, in sommige gevalle, elektron-onttrekkende ester groepe.

X-straal kristalografiese studies het aangedui dat die teenwoordigheid van substituente op die bitiofeenringsisteem, die ringe forseer om in dieselfde vlak te rangskik. Daarby lê die bitiofeenringsisteem *trans* ten opsigte van die swaelatome. Daar word verwag dat hierdie planêre konfigurasie die vloei van elektrone deur die molekuul sal vermaklik.

Vir vergelykingsdoeleindes is ysterkarboniel gekies as oorgangsmetaalkarboniel vir die sintese van mono- en dikern bitiënielkomplekse, aangesien ysterkarboniele maklik alkielbindings aan ligande stabiliseer. Die komplekse, $[\mathrm{FeCp}\{\mathrm{C_4H_2S\text{-}C_4H_3S}\}(\mathrm{CO})_2]$ en $[\mathrm{FeCp}(\mathrm{CO})_2\{\mathrm{C_4H_2S\text{-}C_4H_2S}\}\mathrm{FeCp}(\mathrm{CO})_2]$, is geïsoleer en gekarakteriseer met behulp van spektroskopiese tegnieke. Hierdie komplekse is meer stabiel as die karbeenkomplekse wat vroëer in díe studie verkry is, asook soortgelyke, bekende ysterkomplekse met tiënotiofeen ligande. Die monokern tiënotiofeenkompleks was te onstabiel om geïsoleer te word; terwyl die monokern bitiënielkompleks redelik stabiel was en die dikern bitiënielkompleks selfs lugstabiel was.

UNIVERSITEIT VAN PRETORIA
UNIVERSITY OF PRETORIA
YUNIBESITHI YA PRETORIA

Synthesis and structure of bithiophene complexes

Name of Student: Mandy Czernowalow
Supervisor: Prof. P.H. van Rooyen
Co-supervisor: Prof. S. Lotz
Department: Chemistry
Degree: Magister Scientiae

Summary

Organometallic complexes of thiophene and its derivatives have formed the basis of many studies due to their suitability for applications in the fields of conducting polymers and non-linear optics. This study focused on the investigation of both carbene and alkyl complexes using bithiophene spacers.

Mono- and biscarbene complexes, [M{C(OEt)C_4H_2S-C_4H_3S}] and [M{C(OEt)C_4H_2S-C_4H_2SC(OEt)}M] with M = [Cr(CO)$_5$], [W(CO)$_5$] and [MnCpMe(CO)$_2$], were prepared. The classical Fischer method of synthesis was used to attach transition metal carbonyls to the bithiophene spacers. The reaction of the resulting complexes with oxygen yielded additional products: [M{C(OEt)C_4H_2S-C_4H_2S(O)COEt}] and [EtOC(O) C_4H_2S-C_4H_2S(O)COEt] in the case of M = [Cr(CO)$_5$] and [W(CO)$_5$], but not for M = [MnCpMe(CO)$_2$] as the complexes of manganese are more stable than those of tungsten and chromium. An unexpected, novel organic product, [C_4H_3S-C_4H_2SC(O)C(O)C_4H_2S-C_4H_3S], was formed in the reaction of the chromium carbonyl with bithiophene, but not in the reactions of the tungsten and manganese carbonyls. This can be ascribed to the greater stability of the tungsten and manganese complexes. The mechanism of formation of the organic product could only be speculated upon. Several possible mechanisms were proposed and discussed including: formation prior to alkylation via the coupling of two acylate units; formation during alkylation via the coupling of an acylate unit with a

monocarbene unit; and formation after alkylation involving the coupling of two monocarbene units.

The influence of the carbene moiety on the electronic distribution around the rings is clear from the ^{1}H and ^{13}C NMR data collected. Almost all the NMR signals are shifted downfield of those of the free ligand due to deshielding by the electrophillic carbene moieties and, in some cases, the electron-withdrawing ester groups.

X-ray crystallographic studies indicated that the presence of substituents on the bithiophene ring system forces the rings to align in the same plane. In addition, the ring system was found to be in the *trans* configuration with respect to the sulfur atoms. This planar configuration is expected to aid in the flow of electrons through the molecule.

For the sake of comparison, an iron carbonyl was selected as a transition metal carbonyl for the production of mono- and dinulcear bithienylene complexes as it readily forms alkyl bonds to the ligand. The complexes, $[FeCp\{C_4H_2S\text{-}C_4H_3S\}(CO)_2]$ and $[FeCp(CO)_2\{C_4H_2S\text{-}C_4H_2S\}FeCp(CO)_2]$, were isolated and characterized spectroscopically. They were found to be more stable than the carbene complexes synthesized in this study, as well as similar, known iron complexes with thienothiophene ligands. The mononuclear thienothienyl complex was too unstable to be isolated, while the mononuclear bithienyl complex was quite stable and the dinuclear bithienylene complex was even air stable.

LIST OF COMPOUNDS

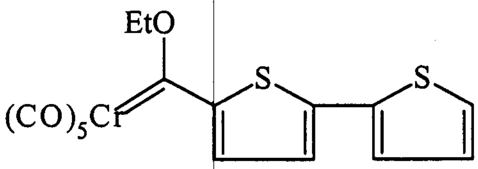

(2-bithienyl)ethoxycarbene pentacarbonyl chromium

1

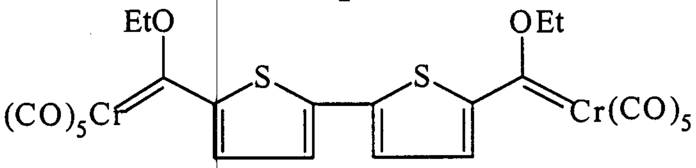

2

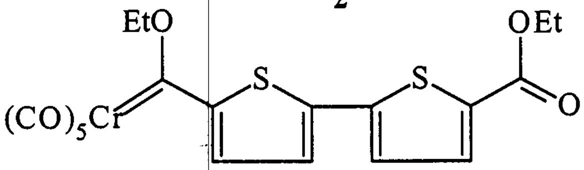

(2-bithienyl)ethoxycarbene pentacarbonyl chromium-5'-ethoxycarboxylate

3

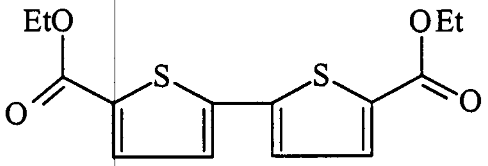

(2,5'-bithienylene)bis{ethoxycarboxylate}

4

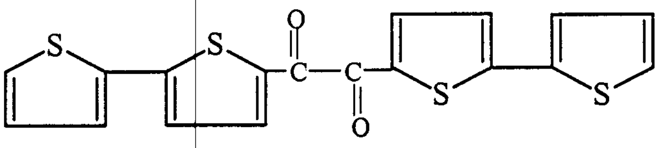

2',2'-bisbithienyl-1,2-dione

5

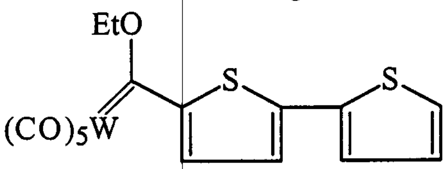

(2-bithienyl)ethoxycarbene pentacarbonyl tungsten

6

LIST OF COMPOUNDS

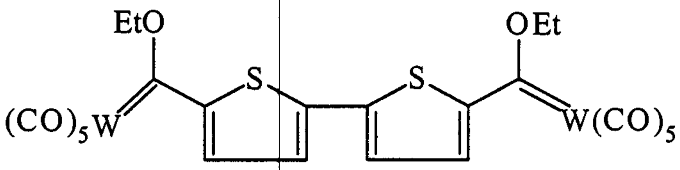

7

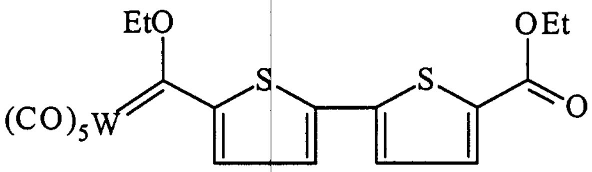

(2-bithienyl)ethoxycarbene pentacarbonyl tungsten-5'-ethoxycarboxylate

8

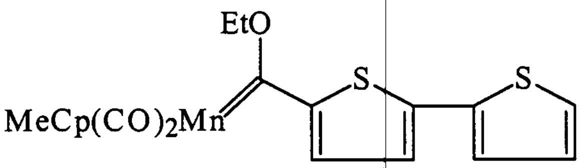

(2-bithienyl)ethoxycarbene methyl cyclopentadienyl dicarbonyl manganese

9

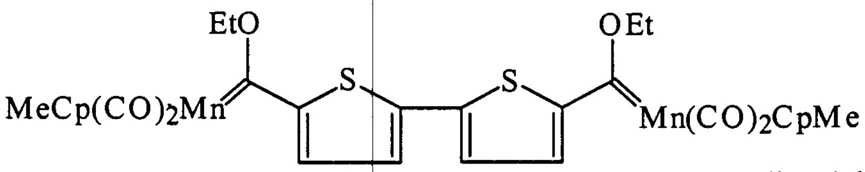

(2,5'-bithienylene)bis{ethoxycarbene methyl cyclopentadienyl dicarbonyl manganese}

10

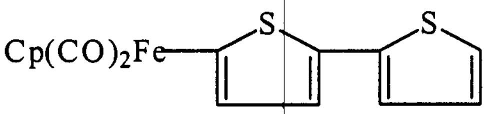

2-bithienyl{cyclopentadienyl dicarbonyl iron}

11

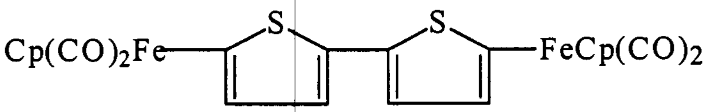

2,5'-bithienylene-bis{cyclopentadienyl dicarbonyl iron}

12

LIST OF ABBREVIATIONS

ADMET	Acyclic diene metathesis
br	Broad
Bu	Butyl
CP	Conducting polymer
Cp	Cyclopentadienyl η^5-C_5H_5
CpH	Cyclopentadiene η^5-C_5H_6
Cp*	Pentamethyl cyclopentadiene η^5-C_5Me_5
d	Doublet
DCC	Dicyclohexylcarbodiimide
dppe	1,2-bis(diphenylphosphino)ethane
Et	Ethyl
IR	Infrared
m	Multiplet
Me	Methyl
MeCp	Methyl cyclopentadiene η^5-C_5H_4Me
NHS	N-Hydroxysuccinimide
NMR	Nuclear Magnetic Resonance Spectroscopy
Ph	Phenyl
PT	Polythiophene
q	Quartet
RCM	Ring-closure metathesis
s	Singlet
t	Triplet
T	Thiophene
TFA	Trifluoroacetic acid
Th	Thienyl group
tTh	Terthienyl
THF	Tetrahydrofuran

TMEDA	Tetramethylethylenediamine

1 INTRODUCTION

1.1 General introduction

1.1.1 Historical overview of organometallic chemistry

Organometallic compounds are those which have direct metal to carbon bonds[1]. L.D. Cadet[1,2] - a French chemist - prepared the earliest organometallic compound in 1760, while trying to synthesize invisible inks from arsenate salts. The compound, As_2Me_4, is a typical example of an "electron-precise" complex, in which the valence electrons of the metal and the carbon atoms are paired to form σ-bonds and the metal is in a formally high oxidation state[1]. Another notable early organometallic reaction was the reaction of Zn with an alkyl halide by Sir Edward Frankland in 1845, in an attempt to synthesize alkyl radicals[3]. More important was the French chemist, V. Grignard's synthesis of the famous organometallic, "Grignard reagents". These were produced by reacting magnesium with alkyl or aryl halides in ether. They have the form [CH_3MgI] and are still used as alkylating agents in synthetic reactions[3]. Organolithium reagents, such as n-butyllithium, are also used in alkylations to produce other organometallic complexes[3].

---

[1] a) M. Bochman, *Organometallics 1, Complexes with Transition Metal-Carbon σ-bonds*, Oxford, New York, **1994**.
b) C. Elschenbroich, A. Salzer, *Organometallics: A Concise Introduction*, VCH Verlagsgesellschaft, Weinheim, Germany, **1992**, 227.

[2] L.D. Cadet de Gassicourt, *Memoires de Mathematique et de Physique*, **1760**.

[3] a) E. Franklind, *Ann.*, 71, **1849**, 171.
b) F.A. Cotton, G. Wilkinson, P.L. Gaus, *Basic Inorganic Chemsitry*, 2nd Edition, John Wiley & Sons, New York, **1987**.
c) J.P. Collman, L.S. Hedges, J.R. Norton, R.G. Finke, *Principles and Applications of Organotransition Metal Chemistry*, University Science Books, California, **1987**.

1.1.2 Transition metal organometallic compounds

Numerous alkyl organometallic compounds of the form $M(CH_2R)_n$ have been synthesized[4] with a wide variety of main group metals in which the polarity of the metal-carbon bond varies from highly ionic - in the case of alkali metals - to covalent - in the case of the p-block metals.

In carbene complexes of the main group metals, overlapping of available s- and p-oribtals[1] forms the metal-carbon bonds. The transition metals have d-orbitals (in addition to the s- and p-orbitals) available and favourably positioned for effective overlap. Transition metals, therefore, exhibit a much fuller diversity of organometallic complexes than the main group metals. The orbitals of the transition metals can hybridize and yield a wide variety of coordination geometries and coordination numbers (1-8 through 4-6 being the most common)[1]. Interaction between the d-orbitals of the transition metal and the π- and π^*- orbitals of unsaturated organic molecules occurs by the metal donating and accepting electron density from the organic molecule - thus stabilizing the bond. Low oxidation state transition metals are stabilized in this manner. This results in transition metal organometallic complexes having very different reactivity and allowing transformations that would not be possible for other organometallic complexes[1,3].

---

[4] W. Herrmann, C. Kocher, *Angew. Chem. Int. Ed. Engl.*, 36, **1997**, 2162.

1.1.3 Applications in organometallic chemistry

Traditionally research in organometallic chemistry has focused on the use of these compounds as catalysts for industrial processes, rather than applications involving stoichiometric organic synthesis[5]. However, over the past twenty years the distinction between the fields of organic and inorganic chemistry has become less clear and this has opened the way for the application of organometallic complexes in stoichiometric organic syntheses. New methods of organic synthesis using organometallic complexes have allowed the formation of carbon-carbon bonds to be controlled in such a way that products with the desired chemo-, regio- and stereoselectivity can be achieved. In other words, the functional group at which the attack takes place, the atom within the functional group that reacts to the attack and the relative isomerism, as well as the absolute isomerism, of the molecule can be controlled using organometallic reagents. This is due to the extremely good stereo- and regio-selectivity of the complexes themselves[5].

Certain stable organometallic compounds can be used as protective groups in order to prevent reactions at certain sites during organic synthesis. An example is shown in **Fig. 1.1**, where Group VI metal(alkoxy)carbenes are reacted with amino acid esters or peptide esters in the presence of NHS (N-hydroxysuccinimide) and DCC (dicyclohexylcarbodiimide) to give (amino)carbene complexes which are stable under the normal peptide coupling conditions and, therefore, allow the amino acid sequencing of the peptide (e.g. the 14 -17 amino acid sequence of the human proinsulin C-peptide).

---

[5] C.M. Lukehart, *Fundamental Transition Metal Organometallic Chemistry*, Brooks/Cole, California, 1985.

Treatment with TFA (triflouroacetic acid) yields the free peptide or amino acid. This is known as N-terminus protection[5].

Organometallic compounds also allow the transfer of less stable organic intermediates by the formation of stable complexes, which can be used as synthons[5]. For example, although the carbene alkylidene moiety, $:CR_2$, is not stable in the free state without electron stabilising and bulky R-substituents, it is an intermediate of many organic reactions.

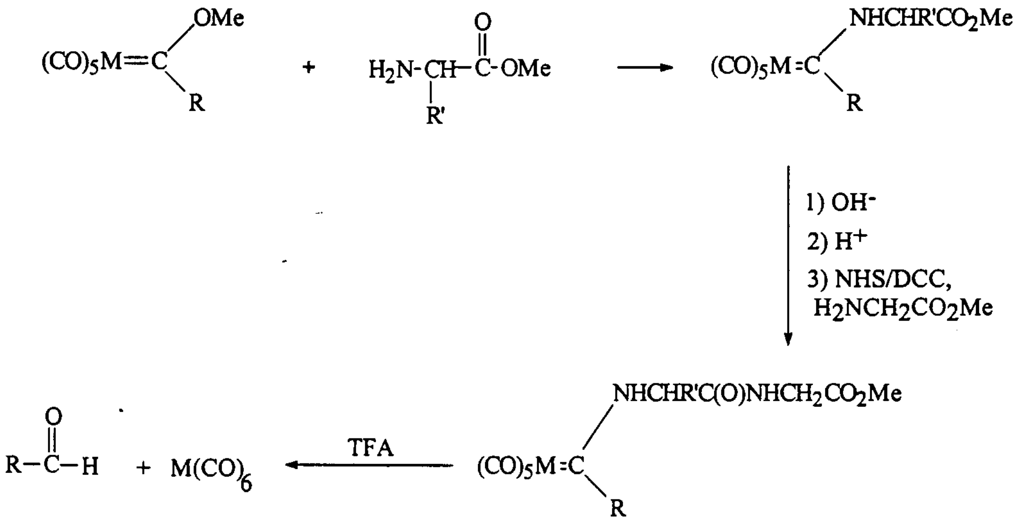

FIG. 1.1: Group VI metal(alkoxy)carbenes are reacted with amino acid esters or peptide esters to give (amino)carbene complexes.

Research has now provided a large number of ways in which, through the use of transition metals, stabilized organometallic carbene complexes can be produced and used to transfer the carbene[1,3].

Another group of metal carbene complexes was discovered by R.R. Schrock and became known as alkylidene complexes[1]. These complexes are useful in the transfer of the alkylidene ligand to unactivated alkenes (shown in **Fig. 1.2**). In the case of cyclopropane, it is interesting to note that the olefin stereochemistry is retained under these conditions.

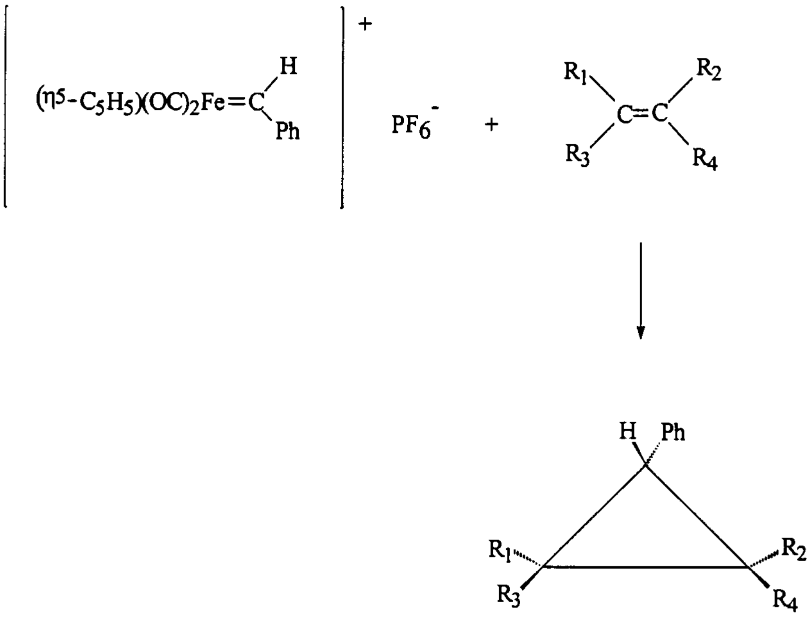

FIG. 1.2: **The transfer of the alkylidene ligand to unactivated alkenes.**

Organometallic complexes can also be employed in the stabilization of carbanions formed when the compound reacts as a Brφnsted acid rather than an electrophile. The metal can easily stabilize the anion that results from such a reaction as shown in **Fig. 1.3**. This type of reaction is used to make α-methylene-γ-butyrolactone, which is used in cancer treatment[6].

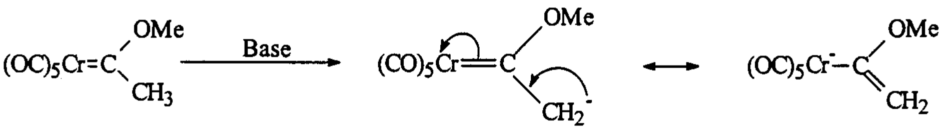

FIG. 1.3: **The metal stabilizes the carbanion.**

---

[6] C.P. Casey, *J. Am. Chem. Soc.*, 96, **1974**, 7808.

Organometallic carbene complexes also play an important role as intermediates in olefin metathesis[7]. The catalytic modification of olefins, referred to as alkene metathesis, has received considerable attention during the last decade. Examples of this include: ring-opening metathesis polymerization (ROMP) and the cross-metathesis of simple olefins such as the conversion of propene into ethylene and pure 1-butene[7]. Alkene metathesis is achievable from $[Mo(CO)_6]$ on Al_2O_3 in heterogeneous catalytic systems and with $[WCl_6]/EtOH/2[Et_2AlCl]$ or ruthenium catalyst homogeneously. What makes alkene metathesis intriguing is the fact that carbene complex intermediates have been established for homogeneous catalysis. The catalytically active carbene complex converts into a metallacyclobutane intermediate which has two possibilities for ring opening. If the ring opens in a way, which differs from the reverse reaction of its formation, the result is a metathesis (redistribution of alkylidene units)- see **Fig. 1.4**. There are numerous accounts of ring-closure metathesis (RCM) and acyclic diene metathesis (ADMET) polymerization. These are accessible via catalysis by the well-defined, functional-group-tolerant transition-metal carbene complexes $[Ru\{C(Ph)H\}(PCy_3)_2Cl_2]$[8] and $[Mo\{C(H)CMe_2Ph\}(NAr)(OR)_2]$[9]. Grubbs *et al.*[10] synthesized and used the former to catalyze the polymerization of highly strained cyclic olefins. Even strained rings and macrocycles are accessible by RCM.

---

[7] a) K.J. Ivin, J.C. Mol, *Olefin Metathesis and Metathesis Polymerization*, Academic Press, San Diego, CA, **1997**. *Alkene Metathesis in Organic Synthesis*, A. Fuerstner (Ed), Springer, Berlin, **1998**.
b) R.H. Grubbs, S. Chang, *Tetrahedron*, 54, **1998**, 4413.

[8] a) P. Schwab, M.B. France, J.W. Ziller, R.H. Grubbs, *Angew. Chem., Int. Ed. Engl.*, 34, **1995**, 2039.
b) P. Schwab, R.H. Grubbs, J.W. Ziller, *J. Am. Chem. Soc.*, 118, **1996**, 100.

[9] R.R. Schrock, J. S. Murdzek, G.C. Bazan, J. Robbins, M. DiMare, M. O'Regan, *J. Am. Chem. Soc.*, 112, **1990**, 387.

[10] S.T. Nguyen, L.K. Johnson and R.H. Grubbs, *J. Am. Chem. Soc.*, 114, **1992**, 3974.

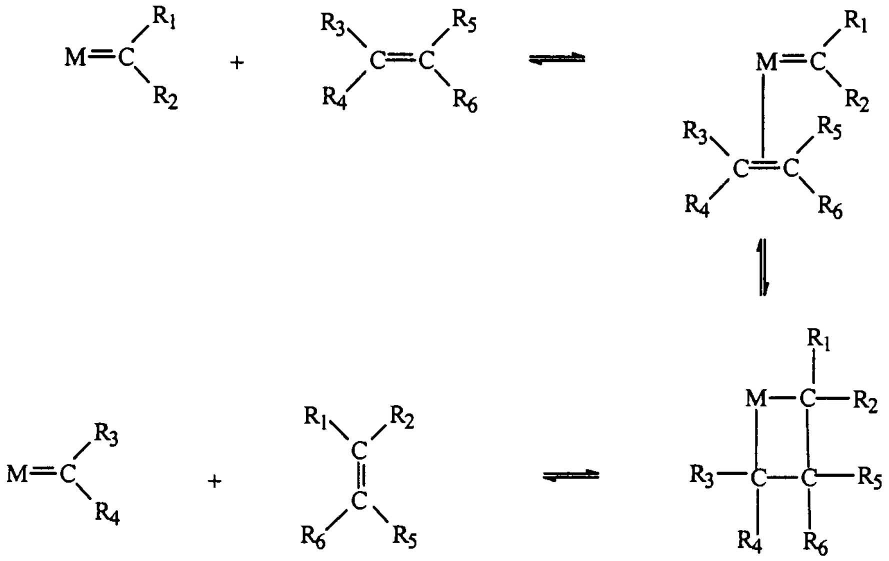

FIG. 1.4: Schematic representation of metathesis showing redistribution of the alkylidene units.

1.2 Metal carbene complexes

Although metal alkyl complexes have a long history, it was not until 1964 that E.O. Fischer discovered the existence of a metal-carbon double bond in organometallic complexes. These became known as carbene complexes because they were formally derived from the coordination of a carbene (:CR_2) to a metal centre. They were given the general formula $[M\{=C(OR)R'\}(CO)_5]$ with M = Cr, Mo, W. These complexes are readily formed from the reaction of air stable, crystalline metal carbonyls with a wide range of organolithium reagents. The complexes are electrophilic in nature and the metals are in a low oxidation state. The bonding is similar to that of CO and is resonance stabilized as shown in **Fig. 1.5**. This figure shows clearly the role of the heteroatom substituent as an electron donor in these complexes[1].

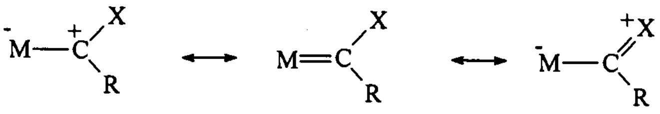

FIG. 1.5: Resonance structures showing the role of the metal and the heteroatom substituent as electron donors.

The metal acts as an electron acceptor, which explains the electrophilic nature of carbons attached to metals and their reactions with lithium alkyls as shown in **Fig. 1.6**.

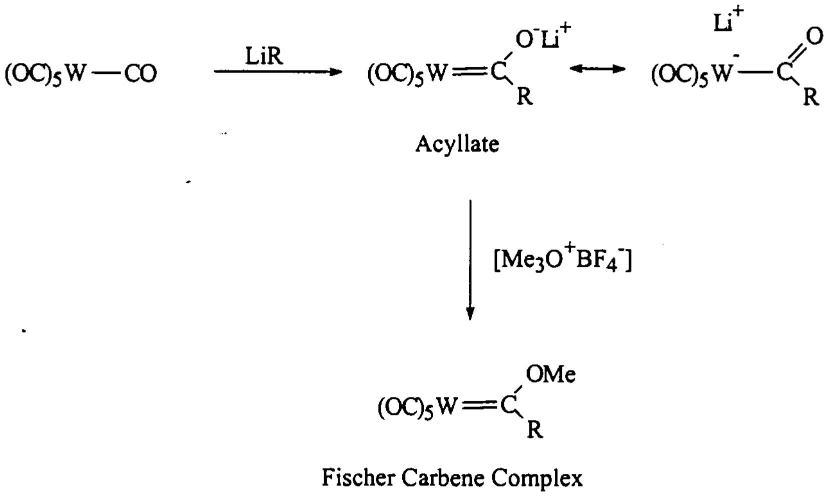

FIG. 1.6: The reaction of metal carbonyls with lithium alkyls to yield Fischer carbene complexes.

Today complexes of this type are known for a variety of metals including chromium, molybdenum, tungsten, iron, ruthenium, rhenium and manganese. They have a very rich chemistry and undergo reactions at a number of sites[11].

---

[11] K.H. Dötz, H. Fischer, P. Hofmann, F.R. Kriessl, U. Schubert, K. Weiss, *Transition Metal Carbene Complexes*, VCH Verlag, Weinheim, **1983**, 218.

Schrock carbene (or alkylidene) complexes differ from the Fischer carbene complexes in that they are nucleophilic and represent the opposite in reactivity and bonding to the electrophilic carbene complexes (**Fig. 1.7**). These complexes are often derived from the coordination of a methylene, or alkylidene substituted methylene (:CR_2) ligand to a metal centre.

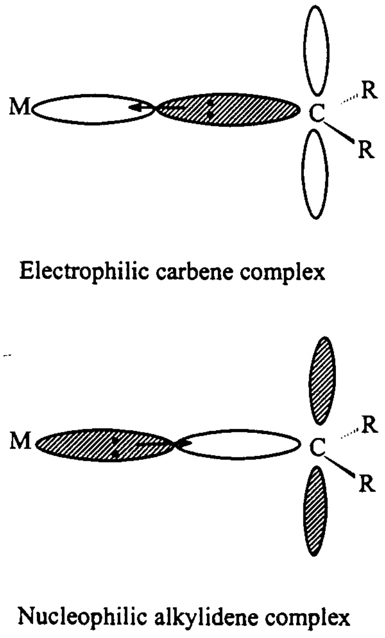

FIG. 1.7: Orbital diagrams showing the difference between the electrophilic carbene and nucleophilic alkylidene complexes.

The metals involved in these complexes have high oxidation states and act as two-electron donors, which explains their reactions with aluminium alkyls (**Fig. 1.8**). The ligands on the metal are strong donor ligands such as alkyl or cyclopentadienyl, and no acceptor ligands. No heteroatom substituents are found in this type of carbene, as their non-bonding electron pairs would not stabilize the complex due to nucleophilic nature of the carbon bonded to the metal.

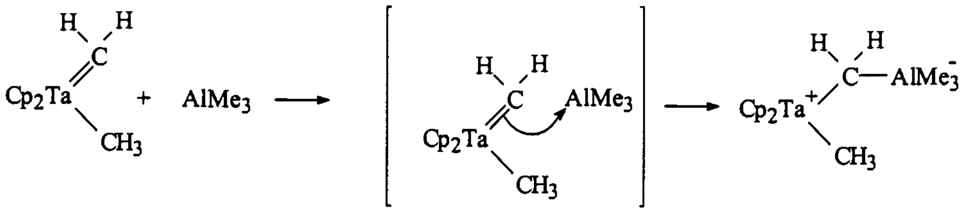

FIG. 1.8: **The reaction of alkylidenes with aluminium alkyls.**

Transition metal carbene complexes have found extensive application as precursors to the synthesis of organic compounds and modified organometallic complexes. Their chemistry includes a number of different reactions such as: (I) reaction with nucleophiles (e.g. aminolysis and related reactions, ylide complex formation); (II) the addition of carbon- and transition metal nucleophiles; (III) reduction and oxidation reactions; (IV) reactions with electrophiles (e.g. the synthesis of neutral and cationic transition metal carbyne complexes); (V) addition-rearrangement reactions (e.g. metal-heteroatom bond formations, carbene side-chain modification and the formation of metal π-complexes); (VI) substitution reactions (e.g. substitution of non-carbene and carbene ligands)[11].

1.3 Thiophenes

1.3.1 Origin and synthesis of thiophenes

Thiophenes have received much attention because of their prevalence in fossil fuels. They are produced by the action of sulfur on hydrocarbons in fossil fuels. Biosynthetic routes to thiophenes have also been developed, but these require the immediacy of di- and oligo-alkynes[12]. Several other synthetic routes have been

---

[12] T.B. Rauchfuss, *Prog. Inorg. Chem.*, 39, 1991, 259.

investigated including the direct reaction of elemental sulfur with alkanes, alkenes or butadienes at elevated temperatures[13].

1.3.2 Properties and structure of thiophenes

Thiophenes are pseudo-aromatic with respect to their structure, properties and reactivity. They are excellent conductors because of the extensive delocalization of electrons within the ring(s). Although, for the sake of convenience, the rings of thiophene and its derivatives are portrayed in this document as having localized double bonds, it must be noted that the electron distribution in the rings is not restricted to this configuration, but electrons are delocalized over the rings due to resonance effects. Thiophenes exhibit superior charge distribution in polymer chains, making them particularly useful in the construction of non-metallic conductors. Thiophenes fall into the category of 5-membered heteroarene compounds - i.e. arenes, which contain a heteroatom in their rings. Rather than behaving like the conjugated dienes or having sulfide chemistry, these compounds behave like highly reactive benzene derivatives due to the delocalization of electrons in the ring. Thiophenes are, however, more nucleophilic than benzene[12].

The structure of thiophene is well represented in **Fig. 1.9**[14].

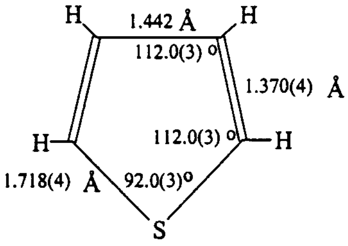

<u>FIG. 1.9</u>: The structure of thiophene.

---

[13] S. Gronowitz, Ed., *Thiophene and its Derivatives*, Vol. 1, Wiley, New York, **1985-1986**.
[14] W.R. Harshbarger, S.H. Bauer, *Acta. Cryst.*, B26, **1970**, 1010.

Note: no ESD is given for C(3)-C(4) bond length as this was calculated as a dependent value, its length determined by the other ring bond lengths and the fitted <CSC and <SCC, such that its value may be affected by errors present in the other fitted factors[14].

The lone electron pair on the sulfur atom in the thiophene ring also takes part in ring stabilization and as a result, there is a high electron density in the ring, making it extremely reactive towards electrophilic substitution. Typical reactions of thiophenes include halogenation, nitration, sulfonation and Friedel-Crafts acylation. They are much more reactive than benzene - behaving more like benzoamines or phenols - undergoing reactions such as the Reimer-Tiemann reaction, nitrozation and coupling with diazonium salts. The reactivity of thiophenes makes the use of milder reagents possible e.g. the weak Lewis acid, $SnCl_4$, in the Friedel-Craft acylation. The controlling step in the reactions of thiophenes with electrophiles is the attachment of the electrophile to the aromatic ring. This takes place at the site, which is able to afford the most stable carbocation intermediate. Reactions therefore predominantly occur at the 2- or 5-position. Attack at these positions results in the positive charge being accommodated by three atoms in the three resonance structures that arise. Attack at the 3- or 4-position would result in only two resonance structures and, therefore, less stabilization of the positive charge.

In order to evaluate the reactions of thiophenes with transition metals, it is necessary to look at the electronic structure of the heterocycle. There are six valence orbitals primarily of p-character (two of which are from the sulfur atom). The five p-orbitals perpendicular to the ring give rise to five non-degenerate π-states. Three of the π-molecular orbitals (MO's) are occupied. Although the symmetries of the π-levels are similar to those of the electronically equivalent cyclopentadiene (CpH) moiety, the presence of the heteroatom lifts any degeneracy. Benzene is a more favourable standard of comparison, as thiophene has a significantly higher basicity than CpH and the coordination chemistries of benzene and thiophene in the η^2, η^4, and η^5 complexes are similar[12]. It is important to note that the lone pairs on the sulfur do not constitute the HOMO and one pair of these is positioned orthogonally to the ring. Rauchfuss[12] describes a wide variety of reactions involving S-bound thiophene-transition metal complexes, which find application in the desulfurization of petroleum using heterogeneous catalysts. S-alkylation of thiophene is difficult and can only be accomplished using strong alkylating agents, such as trialkyloxonium salts, because of the delocalization of non-bonding electrons on the sulfur into the π-system of the ring, which causes a slight positive charge on the sulfur[15,16]. S-coordination diminishes the aromaticity of the thiophene ligand, as shown by the fact that Cp η^1-complexes serve as dienes in reactions with $[Fe_2(CO)_9]$, while the analogous thiophene complexes do not react with this reagent[17].

1.4 Transition metal carbene complexes from metallated thiophenes

Thiophenes exhibit diverse coordination abilities towards the transition metals. Thiophene is activated by transition metals during hydrodesulfurization. The metallation of thiophene occurs even at low temperatures and can result in single or double metallated products. It is therefore ideally suited to the synthesis of Fischer-type mono- and biscarbene complexes. A study[18] has been made of the synthesis and properties of such Fischer carbene complexes, in which it was reported that the

---

[15] A.E.A. Proter,*Thiophene and its Derivaitves*, S. Gronowitz, Ed., Wiley, New York, **1985**, Part 1, 629.
[16] R.J. Gillespie, A.E.A. Porter, W.E. Willmont, *J. Chem. Soc., Chem. Commun.*, 50, **1979**.
[17] M.G. Choi, R.J.Angelici, *J. Am. Chem. Soc.*, 111, **1989**, 8753.
[18] Y.M Terblans, *Thiophene Bimetallic Carbene Complexes*, University of Pretoria, Pretoria, **1996**.

delocalization of the electrons in the thiophene ring allows for electronic communication between the metals.

Furthermore, the same study saw the synthesis of σ,σ-bimetallic complexes of 2,2′-methylenedithienyl, in which the two thiophene rings cannot act as a conjugated π-system and, therefore, communication between the metal functionalities via the ligand is impossible, although the ligand may have some delocalization.

The work carried out by Aoki and co-workers[19] is also of importance. They used acyl metallates to protect the electrophilic (cationic) carbene carbon in the preparation of thienyl carbenes. The carbene salt was used directly, without undertaking alkylation. In this way, the negative charge protects the carbene from attack as other substituents are added and the thiophene ring can be manipulated without the loss of the carbene.

1.5 Bithiophene

1.5.1 Introduction to bithiophene

Bithiophene is a derivative of thiophene and constitutes the focus of this study. Bithiophene derivatives, such as 5-(3-buten-1-ynyl)-2,2′-bithienyl, are well known for their nematacidal properties (which are enhanced by the action of UV-radiation) as well as their photo-induced anti-fungal properties[20]. They are also known to have the ability to inhibit seed germination[21].

1.5.2 Synthesis of bithiophene

Convenient methods for the synthesis of bithiophene have been in existence since

---

[19] S. Aoki, T.Fujimara, E. Nakamura, *J. Am. Chem. Soc.*, 114, **1992**, 2985.
[20] R. Rossi, A. Carpita, A. Lezzi, *Tetrahedron*, 40, **1984**, 2773.

1956[22]. Early methods of synthesis include the use of nickel[23] or palladium[21] catalysts in the coupling of halothiophenes with Grignard reagents derived from halothiophenes. The problem with this method was that it was restricted to functional groups which did not react with organomagnesium reagents. Photochemically induced coupling was also attempted, in which iodothiophenes were coupled with thiophene derivatives. In this case, functional groups were restricted to those which were not reactive towards UV-radiation[24].

Bithiophenes have also been investigated as precursors for the manufacture of polythiophenes, which have important applications in the world of conducting polymers. Boron methodology for the production of bithiophenes for this purpose was investigated by Kagan *et al.*[25] (based on work by Levy[26] and Suzuki[27]), but despite reported yields of 81 %, later work by Pelter and partners[28] showed that almost half the residues were recovered as thiophene, and not bithiophene. Pelter modified the method by using the stepwise addition of thienyl units to readily available trialkoxyboranes. Using a two-phase system consisting of N-borosuccinamide, CH_2Cl_2, methanol and a borax buffer at pH = 9, they produced bithiophene at a 90 % crude yield and an 82 % recovery. They also discovered that changing the base used in the reaction drastically affected the results: using bromine as a base with NaOMe, the recovery dropped to 77 %. They concluded that the base used played an important role in controlling the proportion of α-attack. **Fig. 1.10** shows a general representation of their method.

---

[21] G. Campbell, J.D.H. Lambert, T. Arnason, G.H.N. Towers, *J. Chem. Ecol.*, 8, **1982**, 961
[22] H. Wynberg, A.J. Logothestis, *J. Am. Chem. Soc.*, 78, **1956**, 1958.
[23] R. Rossi, A. Carpita, *Gazz. Chim. Ital.*,115, **1985**, 575.
[24] M. D'Auria, D. Mico, F. D'Onofrio, G. Piancatlli, *J.Org.Chem.*, 52, **1987**, 5234.
[25] J. Kagan, S.K. Arora, *Tetrahedron Lett.*, 24, **1983**, 4043.
[26] A.B. Levy, *Tetrahedron Lett.*, 42, **1979**, 4021.
[27] a) I Akimoto, A. Suzuki, *Synthesis*, **1979**, 146.
b) T. Sotoyama, S. Hara, A. Suzuki, *Bull. Chem. Soc. Jpn.*, 52, **1979**, 1865.

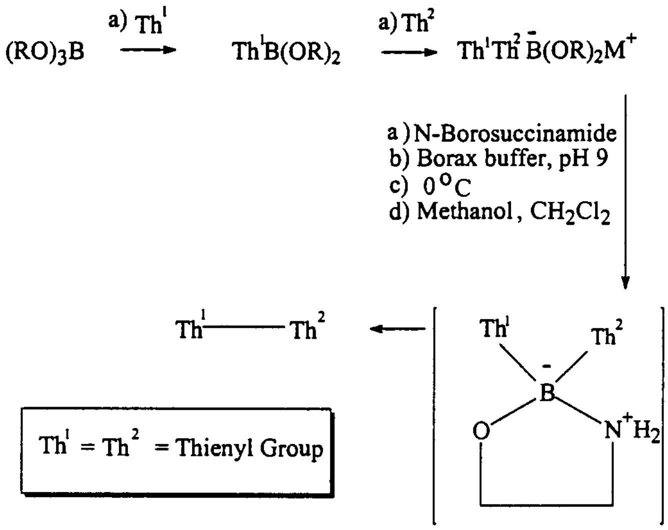

FIG. 1.10: The synthesis of bithiophene[28].

Another synthetic route to bithiophene was that of Larock *et al.*[29], who reported a 96 % yield of bithiophene as a greenish oil which solidified on standing (Melting Point 32-33 °C). Their method involved reacting the thienylmercuric chloride with $[RhCl(CO)_2]_2$ in the presence of LiCl and hexamethylphosphoramide for 24 hours at 80 °C.

Crisp[30] developed a more general method of synthesis of bithiophene and its derivatives as intermediates in the synthesis of biologically active molecules. This involved the use of palladium catalysts in the coupling of iodothiophenes to stannylthiophenes. A variety of functional groups was used on the iodothiophenes and good yields of the desired bithiophene derivatives were obtained. Even in the

---

c) I. Akimoto, M. Sano, A.Suzuki, *Bull. Chem. Soc. Jpn.*, 54, **1981**, 1587.

[28] A. Pelter, H. Williamson, G.M. Davies, *Tetrahedron Lett.*, 25, **1984**, 453.

[29] R.C. Larock, J.C. Bernhardt, *J. Org. Chem.*, 42, **1977**, 1680.

[30] G.T.Crisp, *Synth. Commun.*, 19, **1989**, 307.

case of the most sensitive functional groups (free hydroxy groups and aldehydes) the method proved successful.

1.5.3 Structural features of bithiophene

Visser and co-workers[31] conducted a study of the crystal structures of dithienyls and discovered that 2,2′-dithienyl decomposes during X-ray exposure. Intensities therefore had to be collected at low temperatures (-140 °C). Different crystals had to be used and it seemed impossible to get consistent results. Therefore, only the intensities measured on the zero and fourth layer lines about the b-axis were used. As a result, cell constants and intensities were not very accurate. The space group was indicated unambiguously from systematic absences in the photographs. Molecules were situated at a two-fold position so there is only one independent thiophene ring per cell.

Large inaccuracies and variations in intensities lead to large standard deviations for bond lengths and bond angles. These were compared to theoretically determined values[31]. **Fig. 1.11** shows these.

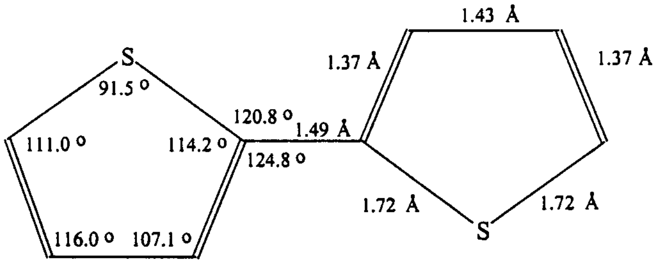

FIG. 1.11: Bond lengths and bond angles of bithiophene.

---

[31] G.J. Visser, G.J. Heeres, J. Wolters, A.Vos, *Acta Cryst.*, B24, **1968**, 467.

In bithiophene crystals, all molecules have the same tilt relative to the [101] direction, namely 7.4 °, and alternating tilts for the *c*-direction, around 46.5 °. No intermolecular distances shorter than those expected for the conventional van der Waals contacts were observed. **Fig. 1.12** shows the crystal structure of bithiophene. There is a notable difference in the gaseous and solid states of bithiophene. In the gas phase the angle of twist around the central bond has an average value of 34 ° with respect to planarity, while Visser[31] showed that, in the solid phase, the molecules are planar and have a *trans*-conformation with respect to the sulfur atoms.

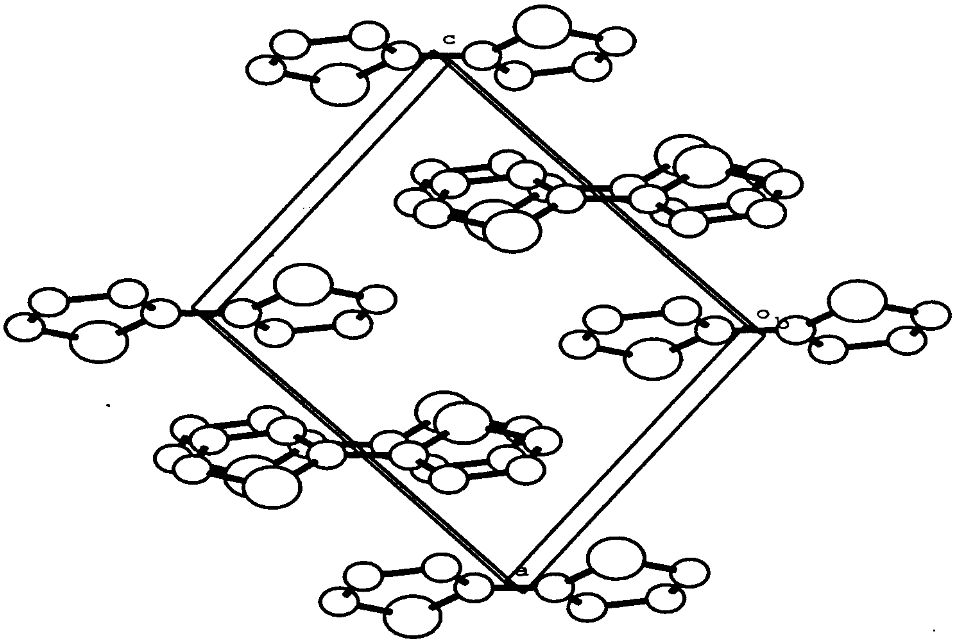

FIG. 1.12: Projection of the unit cell of the crystal structure of bithiophene, viewed along the b-axis[31].

Almennigen *et al.*[32] showed that, in the gas phase, the molecule is flexible with rotations of up to 85 ° possible. The preferred gaseous phase conformation was reported[31] to be the *anti*-gauche conformation with the inter-ring dihedral angle, $\theta =$

---

[32] A. Almennigen, O. Bastiansen, P. Svendsas, *Acta Chem. Scand.*, 12, **1958**, 1671.

146 °. The theoretical studies of Dewar and Trinajstic[33], and the Electron Spin Resonance(ESR) studies of Cavalieri d'Oro [34], all confirm the planar structure, which plays a key role in the potential use of these molecules in conducting materials, as it facilitates charge transfer across the rings. In solution, however, Lumbroso and Carpanelli[35] estimate an angle of rotation of 78 ° and Wachters and Davies[36] estimate 79-97 °, based on measurement of the dipole moment, but these are uncertain because they are sensitively dependent on allowances made for the atom polarization. By considering polarizability anisotropy, and examining apparent polarizations and molar Kerr constants of the rings in 2,2′-bithiophene in CCl_4, Aroney *et al.*[37] found that the preferred solution-state conformation of 2,2′-bithiophene is 23 ° (± 10 °). The large uncertainty arises from the low variability of molar Kerr constants at near *trans* conformations. The alternative 130 ° angle can be excluded on dipole moment evidence alone.

Bucci and co-workers[38] used nematic phase NMR in an attempt to elucidate the structure of 2,2′-bithiophene. They concluded that nematic phase spectra could not give very accurate results concerning conformational analysis because the symmetry of bithiophene results in insufficient observable parameters. The spectra did, however, give a good indication of the conformational preferences and interconversion barriers. Results obtained after rough approximation concur with theoretical calculations performed on the same molecule by Galasso and Trinajstic[39] i.e. a 68:32 ratio of

---

[33] M.J.S. Dewar, N. Trinajstic, *J. Am. Chem. Soc.*, 92, **1970**, 1453.
[34] P. Cavalieri d'Oro, A. Mangini, G.F. Pdulli, P. Spagnolo, M. Tiecco, *Tetrahedron Lett.*, **1969**, 4179.
[35] H. Lumbroso, C. Carpanelli, *Bull. Soc. Chim. Fr.*, **1964**, 3198.
[36] A.J.H. Wachters, D.W. Davies, *Tetrahedron*, 20, **1964**, 2841.
[37] M.J. Aroney, H.K. Lee, R.J.W. Le Fevre, *Aust. J. Chem.*, 25, **1972**, 1561.
[38] P. Bucci, M. Longeri, C.A. Veracini, L. Lunazzi, *J. Am. Chem. Soc.*, 96, **1974**, 1305.
[39] V. Galasso, N. Trinajstic, *Tetrahedron*, 28, **1972**, 4419.

S-*trans* to S-*cis* conformers in solution with a barrier of *ca* 17.4 kJ/mol. In solutions at –80 °C the two conformers are found in an 80:20 ratio, according to Cavalieri d'Oro[34]. Bucci[38] suggests that the S-*trans* conformer is more stable (70 ± 5 %) and the energy required for S-*trans* to S-*cis* interconversion is around 21.7 kJ/mol.

More recently, Aleman[40] applied molecular modeling computational methods in order to the study of conformational preferences of 2,2′-bithiophene. Their results concur with those of Almenningen *et al.*[32]. They reported two minimum energy conformations: the *anti*-gauche conformation (located at $\theta = 142$ °) and the *syn*-gauche conformation for which $\theta = 43$ °. The latter is less favoured than the *anti*-gauche by *ca* 2.17 kJ/mol.

The gauche-gauche ($\theta = 90$ °) conformation forms a barrier between these two conformations. It is less favoured compared to the *anti*-gauche conformation by 6.28 kJ/mol. The results indicated that planar conformations are less stable than twisted conformations; thus the *syn* conformation is less favoured than the *syn*-gauche by 5.6 kJ/mol and the energy difference between the *anti*- and *anti*-gauche conformations is 3.5 kJ/mol.

1.6 Transition metal carbene complexes from metallated bithiophenes

Requirements for large hyperpolarizability are best met in conjugated systems where π-donor and π-acceptor groups are connected via a conducting polyene-type bridge of the required length. This results in a push-pull arrangement of electrons and large second order hyperpolarizabilities. Fischer-type carbene complexes of bithiophene appear to have potential for use in this type of molecular system because of their delocalized nature. With this in mind, Maiorna and co-workers[41] synthesized the mononuclear carbene, $[Cr\{C(X)C_4H_2S\text{-}C_4H_3S\}(CO)_5]$, X= OEt, pyrrolyl and a heteronuclear complex $[(CO)_5Cr\{C(OEt)C_4H_2S\text{-}C_4H_2SC(OEt)\}W(CO)_5]$. These were synthesized via stepwise metallation and reaction with metal carbonyls and subsequent alkylation with $[Et_3O^+BF_4^-]$. Yields were poor and products could not be properly purified and characterized. The aminolysis product was the only one, which showed any hyperpolarizability.

Examples of bithiophene carbene complexes include the synthesis of pentcarbonyl-(diarylcarbene) complexes by reacting pentacarbonyl(arylmethoxycarbene) complexes of tungsten and chromium with lithiated thiophenes and, subsequently, treating the intermediate addition product with silica gel/pentane (**Fig. 1.13**).

The reactions were reported to proceed with ease at low temperatures and the resulting products were reported to be partially thermally labile and diamagnetic[42].

---

[40] C. Aleman, V.M. Domingo, L. Fajari, L. Julia, A. Karpfen, *J. Org. Chem.*, 63, **1998**, 1041.

[41] S. Maiorana, A. Papagni, E. Licandro, A. Persoons, K. Clay, S. Houbrechts, W. Porzio, *Gazz. Chim. Ital.*, 125, **1995**, 377.

[42] E.O. Fischer, W. Held, F.R. Krießl, A. Frank, G. Huttner, *Chem. Ber.*, 110, **1977**, 655.

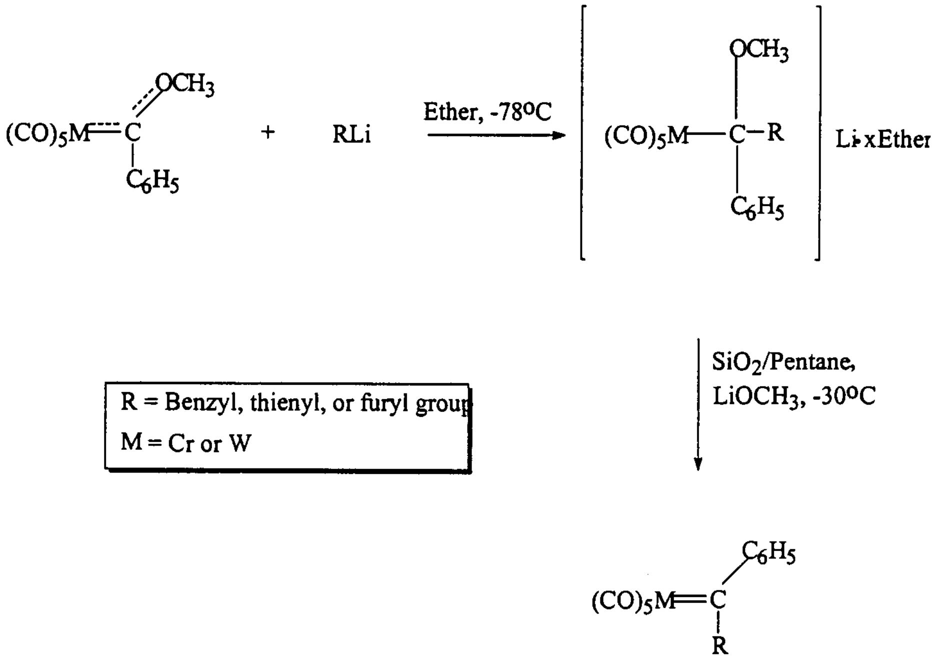

FIG. 1.13: The reaction scheme for the production of pentacarbonyl (diarylcarbene) complexes.

1.7 Ruthenium alkyl complexes of bithiophene

Graf *et al.*[43] examined the formation of ruthenium complexes with bithiophene and other thiophene oligomers in order to formulate a model for the "tuning" of properties of conducting polymers. By reacting [RuCp(CH$_3$CN)$_3$]PF$_6$ or [RuCp*(CH$_3$CN)$_3$]$^+$ with bithiophene, they were able to form [RuCp/Cp*(bithiophene)]PF$_6$. They discovered that the Ru binds η^5 to the outermost ring of the oligomer and affects the conjugation of two rings on either side of the one to which it is bonded. This has implications for the manipulation of conducting polymer characteristics. Very little other information is available for the synthesis of alkyl transition metal complexes of bithiophene.

---

[43] D.D. Graf, N.C. Day, K.R. Mann, *Inorg. Chem.*, 34, **1995**, 1562.

1.8 Applications of bithiophene and its derivatives

1.8.1 Origin of conducting polymers

Substances that have the properties of inorganic semiconductors combined with the processibility, resistance to corrosion and light weight of organic polymers are highly desirable in the world of electronics today. These materials, called conducting polymers (CP's), have numerous applications ranging from bulk applications (such as antistatic coatings) to sophisticated molecular devices (such as electronic components or selective or modified electrodes). They, therefore, have an important place in both industrial and academic research. A short overview will be given here.

Conducting polymers arose from the work of Heeger and MacDiarmid[44] in the late 1970's. They showed that a 12 order of magnitude increase in the conductivity of polyacetylene was possible through charge-transfer oxidative doping.

The essential structural characteristic of CP's is the conjugated π-system, which extends over a large number of monomer units. This results in the use of low-dimensional materials with high anisotropy of conductivity, which increases along the chain direction. The simplest example of such a material is $H-[CH]_x=CH_2$, which comprises alternating single and double bonds. Such a low dimensional structure should have almost no gap between its occupied and unoccupied energy levels (i.e. a band gap, E_g, of 0.0 eV). However, the structure is unstable and interactions between the electrons, phonons (lattice vibrations) and lattice distortions cause an increase in the band gap to E_g= 1.50 eV[45].

Poly(heterocycles), such as polythiophenes (PT), are $sp^2(p_x)$ carbon chains stabilized by the heteroatom, and are better suited to the application than $H-[CH]_x=CH_2$ because

---

[44] C.K. Chaing, Y.W. Park, A.J. Heeger, H. Shirakawa, E.J. Louis, A.G. MacDiarmid, *Phys. Rev. Lett.*, 39, 1977, 1098.

of: (I) their higher environmental stability; (II) their non-degenerate ground state (related to the nonenergetic equivalence of their two limiting mesomeric forms - aromatic and quinoid - see **Fig. 1.14**); and (III) their structural versatility, which allows the modulation of their electronic properties by manipulation of the monomer structure[46].

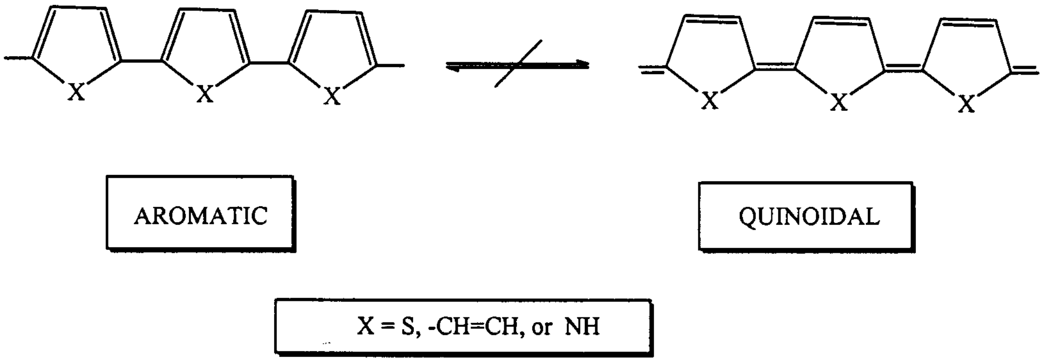

FIG. 1.14: The aromatic and quinoidal structures of aromatic polyheterocycles.

Polyaromatics generally have band gaps larger than 1.50 eV, as their complex structures result in a number of energies contributing to the band gap energy[45]. The bond length alteration energy ($E^{\delta r}$), required to change the lengths of bonds between the rings from single to double bond lengths is one contributing factor. Another factor is the torsional angle or deviation from planarity of the two rings (E^{θ}). A third factor is the aromatic resonance energy of the rings (E^{res}). Finally, the substituent groups on the backbone have inductive and mesomeric effects (E^{sub}), and the solid-state interchain and intermolecular interactions contribute (E^{int}). The band gap energy (E_g) is, therefore, represented by the expression:

$$\mathbf{E_g = E^{\delta r} + E^{\theta} + E^{res} + E^{sub} + E^{int}}$$

---

[45] J. Roncali, *Chem. Rev.*, 97, **1997**, 173.
[46] J. Roncali, *Chem. Rev.*, 92, **1992**, 711.

Polythiophenes are of particular value in this type of research because their properties allow for use in multiple developments such as conductors, electrode materials and organic semiconductors[46]. Much work has been put into manipulating these systems to produce suitable materials for industrial applications.

1.8.2 Synthesis of conducting polymers

Bithiophene was the first thiophene derivative to be electropolymerized[47] and still plays an important role in the development of conducting polymers both as a starting material for the production of thiophene oligomers[48,49,50], as well as being used as a model[46] for adjustments to the properties of conducting polymers. The latter function is important, as larger oligomers are often insoluble and difficult to work with.

There are two main types of synthetic routes employed in the synthesis of CP's:

I) Chemical synthesis: Methods such as polycondensation using nickel complexes[51], nickel catalyzed Grignard coupling[52], plasma polymerization[53], and oxidative polymerization in gas[54] and liquid phases[55,56] have been reported. Few of these methods allow only α,α′-coupling of the thiophene rings and many are not tolerant of electrophilic functional groups. McClain *et al.*[57] devised a method based on the successful synthesis of 2,2′-bithiophene. Poly(3-alkylthiophene)'s with a wide variety

---

[47] A.F. Diaz, *Chem. Scr.*, 17, **1981**, 142.

[48] A. Berlin, G.A.Pagani, F. Sannicolo, *J. Chem. Soc., Chem. Commun.*, **1986**, 1663.

[49] D.D. Cunningham, L. Laguren-Davidson, H.B. Mark, Jr., Chiem van Pham, H. Zimmer, *J. Chem. Soc., Chem. Commun.*, **1987**, 1021.

[50] P. Bauerle, T. Fisher, B. Bidlingmeier, A. Stabel, J. P. Rabe, *Angew. Chem., Int. Ed. Engl.*, 34, **1995**, 303.

[51] J.W.P.Lin, L.P.J. Dudek, *Polym. Sci.*, 18, **1980**, 2869.

[52] M. Kobayashi, J. Chem, T.C. Moraes, .J. Heege, F. Wudl, *Synth. Met.*, 9, **1984**, 77.

[53] R. Hernandez, A.F. Daiz, R.J. Waltman, J. Bargon, *J. Phys. Chem.*, 88, **1984**, 3333.

[54] G. Kossmehl, G. Chatzitheodorou, *Macromol. Chem., Rapid Commun.*, 2, **1981**, 551.

[55] R. Sugimoto, S. Takeda, H.B. Gu, K. Yoshino, *Chem. Express.*, 1, **1986**, 635.

[56] S. Hotta, M. Soga, N. Sonoda, *Synth. Met.*, 26, **1988**, 267.

of functional groups were produced in good yields through the coupling of 2,5-bis(chloromercurio)-3-alkylthiophenes in the presence of copper powder and a catalytic amount of palladium chloride. The synthesis was reported to also produce random copolymers of 3-alkylthiophenes with varying amounts of thiophene or by using monomers of different oxidation potentials.

II) Electrochemical synthesis: Two main routes, i) the cathodic and ii) the anodic routes, are available. The cathodic route[58] comprises the electro-reduction of the complex. It has the disadvantage that the polymer is produced in its neutral form, which leads to rapid passivation of the electrode and limited thickening of the film. The advantage of this method is that it is suitable for use on materials, which are subject to anodic corrosion, such as small band gap semi-conductors[59].

The anodic route[46] is the most widely used route. It has the following advantages: no catalyst is required; direct grafting of the doped conducting polymer onto the electrode surface; easy control of the film thickness by the deposition charge; and the ability to perform the first *in situ* characterization of the growth process (or of the polymer) by electrochemical and/or spectroscopic techniques.

The electropolymerization of bithiophene was first published in 1981[47] and of thiophene in 1982[60].

Although chemical synthesis is probably best for the formation of oligomers of defined structure, the most extensively conjugated and most conductive PT's have been prepared by electrochemical polymerization[46].

1.8.3 Structure of conducting polymers

---

[57] M.D. McClain, D.A. Whittington, D.J. Mitchell, M.D. Curtis, *J. Am. Chem. Soc.*, 117, **1995**, 3887.
[58] G. Zotti, G. Shiavon, *J. Electroanal. Chem.*, 163, **1984**, 385.

The most essential macromolecular structural feature is the extent of the conjugation of the π-system. This controls the size of the energy gap, conductivity and electroactivity of the CP's[61]. In the absence of distortion of the conjugated backbone, the effective mean conjugation length (MCL) is determined by the stereoregularity of the α-α′ linkages in the polymer[62]. Due to their rigid, conjugated structure, unsubstituted CP's are generally insoluble and infusible, which makes them difficult to charaterize by conventional analytical methods. As a result, the determination of the MCL of PT is complex. IR and ^{13}C NMR studies[61,63] of neutral PT's show that α-α′ linkages predominate in their structures.

PT's are, however, known to have a significant amount of α-β′ linkages[64]. The IR spectra of PT's, selectively labeled with deuterium at the α- and/or β-positions, led to a value of 18 α-α′ linked thiophene rings, for the MCL of polythiophene, with an average degree of polymerization of 150[65]. These studies show that the higher the MCL, the more conjugation and, therefore, the better the conductivity of the PT.

In terms of conformational and tertiary structures, PT's are essentially amorphous polymers, but do show some crystallinity (ca 35 %, increasing to 56 % on annealing)[66].

Two models for the crystal structure of these materials exist: orthorhombic unit cell and monoclinic unit cell. In both instances, the models point to the fact that the polymer chains are predominantly planar and have a *transoidal* configuration of the thiophene rings.

---

[59] Z. Xu, G. Horowitz, F.J. Garnier, *J. Electroanal. Chem.*, 246, **1988**, 467.
[60] G. Tourillon, F.J. Garnier, *J. Electroanal. Chem.*, 135, **1982**, 173.
[61] S. Hotta, T. Hosaka, M. Soga, W. Shimotsuma, *Synth. Met.*, 10, **1984**, 95.
[62] K. Tanaka, T. Schichiri, T. Yamabe, *Synth Met.*, **1986**, 271.
[63] T. Yamamoto, K. Sanechika, A. Yamamoto, *Bull. Chem. Soc. Jpn.*, 56, **1983**, 1503.
[64] G. Tourillon, F. Garnier, *J. Phys. Chem.*, 87, **1983**, 2289.
[65] D. Delabouglise, R. Garreau, M. Lemaire, J. Roncali, *New J. Chem.*, 12, **1988**, 155.
[66] Z. Mo, K.B. Lee, Y.B. Moon, M. Kobayashi, A.J. Heeger, F. Wudl, *Macromolecules*, 18, **1985**,

Interchain electron transport is essential for the conductivity of polythiophenes. Miller and Mann[67] studied this and discovered that thiophene oligomers form almost crystalline structures: π-dimers and, even, π-stacks in solution. These stacks enhance interchain electron transfer because there is delocalization of electrons between the rings in the stacks (**Fig. 1.15**). This results in the oxidized polythiophenes having high electrical conductivities. Yu and co-workers[68] took this one step further and suggested that three dimensional π-dimers and π-stacks can be designed by attaching the correct groups to the polymers to facilitate these formations.

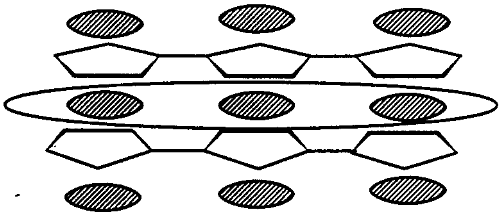

FIG. 1.15: A schematic representation of the π-stacking of polythiophenes, showing the increased electron density between the rings in the stacks.

They did this by attaching methoxy groups to the "inside" β- positions of oligothiophenes. This produced stable cation radicals, from which π-dimers and π-stacks are known to form.

Horne *et al.*[69] studied the isomerization barriers in thiophene oligomers and discovered that, for most of these, the inter-ring isomerization barrier is *ca* 34.8 kJ/mol for rotation in the S_0 state. Barriers for the S_1 state were higher for larger oligomers and this was rationalized by the fact that longer oligomers are able to support a more quinoid-like excited electronic state. The low barriers to

---

1972.

[67] L.L. Miller, K.R. Mann, *Acc. Chem. Res.*, 29, **1996**, 417.

[68] Y. Yu, E. Gunic, B. Zingre, L.L. Miller, *J. Am. Chem. Soc.*, 118, **1996**, 1013.

[69] J.C. Horne, J. Blanchard, E. LeGoff, *J. Am. Chem. Soc.*, 117, **1995**, 9551.

isomerization preclude any long-term order in the polymers. They speculated that the ground state inter-ring isomerization barrier for polythiophenes would be in the same region as that of oligothiophenes. They reported that rotational defects in polythiophenes do not contribute significantly to the material properties, since any meso- or macroscopic material response is averaged over a large number of rotations of each thiophene ring. The small barrier heights calculated for rotation suggest that there is little or no long-term order in the polymers synthesized from oligothiophenes.

1.8.4 Properties of conducting polymers

Optical and charge transfer properties can be accounted for by two models. The "bipolaron" model proposes that the removal of an electron from the conjugated π-system provokes a local distortion of the chain and the appearance of two states in the energy gap, each corresponding to a polaron (or radical cation) with spin 1/2. Theoretically, two adjacent polarons are unstable and lead to the formation of spinless, doubly charged defects (for example bipolarons or dications). These have been proposed to be the dominant charge storage species[70,71]. The role of the heteroatom is not clear. Some[71,72] believe it is negligible; while others[73] believe its dominant effect is via the direct interaction of its p-orbital lone pair with the carbon backbone π-band structure. The problem that arises is that C-C and C-S bond lengths should change during the change in structure from aromatic to quinoid, which takes place during the formation of a bipolaron. The absence of changes in the bond lengths leads to questioning of the "bipolaron" theory and the proposal of another

---

[70] J.L. Bredas, B. Themans, J.M. Andre, R.R. Chance, R. Silbey, *Synth. Met.*, 9, **1984**, 265.
[71] T.C. Chung, J.H. Kaufman, A.J. Heeger, F. Wudl, *Phys. Rev. B.*, 30, **1984**, 702.
[72] G. Tourillon, D. Gourier, F. Garnier, D. Vivien, *J. Phys. Chem.*, 88, **1984**, 1049.
[73] J.W. Mintmire, C.T. White, M.L. Elert, *Synth. Met.*, 16, **1986**, 235.

model, whereby charge transport was said to occur due to the formation of a metallic state through modification of the electron structure. The metallic state model suggests that the oxidation proceeds via the uniform extraction of electrons from the π-band combined with continuous extension of the π- and π*-bands to the Fermi level[74,75]. While the bipolaron theory is still widely accepted, the exact nature of the charged species involved in these properties is a matter for debate. Roncali[46] suggests that a possible cause of the dissention is the difference in the structures and properties of the PT's being studied. It was proposed that polarons and bipolarons differ by the minimum conjugation length required by their spatial extension[70].

Graf *et al.*[76] studied the structure (**Fig. 1.16**) and properties of monomeric π-dimerized and π-stacked forms of the cation radical, 3′,4′-dibutyl-2,5″-diphenyl-2,2′:5′,2″-terthiophene $(Bu_2Ph_2tTh)^{+\bullet}$.

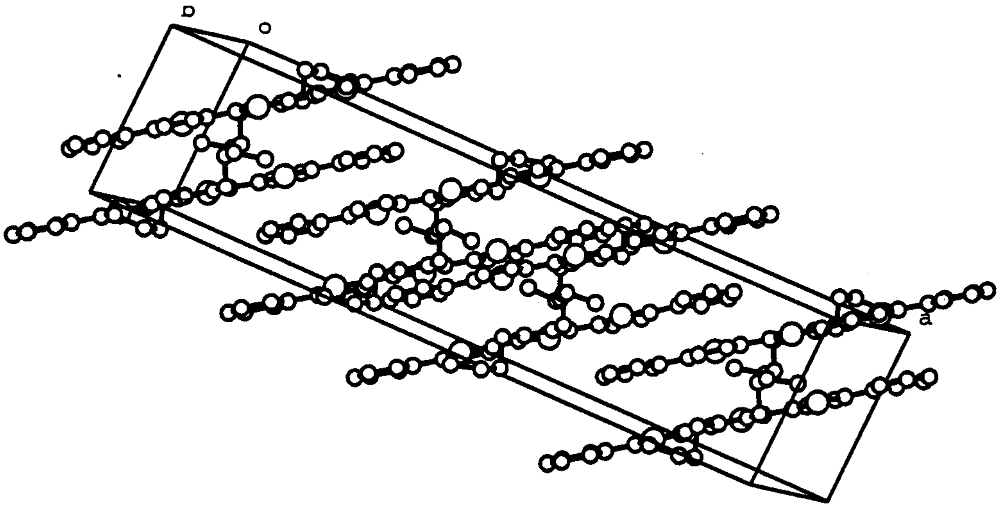

FIG. 1.16a: View of the packing structure of $[Bu_2Ph_2tTh]PF_6$ (at 106K), parallel to the *ac* plane normal with PF_6^- ions left out for clarity[76].

---

[74] G. Tourillon, A.M. Flank, P. Lagarde, *J. Phys. Chem.*, 92, **1988**, 4397.

[75] Y. Jugnet, G. Tourillon, T.M. Duc, *Phys. Rev. Lett.*, 56, **1986**, 1862.

[76] D.D. Graf, R.G. Duan, J.P. Campbell, L.L. Miller, K.R. Mann, *J. Am. Chem. Soc.*, 119, **1997**, 5888.

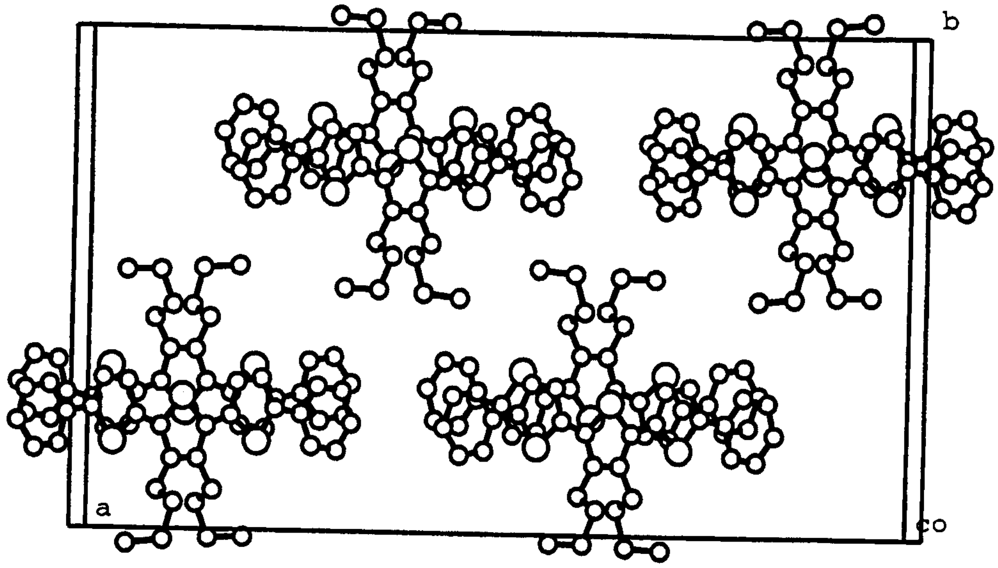

FIG. 1.16b: View of the packing structure of [Bu_2Ph_2tTh]PF_6 (at 106K), down the slipped packing direction (*c* axis)[76].

Fig. 1.17 shows the low- and high-energy bands for the monomeric radical cation, [Bu_2Ph_2tTh]$^+$, labeled as E_{M1} and E_{M2} respectively. Upon π-dimerization, the orbitals of the two monomeric molecules overlap. The three bands of the π-dimer are assigned as the transitions E_{D1}, E_{D2}, E_{D3}, such that the energies of these transitions follows the trend: $E_{D1} > E_{D2} > E_{D3}$. This work supports the theory that a possible conducting mechanism exists through the π-stacks (and not between the π-stacks) which is not adequately modeled by the polaron/bipolaron theory. It is clear that while researchers are still a long way off from fully rationalizing charge transfer mechanisms in these systems, π-stacks and π- interactions are vital to conduction in such molecules as [Bu_2Ph_2tTh]PF_6.

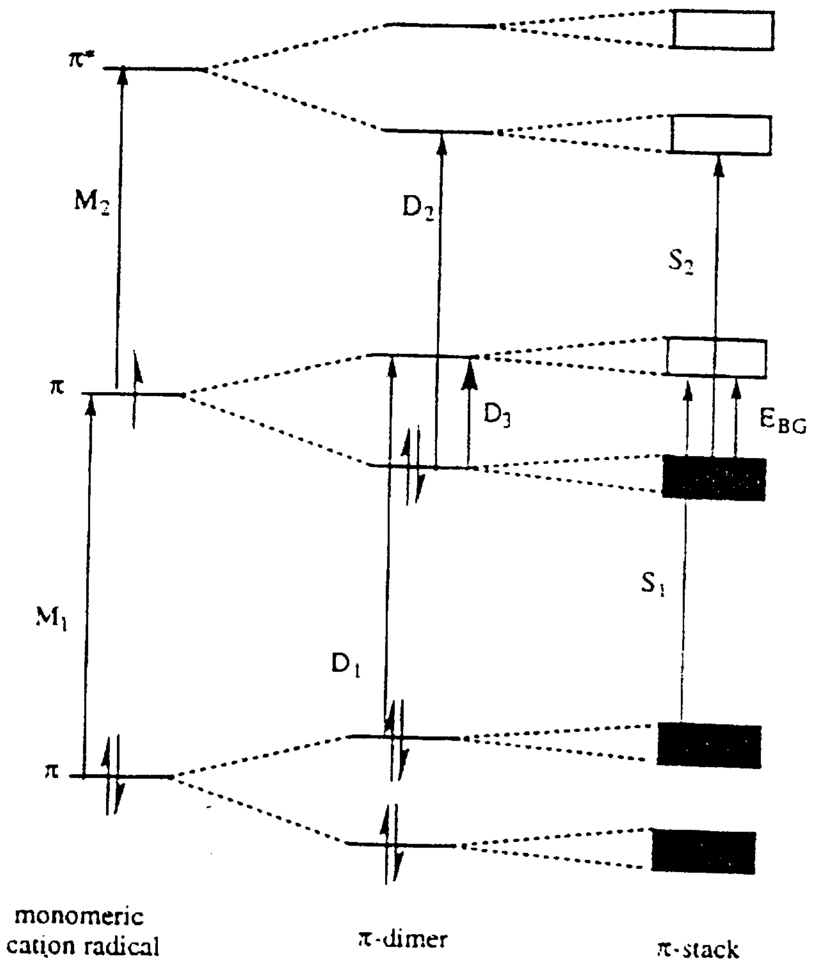

FIG. 1.17: **Qualitative MO diagram for the monomeric, dimeric and π-stacked forms of $[Bu_2Ph_2tTh]PF_6$ in solution and the solid state[76].**

Electrochemical properties arise from the easy, reversible oxidation of these materials. Electrochemical n-doping is, however, less easy to achieve, as the negatively charged form of the polymers is unstable.

Film thickness, the nature of the substrate electrode, and the composition of the electrolytic medium all play a role in the control of charge propagation and mass transport in the polymer, as well as controlling the solvation of the ionic species and of different polymeric forms and the coulombic interactions between the charged sites. The number and spatial localization of charged sites, Ohmic conductivity, and capacitance vary continuously with the doping level and, hence, with electrode potential. This makes the analysis of the factors influencing electrochemical behaviour very difficult. As a result, only theoretical models (based on fixed sites redox polymers) exist for describing electrochemical behaviour[77, 78].

1.8.5 Molecular engineering of conducting polymers

The wide spectrum of applications of these materials necessitates modification of structure, form and properties of the polymers in order to meet the requirements of the application. The method of modification is determined by the required property and the level at which the modification must occur (i.e. molecular, macromolecular, microscopic). Three approaches exist: (I) Association of the CP with other materials (or chemical entities) in order to produce hybrid materials which have properties common to both the starting materials, and in which these properties exist synergically.

Of particular importance is the incorporation of transition metals (such as Ag, Pt and Cu), which were electrodeposited into polymethylthiophene[79].

Dinuclear Pt complexes of rigid-rod alkynes with extended π-conjugation via the oligothiophene linkage units in the backbone, were prepared and characterized by Lewis[80]. Zinc has also been included into polymethylthiophene[81]. Molybdenum has

---

[77] E. Laviron, *J. Electroanal. Chem.*, 122, **1980**, 37.

[78] C. P. Andrieux, J.M. Bouchiat, J.M. Saveant, *J. Electroanal. Chem.*, 131, **1982**, 1.

[79] a) G. Tourillon, E. Dartyge, H. Dexpert, A. Fontaine, A. Jucha, P. Lagarde, D.E. Savers, *J. Electroanal. Chem.*, 178, **1984**, 357.
b) G. Tourillon, F. Garnier, *J. Phys. Chem.*, 88, **1984**, 5280.
c) D. Gouriet, G. Tourillon, *J. Phys. Chem.*, 90, **1986**, 5561.

[80] J. Lewis, N.J. Long, P.R. Raithby, G.P. Shields, W.Y. Wong, M. Younus, *J. Chem. Soc., Dalton Trans.*, **1997**, 4283.

[81] H. Shinohara, M. Aizawa, H. Shirakawa, *J. Chem. Soc., Chem. Commun.*, **1986**, 209.

been introduced into terthiophenes to yield electrochemically conductive films[82]. Ruthenium and osmium inclusions into oligothiophenes and oligothienylacetylides have been extensively studied[83]. Several studies have also been conducted on transition metal σ-acetylide functionalized oligothiophenes[84] due to their facile metal-to-ligand charge transfer capabilities. A new class of nanostructures was also derived using (amongst others) [$FeOCl_4$] as the host matrix for intercalative polymerization of thiophenes[85].

(II) Synthesis of block copolymers (such as those of thiophenes and pyrroles) which has been investigated in numerous studies[86]. These have displayed excellent confinement characteristics of the π-conjugated electrons.

(III) Derivatization of the monomer prior to polymerization. This would seem to be the simplest method of modifying the properties of CP's, but it requires that the functional group be coupled to the monomer in such a way as to remain compatible with both polymerization and conservation of an extensively conjugated π-system in

---

[82] D.H. Kim, B.S. Kang, S.M. Lim, K.M. Bark, B.G. Kim, M. Shiro, Y.B. Shim, S.C. Shin, *J. Chem. Soc., Dalton Trans.*, **1998**, 1893.

[83] a) D.D. Graf, K.R. Mann, *Inorg. Chem.*, 36, **1997**, 141.
b) D. D. Graf, K.R. Mann, *Inorg. Chem.*, 36, **1997**, 150.
c) Y. Zhu, D.B. Millet, M.O. Wolf, S. J. Rettig, *Organometallics*, 18, **1999**, 1930.

[84] a) E. Viola, C. Lo Strezo, R. Crescnzi, G. Frachey, *J. Organomet. Chem.*, 493, **1995**, C9
b) A. Buttinlli, E. Viola, E. Antonelli, C. Lo Strezo, *Organometallics*, 17, **1998**, 2574.
c) M.C.B. Colbert, J. Lewis, N.J. Long, P.R. Raithby, M. Younus, A.J.P. White, D.J. Williams, N.N. Payne, L. Yellowlees, D. Beljonne, N. Chawdyhury, R. H. Friend, *Organometallics*, 17, **1998**, 3034.

[85] a) M.G. Kanazidis, L. M. Tonge, T.J. Marks, H.O. Marcy, C.R. Kannewurf, *J. Am. Chem. Soc.*, 109, **1987**, 3797.
b) P. Enzel, T. Bein, *J. Chem. Soc., Chem. Commun.*, **1989**, 1326.
c) M.G. Kanatzidis, Wu Chun-Guey, H.O. Marcy, D.C. De Groot, C.R. Kannewurf, *Chem. Mater.*, 2, **1990**, 222.

[86] a) F. Meyers, A.J. Heeger, J.L. Bredas, *J. Chem. Phys.*, 97, **1992**, 2750.
b) J.P.l Ferraris, T.R. Hanlor, *Polymer*, 30, **1989**, 1319.
c) P.I. Burn, A.B. Holmes, A. Kraff, D.D.C. Bradley, A.R. Brown, R.H. Friend, R.W. Gymer, *J. Chem. Soc., Chem. Commun.*, **1992**, 32.
d) J.P. Parakka, J.A. Jeevarajan, A.S. Jeevarajan, L.D. Kispert, M.P. Cava, *Adv. Mater.*, 8, **1996**, 54.
e) J.P. Parakka, M.P. Cava, *Synth. Met.*, 68, **1995**, 275.

the resulting polymer in order to preserve the relevant electronic, optical and electrochemical properties. The derivatization of monomers has, therefore, been the focus of several investigations. These include studies on: the effect of electronegativity of the substituents[79, 87]; the use of methyl substituents on the monomers and conjugated systems as monomers [88,89]; the use of heteroatoms as functional groups [90]; and the use of branched monomers and side chain substituents[91]. Work directed specifically towards bithiophene as a monomer focused largely on bridged bithiophenes[92,93].

Benincori *et al.*[94] highlighted another aspect of monomer manipulation to influence polymer properties. They studied the effect of controlling the torsion angle (θ) at the inter-ring bond in bithiophene monomers on the properties of polybithiophenes. Molecular modeling can be used in all these approaches to elucidate the best possible material for the application.

1.8.6 Molecular modeling of conducting polymers

---

[87] a) R.J. Waltman, J. Bargon, *Can. J. Chem.*, 64, **1986**, 76.
b) R.J. Waltman, J. Bargon, A.F. Diaz, *J. Phys. Chem.*, 87, **1983**, 1459.
c) H.S. Li, J. Roncali, F. Garnier, *J. Electroanal. Chem.*, 263, **1989**, 155.
d) S. Tanaka, M. Sato, K Kaeriyama, *Synth. Met.*, 25, **1988**, 277.
e) J.P. Ruiz, K. Nayak, D.S. Marynick, J.R. Reynolds, *Macromolecules*, 22, **1989**, 1231.

[88] G. Tourillon, F. Garnier, *J. Phys. Chem.*, 87, **1983**, 2289.

[89] J. Roncali, F. Garnier, M. Lemaire, R. Garreau, *Synth. Met.*, 15, **1986**, 323.

[90] R.D. McCullough, S.P. Williams, *J. Am. Chem. Soc.*, 115, **1993**, 11608.

[91] a)S. Tanaka, M. Kumei, *J. Chem. Soc., Chem. Commun.*, **1995**, 815.
b)R.D. McCullough, R.D. Lowe, *J. Chem. Soc., Chem. Commun.*, **1992**, 70.
c)T.A. Chen, R.D. Rieke, *J. Am. Chem. Soc.*, 114, **1992**, 10087.

[92] G. Zotti, G. Schiavon, A. Berlin, G. Fontana, G. Pagani, *Macromolecules*, 27, **1994**, 1938.

[93] T.M. Lambert, J.P. Ferraris, *J. Chem. Soc., Chem. Commun.*, **1991**, 752.

[94] T. Benincori, E. Brenna, F. Sannicolo, L. Trimarco, G. Moro, D. Pitea, T. Pilati, G. Zerbi, G. Zotti, *J. Chem. Soc., Chem. Commun.*, **1995**, 881.

This is a novel and useful technique, which has recently been implemented to design and tailor new products in various fields of chemistry. It enables chemists to examine the properties and predict the reactivities of compounds before embarking on the experimental work. Modeling methods have been used, among other applications, to: predict and refine complex crystal structures, calculate surface structures[95,96] and surface energies[97], study sorption and reaction pathways in catalysis[98], and to investigate the transport and defect properties of ionic solids[99,100]. These methods are also used[101] in the development of electronically conducting polymers especially in studying the highly unstable radical cations. Quantum mechanical calculations are used to map the location of the unpaired electron in the radical cation and this enables the prediction of how and where coupling will take place. In this way, a suitable monomer can be tuned by selecting substituents and observing their effect on the spin density distribution. Spin density distribution can then be fine tuned to yield maximum α-coupling and minimal branched coupling so that the highest possible degree of conjugation is achieved. All this can be done without any experimental work.

1.8.7 Applications of thiophene-based conducting polymers

As was mentioned earlier, these are varied and numerous and more possible applications are being reported all the time. Aside from their obvious usefulness in electronic conductors, a few main areas of application comprise:

---

[95] M.W. Deem, J. Newsam, *J. Am. Chem. Soc.*, 114, **1992**, 7189.
[96] M.D. Shannon, *Nature*, 353, **1991**, 417.
[97] W.C. Mackrodt, *Adv. Ceram.*, 23, **1987**, 293.
[98] C.R.A. Catlow, J.M. Thomas, *Phil. Trans. R. Soc. Lond. A.*, 341, **1992**, 255.
[99] M..J. Gillan, *Physica B*, 131, **1985**, 157.
[100] C.R.A. Catlow in *Defects in Solids*, A.V. Chadwick, M. Terenzi (Eds), NATO SI series B, vol. 47, New York Plenum Press, **1986**, 269.

I) Electronic transistors

Silicon transistors are fabricated by expensive processes, at high temperatures, in ultra-clean environments, and require the use of precision optics. Organic molecular transistors could be produced under cheaper, less rigorous conditions. Transistors made of organic molecules on a plastic substrate would be more durable and flexible and could be used in such applications as unbreakable computer screens.

Katz and co-workers[102] report that they have been developing laboratory synthesized transistors from thiophene hexamers such as dihexyl-α-hexathiophene. The hexyl groups enable the hexamer to be better aligned when deposited on the surface, thereby enhancing the performance of the semiconductor. These materials perform comparably well with transistors made under more expensive conditions such as vacuum evaporation.

II) Photoconductive materials and non-linear optics

Photochemical cells, photovoltaic devices and photochargeable devices have been developed using polythiophenes and are constantly being improved upon[46].

Photochromism is a reversible structural isomerism, which changes the colour and other properties of the compound and is of particular interest to researchers studying optical memory, switching and display media.

CP's, which display these properties, are considered useful as substitutes for metals because of their greater durability.

Upon doping, polythiophenes undergo a colour change, which makes them well suited to this type of application. Poly(3-alkylthiophenes) also undergo this type of change, but have increased solubility and, therefore, have better processibility than polythiophenes. Poly(thiophenalkanesulfonates) are self-doped, water-soluble CP's

---

[101] P Cox, *Chemistry in Britain*, March, 1997, 44.

and are, therefore, extremely well suited to optical applications[103]. Some examples of research conducted in this area follow.

Masahiro[104] discovered that some fluorinated diarylalkenes (such as dithienylperfluorocyclopentenes – see **Fig. 1.18**) have photochromic properties.

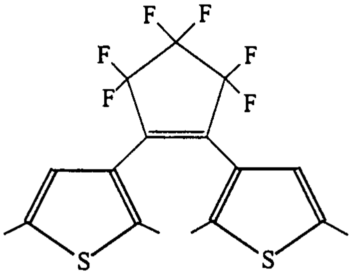

FIG. 1.18: Fluorinated dithienylalkene.

In the case of the dithienyl derivative, irradiation, by 313nm light, of the white crystal causes it to turn red. Irradiation with light in the visible region reverses the process.

Wu *et al.*[105] synthesized ruthenium σ-acetylides with an end-capping electron acceptor and a thienyl entity in the conjugation chain. They found that intense charge transfer occurred between the ruthenium donor and the organic acceptor, resulting in second order nonlinear optical properties (**Fig. 1.19**).

III) Chemosensors

Polythiophenes and other CP's can be applied as chemosensors - to detect specific molecules or classes of molecules. Swager[106] reports on a universal method of signal

---

[102] H.E. Katz, Z. Bao, J. Laquindanum, A. Dodabalapur, A.J. Lovinger, in *Chemical and Engineering News*, April, **1998**, 62.

[103] A.O. Patil, A. J. Heeger, F. Wudl, *Chem. Rev.*, 88, **1988**, 183.

[104] I. Masahiro, *Bull. Chem. Soc. Jpn.*, 75, **1998**, 985.

[105] I.Y. Wu, J.T. Lin, J. Luo, C.S. Li, C. Tsai, Y.S. Wen,C.C. Hsu, F.F.Yeh, S. Liou, *Organometallics*, 17, **1998**, 2188.

[106] T.M. Swager, *Acc. Chem. Res.*, 31, **1998**, 201.

amplification in molecular wires, which can be used as molecular chemosensors with enhanced sensitivity, and diversity of application.

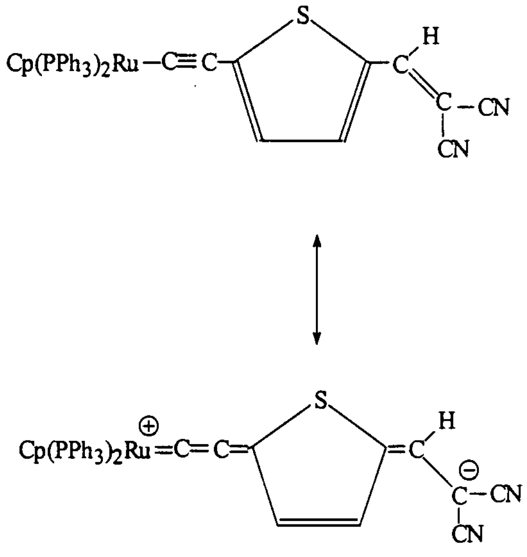

FIG. 1.19: "Push-pull" charge transfer process in ruthenium σ-acetylides.

An example of such application is the possible use of nucleobase-functionalized polythiophenes, first studied by Bauerle *et al.*[107], in handheld DNA testers. Wilson[108] reports them to be investigating more electroactive, water-soluble polythiophenes and plan to do experiments in the detection of up to 15 strands of DNA.

The development of self-assembling poly(3-substituted thiophenes) in water was reported by McCullough and co-workers[109]. These molecules display excellent chemoselective ionochromic sensing in addition to their ability to self assemble in water with almost 100% regioregularity. They, therefore, show excellent potential for use as conducting polymer sensors. Their high electrical conductivities and nonlinear optical properties can also be applied in other areas.

---

[107] P. Bauerle, A. Emge, A. Meyer, *Adv. Mat.*, 3 **1998**, 324.
[108] E.K. Wilson, *Chemical and Engineering News*, May, **1998**, 47.
[109] R.D. McCullough, P.C. Ewbank, R.S. Lowe, *J. Am. Chem. Soc.*, 119, **1997**, 633.

Polythiophenes are gas sensitive for example exposure to NO or NO_2 increases their conductivity while H_2S and NH_3 have the opposite effect[110,111]. Polythiophene-based gas detectors have been proposed, but their selectivity is poor[46].

1.9 Hydrodesulfurization of thiophene and its derivatives

Crude oil contains a variety of organo-sulfur compounds, which need to be removed before it can be used in the petroleum industry. Many of these are removed by passing high-pressure hydrogen gas over a heated heterogeneous catalyst. This is known as Hydrodesulfurization (HDS).

Residual sulfur compounds are present mainly in the form of thiophene and thienyl derivatives - predominantly benzothiophene and dibenzothiophene. These are particularly difficult to degrade and, as a result, many studies have been conducted into methods to improve the adsorption of such compounds onto the catalyst surface and then desulfurize it[112].

Thiophene undergoes HDS as shown in **Fig. 1.20**, through hydrogenolysis of the C-S bonds[12]. Subsequent reduction of the double bonds can follow. The alkylation of thiophene rings and the subsequent reduction by HDS has made the synthesis of many compounds possible[113]. Thiophene can also be desulfurized to yield alkenes of the type ($RCH_2CH{=}CHCH_2R'$) by employing a Nickel boride catalyst.

---

[110] K. Yoshino, H.S. Nalwa, J.G. Rabe, W.F. Schmidt, *Polym. Commun.*, 26, **1985**, 103.

[111] T. Hanawa, S. Kuwabata, H. Hoshimoto, H. Yoneyama, *Synth. Met.*, 30, **1989**, 173.

[112] C. Bianchini, J.A.Casares, M.V. Jimenez, A.Meli, S. Moneti, F. Vizza, V. Herrera, R. Sanchez-Delgado, *Organometallics*, 14, **1995**, 4850.

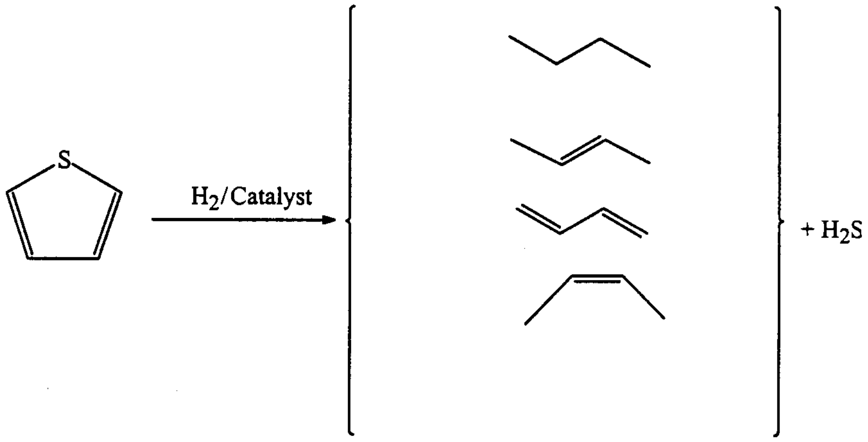

FIG. 1.20: Schematic representation of the HDS of thiophene.

Although the exact mechanisms of Raney nickel reactions are still under investigation, it is known that the reduction of thiophene occurs via the formation of butadiene and butene, rather than through 1-butanethiol or other sulfur compounds.

The sulfur is, therefore, removed first, before the double bonds are reduced[14]. Investigations into the mechanisms by which thiophene and its derivatives adsorb to the catalyst surface have been extensive and include molecular modeling and computational studies, which are often based on the study of a model molecule, such as thiophene, and its bonding to metal or metal sulfide crystals[114]. These led to the conclusion that thiophene is a very versatile molecule exhibiting many more modes of binding and reactions than anticipated. While these studies do not provide a definitive mechanism for thiophene HDS, they make several valuable postulates. It seems that thiophene coordinates to the metal surface through the sulfur atom in a number of ways[115]: I) as a formal two-electron donor (in the η^1(S) and η^2 modes where it occupies one site on the metal) which promotes reactions that may occur in

---

[113] J. March, *Advanced Organic Chemistry*, 4th Edition, John Wiley &Sons, New York, **1992**.
[114] M. Neurock, R.A. van Santen, *J. Am. Chem. Soc.* 116, **1994**, 4427.
[115] R.J. Angelici, *Bull. Chem. Soc. Belg.* 104, **1995**, 265.

HDS, but in which the thiophene is very weakly coordinated to the metal and easily removed by other reagents. II) η^4 coordination mode where it acts as a four-electron donor and occupies two coordination sites on the metal. The stability of this coordination depends upon the metal's need for four electrons. In this form, the ligand is very reactive - especially towards reactions which lead to the cleavage of the C-S bond, which can be useful in HDS. III) η^5 is the most common coordination for thiophene binding in organometallic complexes. Here it acts as a six-electron donor and formally occupies three coordination sites on the metal. The metal removes electron density from the ring, making it more susceptible to nucleophilic attack by a variety of reagents including metal hydrides. All four possibilities can occur on the catalysts for HDS. These generally appear to form the most stable complexes when the metal is in a low oxidation state (- two or less). η^4 and η^5 coordinations are reported to be the most reactive and mechanisms for HDS based on their reactivities have been proposed[116,117]. The other two are less well studied due to the weak coordination of the thiophene to the metal. Rauchfuss[12] mentions and discusses several methods for the HDS of thiophene:

(I) Heterogeneous catalysis using commercial catalysts such as molybdenum and cobalt in a 3:1 ratio on aluminium, or other catalysts such as metals in the platinum subgroup[118]. (II) The use of iron and the production of thiaferroles, $[S(C_4H_3)_2Fe_2(CO)_6]$, from the reaction of 2,2′-bithiophene and $[Fe_3(CO)_{12}]$ which in essence consitutes the replacement of the sulfur on the thiophene ring with a transition metal (Fe, in this case)[119,120]. (III) C-S cleavage through the use of $[(C_5Me_5)Rh]$ and $[(C_5Me_5)Ir]$ reagents. (IV) Cleavage of coordinated thiophenes by hydride-organic

---

[116] R.J. Angelici, *Acc.Chem. Res.*, 21, **1988**, 387.
[117] J. Chen, L.M. Daniels, R.J. Angelici, *J. Am. Chem. Soc.*, 113, **1991**, 2544.
[118] R.R. Chianelli, *Catal. Rev. Sci. Eng.*, 26, **1984**, 361.

nucleophiles such as [$LiAlH_4$] and [$NaBHEt_3$]. (V) Base-hydrolysis of thiophene complexes in dicationic thiophene sandwich complexes, such as [RhCp*(2,3,4,5-tetramethyl-thiophene)]$^{2+}$, and π-thiophenes, such as [Ru(2,3,4,5-tetramethylthiophene)$_2$]$^{2+}$. (VI) Thiophene desulfurization using nickel hydride reagents[121,122]. This is especially useful in the desulfurization of dibenzothiophenes. Caldwell and Land[123] studied the desulfurization of thiophene on a palladium surface and noted that this occurred via the scission of the C-S bond, the formation of a C_4H_x (X=4,5) and the hydrogenation and desorption of this intermediate to yield 1,3-butadiene. C-S bond cleavage results in the deposition of a film of sulfur on the electrode surface, which remains there even at elevated temperatures due to strong interactions between absorbed sulfur and palladium.

Bianchini *et al.*[124] proposed another method of C-S bond cleavage via the reaction of 2,2′-dithiophene with [Rh(triphos)H_3] (triphos = $MeC(CH_2PPh_2)_3$). This gave rise to butadienyl methyl sulfides for which a general synthetic method was lacking at the time.

The synthesis of organometallic complexes of thiophene and its derivatives has formed an integral part of the investigation into models of thiophene adsorption at metal sites on catalytic surfaces. Hence, studies such as the one documented here find application in this type of chemistry.

Benzothiophene (BT) and dibenzothiophene (DBT) are among the most difficult thiophene derivatives to hydrodesulfurize because they are very stable structures. It

---

[119] T.A. Manuel, *Inorg. Chem.*, 3, **1964**, 1795.
[120] G. LeBorgne, D. Grandjean, *Acta Cryst.*, B33, **1977**, 344.
[121] J.J. Eisch, L.E. Hallenbeck, K.I. Han, *J. Org. Chem.*, 48, **1983**, 2963.
[122] J.J. Eisch, L.E. Hallenbck, K.I. Han, *J. Am. Chem. Soc.*, 108, **1986**, 7763.
[123] T.E. Caldwell, D.P. Land, *Polyhedron*, 16, **1997**, 3197.
[124] C. Bianchini, M.V. Jimenez, A. Meli, F. Vizza, *Organometallics*, 14, **1995**, 4858.

was found[125,126] that DBT can be broken down to form a mixture of biphenyl and H_2S or hydrogenated to 2-phenylthiophenol. Both reactions can be performed under catalytic or stoichiometric conditions.

1.10 Aims of this Study

The publication by Maiorna and co-workers[41] in which they synthesized the mononuclear carbene, $[Cr\{C(X)C_4H_2S\text{-}C_4H_3S\}(CO)_5]$, X= OEt, pyrrolyl and a heteronuclear complex $[(CO)_5Cr\{C(OEt)C_4H_2S\text{-}C_4H_2SC(OEt)\}W(CO)_5]$ encouraged us to further investigate bithiophene chemistry - particularly bithiophene mono- and biscarbene complexes. We hoped to characterize the products more fully and investigate the role of their structure in electronic communication properties. Research in our laboratories has focused on the exploitation of thiophene and conjugated thiophene derivatives as spacer ligands in σ,π- and σ,σ-binuclear complexes for some years[127].

In this study, the main concern was the synthesis of both mono- and dinuclear, σ-bonded carbene complexes of the thiophene derivative, bithiophene, and the investigation of the properties of these compounds and their decomposition pathways. Metal carbonyls: $[Cr(CO)_6]$, $[W(CO)_6]$, and $[Mn(MeCp)(CO)_3]$ were employed to prepare the mono- and biscarbene complexes of bithiophene and subsequently these

---

[125] C. Bianchini, M.V. Jimenez, A. Meli, S. Monetti, F. Vizza, V. Herrera, R.A. Sanchez-Delgado, *Organometallics*, 14, **1995**, 2342.

[126] a) J.J. Garcia, B.E. Mann, H. Adams, N.A. Bailey, P.M. Maitlis, *J. Am. Chem. Soc.*, 115, **1993**, 12200.
b) J.J. Garcia, B.E. Mann, H. Adams, N.A. Bailey, P.M. Maitlis, *J. Am. Chem. Soc.*, 117, **1995**, 2179.

[127] a) T.A. Waldbach, P.H. Van Rooyen, S.Lotz, *Angew. Chem. Int. Ed. Engl.*, 32, **1993**, 710.
b) T.A. Waldbach, P.H. Van Rooyen, S. Lotz, *Organometallics*, 12, **1993**, 4250.
c) Y.M Terblans, H.M. Roos, S. Lotz, *J. Organomet. Chem.*, 566, **1998**, 133.
d) M. Landman, *unpublished work*, **2000**.
e) A. du Toit, M. Landman, S. Lotz, *J. Chem. Soc., Dalton Trans.*, **1997**, 2955.

and the relevant decomposition products were fully characterized. Possible decomposition pathways were proposed when possible.

As a means of comparison, we also aimed to synthesize and characterize the mono- and bisalkyl iron complexes of bithiophene in order to compare the carbene and alkyl complexes. [FeCp$(CO)_2$I] was used to synthesize the mono- and bisalkyl bithiophene complexes.

In addition, we aimed to investigate the effects of carbene and alkyl substituents on thiophene ring orientation, as this would have an influence on electronic communication over the rings.

2 CHROMIUM CARBENE COMPLEXES OF BITHIOPHENE

2.1 Introduction

2.1.1 Carbene complexes of arenes and heteroarenes

I) Monocarbene complexes

Fischer and Maasböl[1] first discovered carbenes and produced the first example of a carbene containing an aromatic group, $[W(CO)_5C(OMe)Ph]$. Mills and Redhouse[2] then published structural data on the carbenes: $[W(CO)_5C(OMe)Ph]$ and $[Cr(CO)_5C(OMe)Ph]$, from which the sp^2 nature of the carbene carbon was evident. Later studies[3] showed that the transition metal has a $d(t_{2g})$-p π-interaction with the carbene carbon and that the lone pair on the heteroatom (X) also plays an important role in the stabilization of the "singlet" carbene carbon through p_C-p_X π-bonding (**Fig. 2.1**).

Phenyl or heteroarene substituents on the carbene may act as electron-withdrawing or electron-donating substituents as they become incorporated into the delocalized π-system of the carbene carbon.

---

[1] E.O. Fischer, A. Maasböl, *Angew. Chem.*, 76, **1964**, 645.

[2] O.S. Mills, A.D. Redhouse, *J. Chem. Soc.A.*, **1968**, 642.

[3] a) E.O. Fischer, *Angew. Chem. Int. Ed. Engl.*, 13, **1974**, 651.
b) F.A. Cotton, C.M. Lukehart, *Prog. Inorg. Chem.*, 16, **1972**, 487.

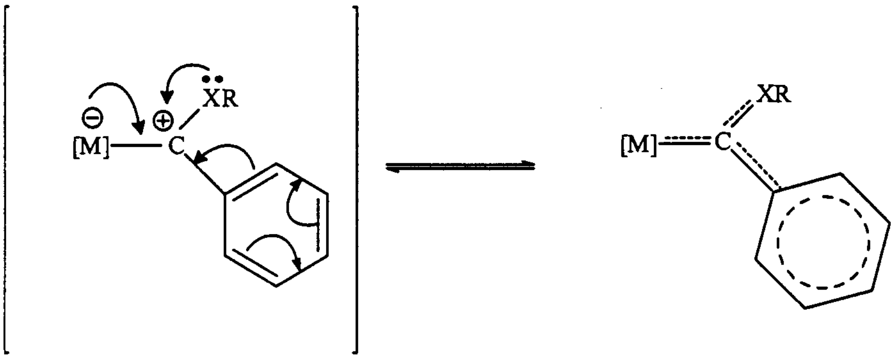

FIG. 2.1: **The role of the substituent in the stabilization of the carbene carbon.**

In complexes such as [W(CO)$_5$C(Ph)Ph], (synthesized from [W(CO)$_5$C(OEt)Ph])[4] the aromatic groups act as electron-donating groups, while, in such complexes as [MnCp(CO)$_2$C(OMe)Ph], [W(CO)$_5$C(OEt)Ph] and [Cr(CO)$_5$C(OEt)Ph], the carbonyl ligands have some electrophilic influence.

Fischer[5] experimented further and discovered that dinuclear metal carbene complexes, such as [Mn$_2$(CO)$_9$C(OEt)Ph], could also be formed. Although Fischer-type carbene complexes of iron are not readily accessible due to the preferred alkylation of the metal centre, rather than the oxygen[6], the iron carbene complex [Fe(CO)$_4$C(OEt)Ph] was synthesized by Cardin and co-workers[7]. Toerien *et al.*[8] added thiazolyl- and isothiazolyl-lithium to [FeCp(CO)$_2$Cl], followed by alkylation or protonation of all the products, this yielded iron carbene complexes of the type shown in **Fig. 2.2**.

In the thiazolylidene complexes, the N-atom is in a position typical for aminocarbene complexes (i.e. the α-position with respect to the coordinated carbene carbon). This

---

[4] C.P. Casey, *J. Am. Chem. Soc.*, 95, **1973**, 5833.

[5] E.O. Fischer, E. Offhaus, *Chem. Ber.*, 102, **1969**, 2549.

[6] a) M.F. Semmelhack, R. Tamar, *J. Am. Chem. Soc.*, 105, **1983**, 4099.
b) S. Lotz, J.L.M. Dillen, M.M. van Dyk, *J. Organomet. Chem.*, 371, **1989**, 371.

[7] D.J. Cardin, B. Cetinkaya, M.F. Lappert, *Chem. Rev.*, 72, **1972**, 545.

[8] J.G. Toerien, M. Desmet, G.J. Kruger, H.G. Raubenheimer, *J. Organomet. Chem.*, 479, **1994**, C12.

is not the case, however, for the isothiazolylidene complex, in which the nucleophilic heteroatom is situated γ to the carbene carbon.

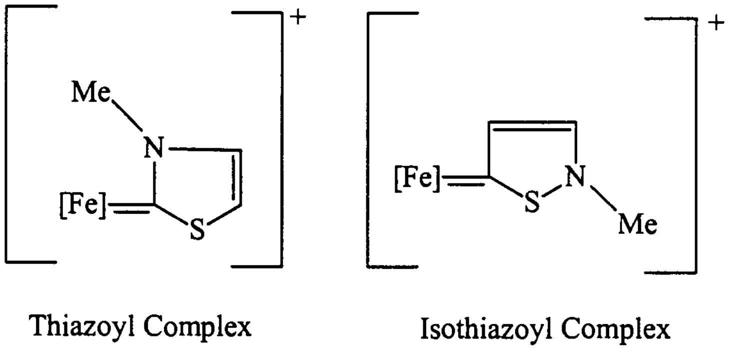

FIG. 2.2: Iron carbene complexes from thiazolyl and isothiazolyl ligands.

Heterocyclic carbenes from imidazolium and pyrazolium salts form very stable complexes with certain transition metals. Wanzlick[9] and Öfele[10] discovered this during their synthesis of the carbenes: pentacarbonyl(1,3-diphenylimidazoline-2-ylidene)chromium(0) and bis(1,3-diphenylimidazoline-2-ylidene)mercury-(II)diperchlorate. They were unable to isolate the free carbenes. Arduengo[11] discovered a way to produce isolable N-heterocyclic carbenes, in which the metal-carbon bond is more stable than in the Fischer- and Schrock carbenes. Angelici and co-workers[12] recently synthesized a cationic, 2-thienylidene carbene complex with rhenium as the metal. This complex forms by C-H bond activation in the S-thiophene complex.

---

[9] H.W. Wanzlick, H.J. Schonherr, *Angew. Chem. Int. Ed. Engl.*, 7, **1968**, 141.

[10] K. Öfele, *J. Organomet. Chem.*, 12, **1968**, 42.

[11] a) A.J. Arduengo, R.L. Harlow, M. Kline, *J. Am. Chem. Soc.*, 113, **1991**, 361.
b) A.J. Arduengo, F. Davidson, H.V.R. Dias, J.R. Goerlich, D. Khasnis, W.J. Marshall, T.K. Prakasha, *J. Am. Chem. Soc.*, 119, **1997**, 12742.

[12] M.J. Robertson, C.J. White, R.J. Angelici, *J. Am. Chem. Soc.*, 116, **1994**, 5190.

The intermediate [ReCp(NO)(PPh$_3$)(2-thienyl)] does not regenerate the S-thiophene complex upon reprotonation, but instead becomes protonated at the 3-position and forms the thienylidene carbene complex (**Fig. 2.3**).

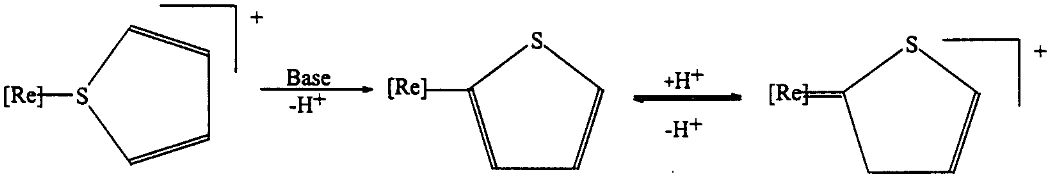

<u>FIG. 2.3</u>: Formation of a cationic thienylidene rhenium carbene complex. [Re] = [ReCp(NO)(PPh$_3$)].

Pentacarbonyl(dithienylcarbene) complexes have been produced by reacting pentacarbonyl(arylmethoxycarbene) complexes of tungsten and chromium with lithiated thiophenes and, subsequently, treating the intermediate addition product with silica gel/pentane. The reactions were reported to proceed with ease at low temperatures and the resulting products were reported to be partially thermally labile and diamagnetic[13].

Chromium monocarbene complexes of the type [Cr(CO)$_5$C(OR)R'] where R'= 2-thienyl or 2-furyl were synthesized by Connor *et al.*[14] in order to compare the influences of the different R-groups on the stability of the empty p$_z$-orbital of the carbene carbon.

Maiorana and co-workers[15] did some preliminary work on the synthesis of monocarbene complexes of bithiophene, in order to establish the effects of a "push-

---

[13] E.O. Fischer, W. Held, F.R. Krieβl, A. Frank, G. Huttner, *Chem. Ber.*, **1977**, 110, 655.

[14] J.A. Connor, E.M. Jones, *J. Chem. Soc. A.*, **1971**, 1974.

[15] S. Maiorana, A. Papagni, E. Licandro, A. Persoons, K. Clay, S. Houbrechts, W. Porzio, *Gazz. Chim. Ital.*, 479, **1994**, C12.

pull" electronic system set up along the carbene, by placing transition metals with multiple electron-withdrawing carbonyl groups on one side of a thiophene ring and using the other thiophene ring as an electron donor. Aside from some rudimentary spectra and a superficial evaluation of the non-linear optical properties of the materials, as far as we are aware, the work was not followed up until now.

II) Biscarbene complexes

The first dinuclear biscarbene complexes were also synthesized by Fischer in 1982[16]. These were prepared from dilithiated *o*- and *p*-phenylene, which were reacted with metal carbonyl complexes of tungsten, chromium and molybdenum, to yield phenylene biscarbene complexes.

Dinuclear chromium and tungsten biscarbene complexes of biphenylene were later produced by Hoa Tran Huy *et al.*[17]. They conducted an X-ray diffraction study of the chromium complex and found that the molecule was centrosymmetric and that the rings were strictly coplanar as opposed to the twisted conformation of the rings in free biphenylene[18] (**Fig. 2.4**).

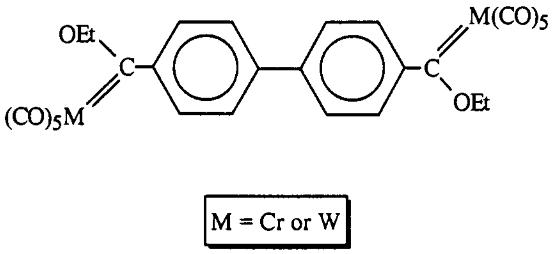

FIG. 2.4: Biphenylene dinulcear biscarbene complexes.

---

[16] E.O. Fischer, W. Roll, N. Hoa Tran Huy, K. Ackermann, *Chem. Ber.*, 115, **1982**, 2951.
[17] N. Hoa Tran Huy, P. Lefloch, F. Robert, Y. Jeannin, J. Organomet. Chem., 327, **1987**, 211.
[18] G. Charbonneau, Y. Delugeard, *Acta Cryst. B*, 33, **1977**, 1586.

Terblans *et al.*[19] recently synthesized the dinuclear carbenes of tungsten, and chromium using thiophene as the bridging ligand (**Fig. 2.5**).

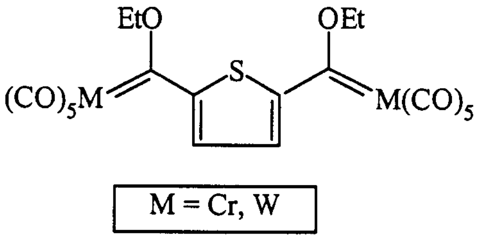

FIG. 2.5: Carbene complexes with thiophene as the bridging ligand.

It was hoped that by refluxing these products in carbon disulphide, hexane and acetone, a product could be isolated in which the thiophene bridging ligands would be coupled, resulting in an extended spacer between the two metal centres. No evidence of such coupling was found, but the corresponding *o*-ethylthienyl carboxalate monocarbene and the *o*-ethylthienyl thiocarboxylate monocarbene complexes were isolated.

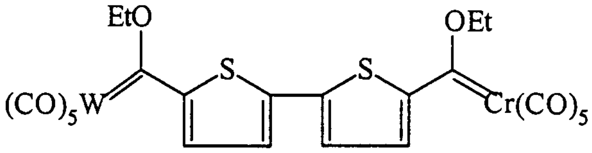

FIG. 2.6: Heteronuclear biscarbene complex of bithienylene[15].

The usefulness of thiophenes in non-linear optical and electronic applications has lead to the investigation into the use of longer spacer groups between metal centres. As a result, focus has turned to bithiophene. Marianno and co-workers[15] synthesized the

---

[19] Y. M. Terblans, H.M. Roos, S. Lotz, *J. Organomet. Chem.*, 566, **1998**, 133.

first mixed metal biscarbene complex of bithiophene, but were unable to purify it as the chosen method of synthesis proved inefficient (**Fig. 2.6**).

Section A: Chromium bithiophene complexes

2.2 Synthesis of chromium bithiophene biscarbene complexes

In this study, we investigated further the work started by Mariano *et al.*[15] and examined the structures and, where possible, the decomposition mechanisms of bithiophene complexes more closely.

Terblans *et al.*[19] reported that they were unable to dilithiate thiophene in tetrahydrofuran (THF) and had to use hexane as the solvent of choice for the production of dilithiated thiophene. Furthermore, they found that, while the first proton is readily removed, the second could only be abstracted sufficiently quickly at elevated temperatures. Maiorana[15] also used hexane to produce dilithiated bithiophene. Our experiences with bithiophene differed from this, as we were able to successfully dilithiate bithiophene in THF at very low temperatures (-50 °C). This could be explained by increased stabilization of the negative charge over the two rings relative to that over one ring, resulting in the abstraction of the second proton being more difficult in the case of thiophene.

The monocarbene and biscarbene chromium complexes of bithiophene were synthesized via the classical Fischer method, using THF as the solvent. The butyllithium: TMEDA complex was able to abstract both the 5- and 5'-protons from the bithiophene rings when two equivalents of the base were reacted with one equivalent of bithiophene. Both protons were removed at low temperatures. The metal carbonyl was added, at which point nucleophilic attack by the dianion of the bithienylene occurs at the carbonyl carbons of two metal carbonyls to form the dilithium diacylmetallated product. The lithium salt is quenched with $Et_3O^+BF_4^-$ to afford the desired dinuclear biscarbene complex. In addition to the biscarbene complex, the monocarbene complex and two other compounds were produced. **Fig. 2.7** shows the reaction scheme.

The red monocarbene complex, **1**, was characterized by ^1H and ^{13}C NMR spectroscopies, as well as infrared spectroscopy and mass spectrometry. The purple biscarbene complex, **2**, was also isolated and characterized by spectrosopic methods. The product, **3**, was isolated and characterized spectroscopically. It appears to have resulted from the decomposition of the biscarbene, in which one metal fragment is lost by attack from oxygen. The structure of this product is based on spectroscopic data. In addition, spectroscopic evidence was found for the formation of a bisester compound, **4**, indicating that **3** also reacts with oxygen in a similar manner to **2**. This was not observed for the dinuclear biscarbene complex of thiophene, and must be ascribed to the influence of a second thienyl ring in bithiophene.

A proposed mechanism for the decomposition of the dinuclear biscarbene complex is shown in **Fig. 2.8**. The biscarbene complex decomposes to yield ester functionalities on the bithiophene. This can be ascribed to the features of the bithiophene substituent. The carbene moieties are very reactive and, therefore, react with trace amounts of oxygen to yield the ester. The mechanism for this reaction is based on a peroxy metallacyclic intermediate analogous to the cyclometallabutane intermediate (see **Fig. 1.4**) of the mechanism accepted for alkene metathesis.

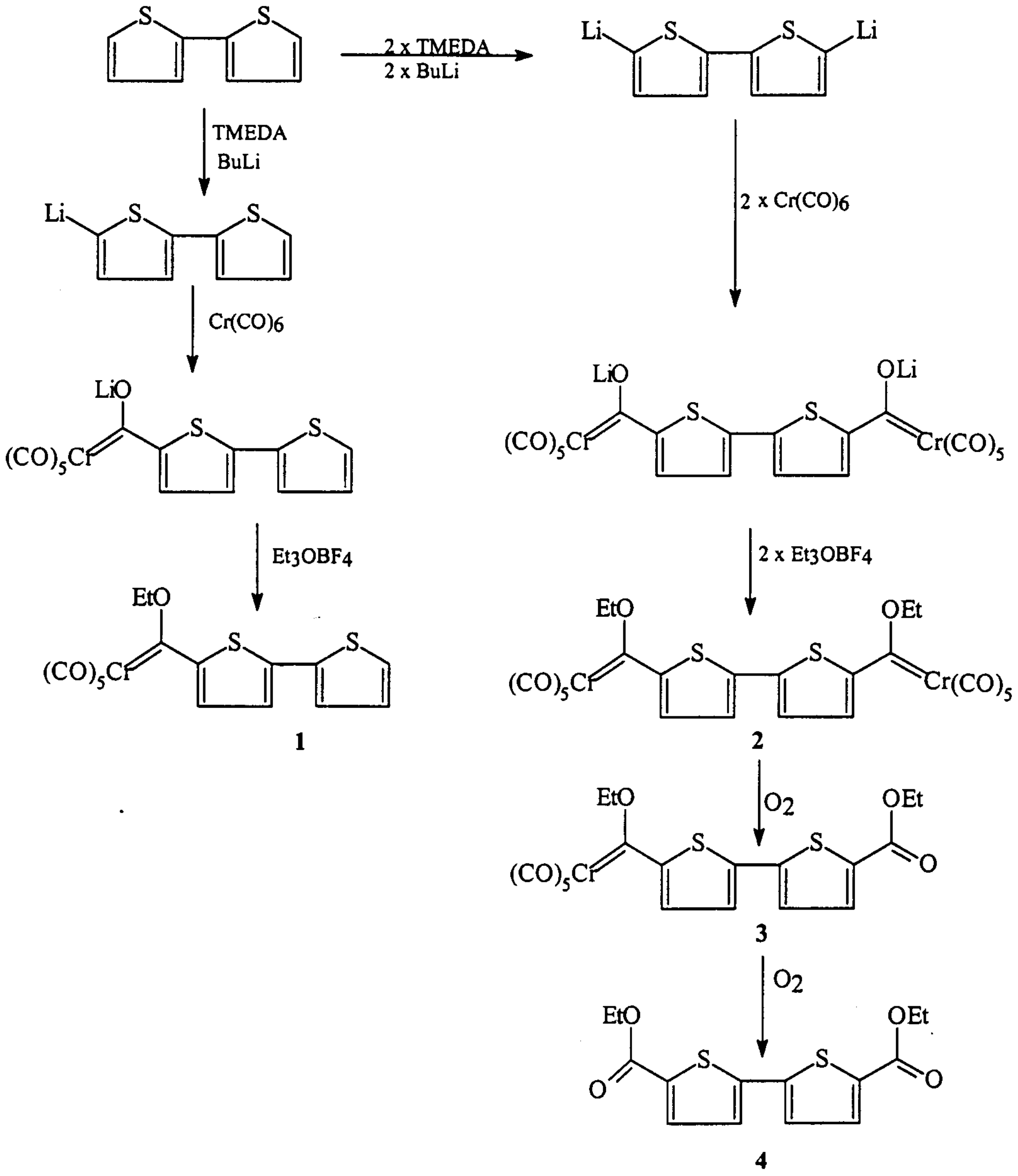

FIG. 2.7: The reaction scheme for the production of complexes 1-4.

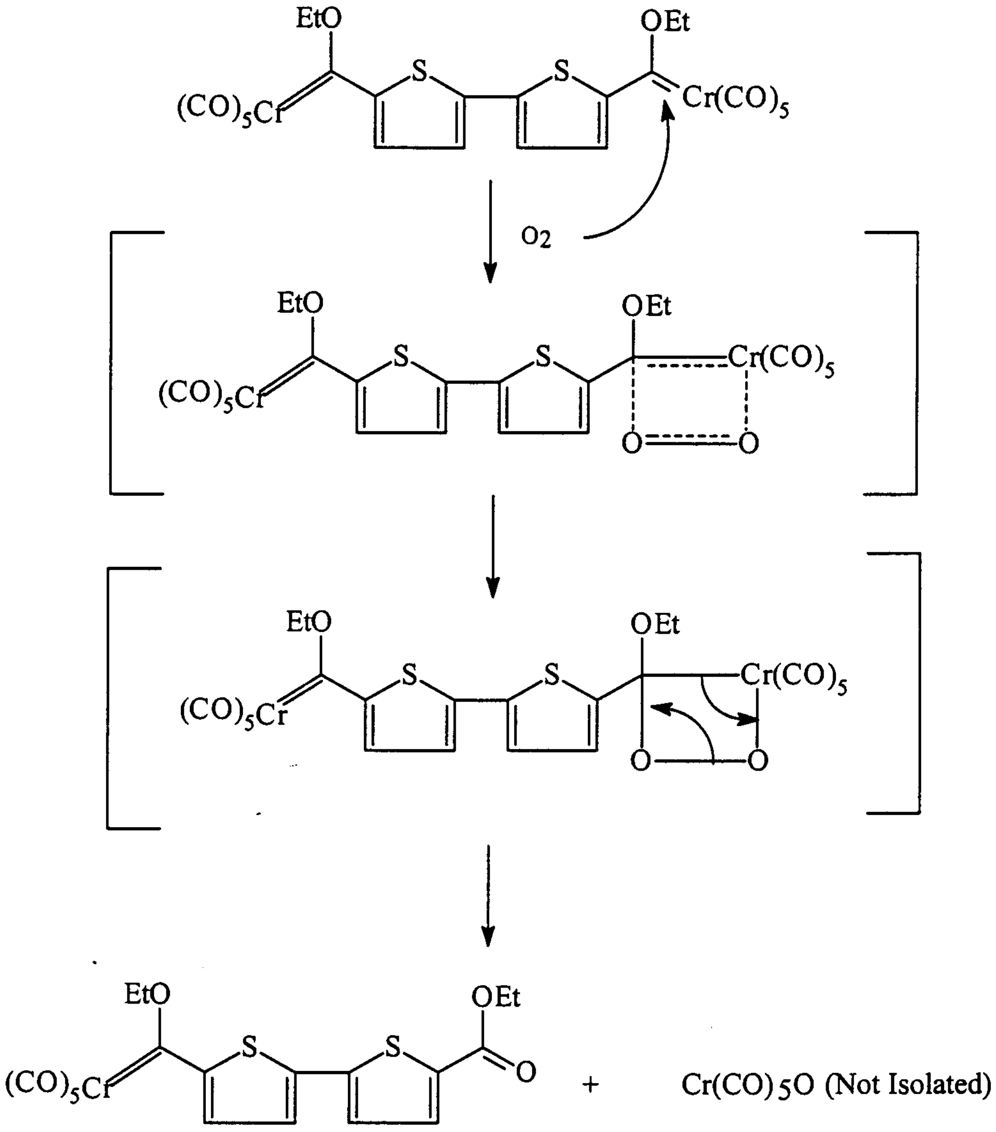

3

FIG. 2.8: **Mechanisms of the reaction of the biscarbene complex with oxygen.**

2.3 Spectroscopic characterization of chromium bithiophene carbene complexes.

Fig.2.9 shows the labeling system used for the discussion of spectroscopic data.

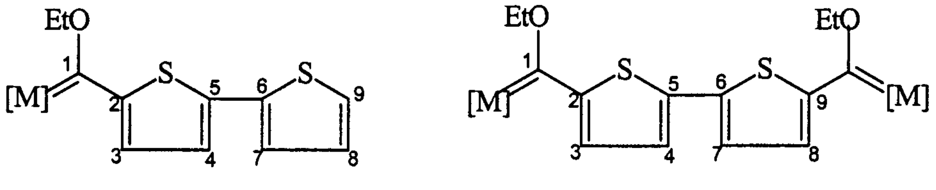

Monocarbene

Biscarbene

[M] = $Cr(CO)_5$ or $W(CO)_5$ or $Mn(CO)_2CpMe$

FIG. 2.9: Labeling system used in the discussion of spectroscopic data.

2.3.1 ^{1}H NMR spectroscopy

All NMR spectra were recorded in deuterated chloroform as a solvent. The ^{1}H NMR data are represented in **Table 2.1**.

Table 2.1: ^{1}H NMR data for 1, 2, 3 and 4.

Proton	**Chemical Shifts (δ, ppm) and Coupling Constants (J, Hz)**							
	1		**2**		**3**		**4**	
	δ	**J**	**δ**	**J**	**δ**	**J**	**δ**	**J**
H_3	8.16(d)	4.3	8.16(d)	4.2	8.23(d)	5.8	7.69(dd)	3.8
H_4	7.29(d)	4.3	7.45(d)	4.3	7.45(d)	5.8	7.51(dd)	3.2
H_7	7.36(d)	5.3	7.45(d)	4.2	7.41(d)	5.8	7.51(dd)	3.2
H_8	7.06(dd)	5.3, 2.9	8.16(d)	4.2	7.80(d)	5.8	7.69(d)	3.8
H_9	7.39(d)	2.9	-	-	-	-	-	-
$O\mathbf{CH_2}CH_3$-M	5.14(q)	7.0	5.17(q)	7.1	5.17(q)	6.8	-	-
$O\mathbf{CH_2}CH_3$-O	-	-	-	-	4.34(q)	7.0	4.34(q)	7.1
$OCH_2\mathbf{CH_3}$-M	1.66(t)	7.0	1.68(t)	7.0	1.67(t)	7.3	-	-
$OCH_2\mathbf{CH_3}$-O	-	-	-	-	1.35(t)	8.0	1.37(t)	7.1

The data support the proposed molecular structures of the complexes. Instrumental limitations in the past led to poor ^{1}H NMR characterization of bithiophene. In 1956 Wynberg[20] reported that the spectrum contained three signals: 7.20 ppm (t, J = 3.6 Hz), 7.02 ppm (d, J = 3.9 Hz) and 7.01 ppm (d, J = 3.6), but made no attempt to assign these signals any further. In 1983, Kagan[21] reported a multiplet at 7.0 - 7.25 ppm, but he also did not attempt any further assignment of signals. We therefore analysed free bithiophene using improved ^{1}H NMR techniques and were able to make the following assignments: the signal for **H_3** (and the equivalent **H_8**) can be found at 7.01 ppm (dd, J_3 = 3.7 Hz). **H_2** is equivalent to **H_9** and the signal for these protons appears at 7.20 ppm (d, J_3 = 5.2 Hz). **H_4** is equivalent to **H_7** and the signal for these protons appears at 7.18 ppm (d, J_3 = 5.2 Hz). Due to the greater resolution achievable with modern techniques, it is also possible to see that the peaks in both doublets are split further. This can be ascribed to long-range (4-bond) coupling. At 7.21 ppm (d, J_4 = 0.8 Hz) and 7.20 ppm (d, J_4 = 1.1 Hz) signals arise due to **H_2-H_4** coupling. Signals at 7.19 ppm (d, J_4 = 1.0 Hz) and 7.18 ppm (d, J_4 = 1.05 Hz) indicate **H_4-H_2** coupling.

The influence of bonding to the metal fragment and the presence of the electrophilic carbene carbon linker on the chemical shifts of the protons in complexes **1**, **2** and **3** is obvious when comparing the values for free bithiophene with those in **Table 2.1**. The carbene moiety is electrophilic and causes draining of electron density from the double bonds in the rings. As a result, the protons in the complexes are shifted downfield with respect to those of the uncoordinated ligand.

---

[20] H. Wynberg, A.J. Logothesis, *J. Am. Chem. Soc.*, 78, **1956**, 1958.
[21] J. Kagan, S.K. Arora, *Tetrahedron Lett.*, 24, **1983**, 4043.

The coordination shift, $\Delta\delta$, is defined as the difference in chemical shift between the chemical shift of the metal bonded unit and the free ligand[22], such that:

$$\Delta\delta = \delta(\text{complex}) - \delta(\text{ligand})$$

Metal bonded protons are generally regarded as hydridic and experience particularily strong shielding. As a result, they have very large $\Delta\delta$ values. Proton shielding increases with increased metal atomic number (for metals in the same group). Protons attached to metal-bonded carbon atoms display a much smaller span of chemical shifts for $\Delta\delta$[22].

In **1**, the signals for **H_3** and **H_9** occur further downfield than that for **H_4** due to the effects of the π- resonance between the two structures - shown in **Fig. 2.10**.

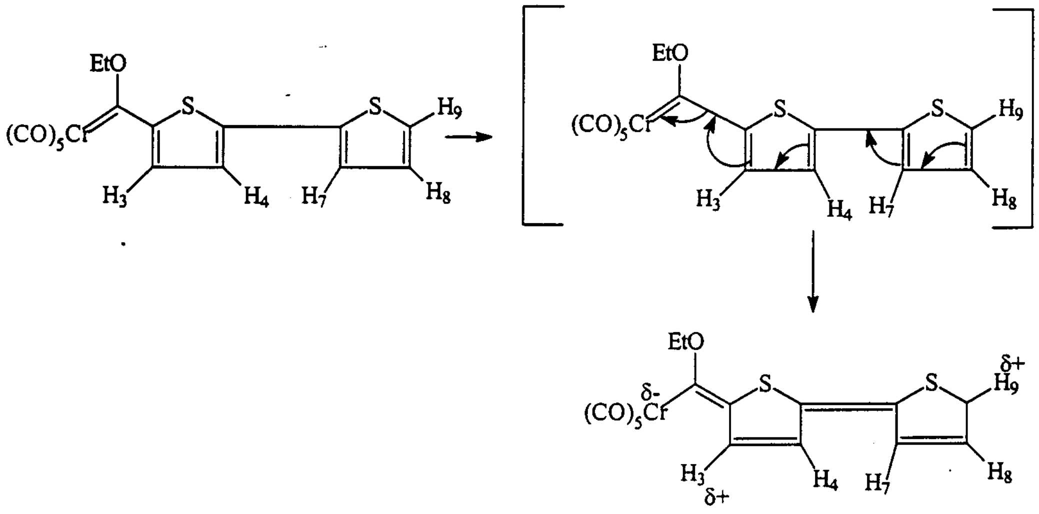

FIG. 2.10: The proposed electron drainage from the bithiophene rings in 1.

It is clear from the diagram that protons **H_4**, **H_7** and **H_8** are less affected by the delocalization, while protons **H_3** and **H_9** become less shielded. This deshielding of protons **H_3** and **H_9** causes the shift downfield. **H_3** will shift further downfield than **H_9**

---

[22] Ch. Elschenbroich, A. Salzer, *Organometallics, A Concise Introduction*, VCH Publishers Inc. New York, 2nd Edition, 1992.

as it is much closer to the electrophilic carbene carbon. The downfield shift in the case of **H_9** is only marginal as it is quite far away from the carbene. There is a doublet of doublets at 7.06 ppm, which arises due to **H_8** coupling with **H_7** and **H_9**. The assignment of peaks was not based only on chemical shifts, but also by considering the coupling constants. In the case of the doublet of doublets for proton **H_8**, the coupling constants for coupling with **H_7** and with **H_9** are given.

In **2**, all the protons (except **H_3**) are shifted downfield from the values for **1**. This is because there are now two carbene ligands involved in the resonance system and, therefore, each proton can be regarded as having a slight positive charge due to draining of electron density from the rings and the resulting deshielding of the protons by the two electrophilic carbene groups. This is shown in **Fig. 2.11**. Interestingly, **H_3** has the same chemical shift in both the mono- and biscarbene complexes, which could suggest that very little electron density of the unattached thiophene ring in **1** is transferred to the ring closest to the electrophilic carbene carbon. The resonances of other protons in the distant ring, as well as the chemical shifts of the protons in uncoordinated bithiophene, however, do not support this explanation. One should also remember that both the ethoxy and the metal fragment will stabilize the carbene carbon and that these effects (which greatly affect C_3) will probably be different for carbene carbons in the mono- and the biscarbene complexes.

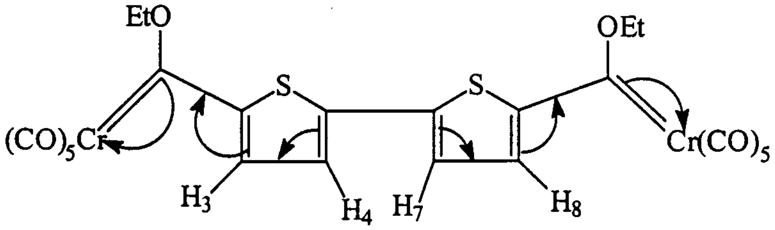

FIG. 2.11: Competitive shifting of electron density from the bithiophene rings by the biscarbene units.

In the case of **3**, both the ester and the carbene carbon have electron-withdrawing and, hence, deshielding capabilities. The protons nearest the carbene are found further downfield from those nearest the ester, indicating that the carbene group has stronger electron-withdrawing properties than the ester group. Thus, $\mathbf{H_3}$ is found further downfield than $\mathbf{H_8}$. Correspondingly, we assigned $\mathbf{H_4}$ downfield from $\mathbf{H_7}$.

A quartet at around 4.34 ppm and a triplet at around 1.35 ppm appear in the spectra of **3** and **4**, which are not present in the spectra of **1** and **2**. These indicate the presence of the ester functionalities. In both cases, metal fragments of the carbene ligands have been replaced by oxygen to yield ester groups. In **3** only one metal fragment is lost, while in **4** both are lost.

The spectrum of **4** also shows the protons having shifted downfield relative to the chemical shifts of free bithiophene. This is because of the electron-withdrawing properties of the two ester groups. The fact that the downfield shift is less for this compound than for the biscarbene complexes of bithiophene can be ascribed to the weaker electron-withdrawing properties of the ester group compared with the carbene moiety.

In **4** the signals for the ethoxy groups attached to the carbene disappear completely due to the formation of esters on both sides of the ligand and the loss of the carbene substituents. A doublet of doublets is observed for each of the two types of ring protons of **4** because of the presence of two isomers of the bisester. Sulfur atoms in the rings are *cis* and *trans* to each other due to restricted rotation around the bond joining the two thiophene rings, resulting in these rotational isomers. There are, therefore, two types of molecules present in solution, each with different chemical environments for the protons concerned and thus two signals.

The protons in the methylene regions of **1**, **2** and **3** show similar chemical shifts for the **CH_2** protons in the carbene ethoxy substituent, which follows logic since **3** is derived from **2**. By contrast the methylene portions of the terminal ester ethoxy group is shifted upfield from the resonances by about 0.8 ppm.

2.3.2 ^{13}C NMR spectroscopy

The ^{13}C NMR data for complexes **1**, **2** and **3** and **4** are shown in **Table 2.2**.

Table 2.2: ^{13}C NMR data for 1, 2, 3 and 4.

Carbon	**Chemical Shifts (δ, ppm)**			
	1	**2**	**3**	**4**
Carbene	312.1	314.3	313.7	-
C_2	166.5	154.3	159.1	151.6
C_3	145.5	144.3	142.1	132.3
C_4	125.2	127.1	128.3	129.3
C_5, C_6[a]	147.3, 142.8	141.8	128.5, 127.4	133.9
C_7	127.5	127.1	128.1	129.3
C_8	128.4	144.3	134.1	132.3
C_9	126.3	154.3	150.0	151.6
OCH_2CH_3-M	75.7	76.5	75.9	-
OCH_2CH_3-O	-	-	61.5	53.4
OCH_2CH_3-M	15.2	15.2	15.2	-
OCH_2CH_3-O	-	-	14.3	14.1
(O)COEt	-	-	176.1	178.9
$M(CO)_5$	223.3(*trans*) 217.2(*cis*)	223.3(*trans*) 216.9(*cis*)	223.8(*trans*) 217.0(*cis*)	- -

[a] Cannot discriminate between resonances of **C_5** and **C_6**.

There is a large variation observed in the chemical shifts of carbene carbons, which is related to the metal and to the other carbene substituents. These chemical shifts range from 200 ppm for aminocarbene complexes[23] to 400 ppm for certain silicone complexes[24]. The metal plays an important role in the chemical shift of the carbene carbon via interaction of the metal d-orbitals with the p_z-orbital of the carbene carbon.

---

[23] B.A. Anderson, W.D. Wulff, A. Rahm, *J. Am. Chem. Soc.*, 115, **1993**, 4602.
[24] E.O. Fischer, T. Selmay, F.R. Kreissl, U. Schubert, *Chem. Ber.*, 110, **1977**, 574.

Carbene carbons in metal complexes can be said to have a significant positive charge due to deshielding of the carbenium carbon on bonding.

For complexes of chromium and tungsten, $[M(CO)_5\{C(OEt)\}R]$, the chemical shifts of carbene carbons, as a function of R, decreases as follows: R = Me > Ph > 1-ferrocenyl > 2-thienyl > 2-furyl[14]. This decrease follows the trend of the lowering of donor properties among these R groups.

The ^{13}C NMR data for free bithiophene is given by Crisp[25] as δ 123.6, 124.2, 127.7 and 137.3. Comparing these values with those in **Table 2.2**, it is clear that the presence of the carbene and/or ester groups has a marked effect on the chemical environment of the carbon atoms by deshielding them and causing a downfield shift in the signals.

Comparison of the chemical shifts for the carbene moieties of **1**, **2** and **3**, shows that the signals for the carbene carbons are practically the same.

Typically, the terminal metal-carbonyl carbons have chemical shifts of between 150 ppm and 240 ppm[22]. Shielding of the carbonyl group increases, within a metal group, with increasing atomic number, thus for $Cr(CO)_6$, $Mo(CO)_6$, and $W(CO)_6$, the chemical shifts are 212 ppm, 202 ppm and 192 ppm respectively. In the spectra of carbene complexes, the carbonyl moiety is represented by two signals, which denote the *cis*- and *trans*-conformations of the carbonyl ligands. Metal carbonyls appear to be little affected by changes in the substituents on the carbene carbon.

Quaternary carbons, **C_5** and **C_6**, could not be assigned individually as there is no reliable way of deciding which would appear furthest downfield.

---

[25] G.T. Crisp, *Synth. Commun.*, 19, **1989**, 307.

2.3.3 Infrared spectroscopy

Unlike M-C stretching frequencies, C-O stretching vibrational frequencies can be viewed as independent of other vibrations in the molecule. The ν_{CO} vibrational bands, arising from the carbonyl ligands, appear at lower energies than those of the corresponding precursor metal carbonyl complexes. The weaker π-acceptor properties of the carbene ligand, compared to the carbonyl group, are evident from this.

Three absorption bands appear in the Infrared spectra of pentacarbonyl metal carbene complexes namely: two A_1 and one E band. One A_1 band is infrared inactive, but obtains intensity as a result of the coupling to the other, infrared active, A_1 vibration. This is as expected of C_{4v} symmetry. The presence of bulky substituents on the carbene carbon can cause the E band to split and the formally IR-forbidden, B band appears. This is a result of the distortion of the equatorial plane of carbonyls[26].

In dichloromethane as a solvent, the infrared active $A_1^{(2)}$ and E bands are found to be overlapping. Hexane is, therefore, the solvent of choice in order to have both bands visible, but due to solubility constraints dichloromethane was used for **1** and **2**, while **3** and **4** were measured in hexane. The $A_1^{(2)}$ band is generally observed as a shoulder on the higher wavenumber side of the E band.

The Infrared data for **1**, **2**, **3** and **4** are summarized in **Table 2.3**.

Table 2.3: Infrared data for 1, 2, 3 and 4^a.

Band	**Stretching Vibrational Frequency, ν_{CO}, cm^{-1}**		
	1	**2**	**3**
$A_1^{(1)}$	2056(m)	2054(m)	2057(m)
B	1982(w)	1982(w)	1983(w)
$A_1^{(2)}$	1945	1943	1957(m)
E	1945	1943	1948(vs)

$^a\nu_{CO}$ for the carbonyl of **4** is found at 1721 cm^{-1}.

Fig. 2.12 shows the IR spectrum of **3**. The $A_1^{(2)}$ and B bands are clearly visible.

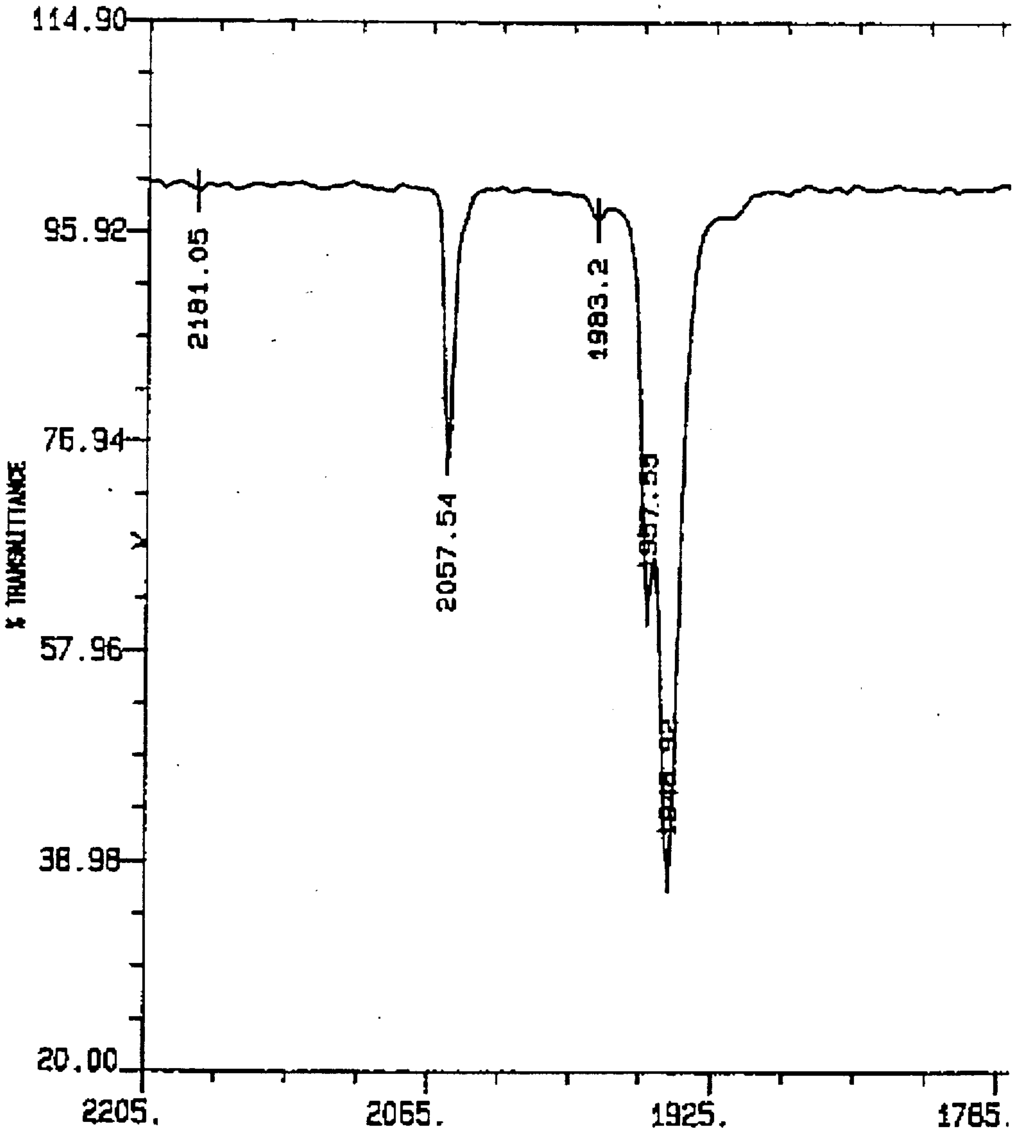

FIG. 2.12: **The Infrared spectrum of 3.**

---

[26] P.S. Bratermann, *Metal Carbonyl Spectra*, Academic Press, London, 1975.

2.3.4 Mass spectrometry

Fragmentation data of **1**, **2**, **3** and **4** are summarized in **Table 2.4**. The spectra of **1** and **3** display a molecular ion peak, M^+, and a general fragmentation pattern in which the carbonyls are lost initially, followed by the loss of the COEt fragment. For **4**, the M^+ peak still appears, but the fragmetation pattern begins with the loss of an OEt fragment, rather than a carbonyl. For **2**, the M^+, M^+**-CO** and M^+**-2CO** peaks were not observed. These are seldom observed for dinuclear biscarbene complexes of thiophene and its derivatives[27]. The fragment ion of highest *m/z* value, which could be assigned, corresponded to M^+**-3CO**.

Table 2.4: Fragmentation data for 1, 2, 3 and 4.

Fragment	1		2		3		4	
	m/z	I/%	*m/z*	I/%	*m/z*	I/%	*m/z*	I/%
M^+	414.3	7.8	n.o.†	n.o.	485.9	4.7	310.1	100.0
M^+-OEt	-	-	-	-	-	-	265.0	44.9
M^+-CO	386.3	10.5	n.o.	n.o.	457.9	5.7	237.0	41.8
M^+-2OEt	-	-	-	-	-	-	193.0	8.2
M^+-2CO	358.2	9.0	n.o.	n.o.	429.9	4.1	165.0	19.5
M^+-3CO	330.2	10.2	577.6	6.8	401.9	4.0	-	-
M^+-4CO	302.2	25.7	549.6	1.3	373.9	23.5	-	-
$N^+ = M^+$-5CO	274.1	100.0	521.5	0.3	346.0	87.4	-	-
N^+-COEt	217.1	50.7	464.4	0.4	288.9	26.9	-	-
N^+-OCOEt	-	-	-	-	216.9	10.2	-	-

† n.o. = not observed.

---

[27] S. Lotz, *Personal Communication*, **2000**.

Section B: A novel organic by-product of the reaction

2.4 Formation and characterization of 5

2.4.1 Possible reaction mechanisms for the formation of 5

An unexpected product, **5**, was found after crystallizing a mixture containing **1**. The nature of **5** calls for some speculation about its origin. This is merely speculative as no experimental evidence for the formation of the product was gathered. Four reaction routes are given in **Fig. 2.13a** - **Fig. 2.13c**, representative of different stages during the reaction. It cannot be ruled out that **5** was already present in the mixture used to crystallize **1**.

The first mechanism assumes that the formation of **5** occurred prior to alkylation. **Fig. 2.13a** shows the mechanism of formation via the coupling of two acylate units. The second proposal is shown in **Fig. 2.13b** and assumes the formation of **5** takes place during alkylation via the coupling of an acylate unit with a monocarbene unit and the third (**Fig. 2.13c(ii)**) assumes **5** arises from the coupling of monocarbene complexes, **1**.

The first two mechanisms are based on the widely accepted coupling of two metal-carbon double bonds to form a four-membered ring. This step is necessary to couple the two bithienyl units. More problematic is to obtain two adjacent carbonyl groups in the final product. In the first proposed mechanism, this is achieved by opening the ring towards the chromium atoms and by retaining the carbon-carbon bond. The formation of the reduced dichromium monocarbonyl dianion with **5** is acceptable. **Fig. 2.13b** shows the second proposed mechanism, repeating the procedure in the first proposed mechanism, but now with one acylate and one carbene complex. The metal acylate is opened asymmetrically at the acylate with the generation of a new carbene complex after the elimination of the ethoxy group at the carbene site. The final step of the mechanism requires oxygen and has been established in similar systems. The intermolecular carbon-carbon coupling reaction involving acylates is without president in literature. By contrast, it is well known that two carbene ligands couple intermolecularily to afford the bisalkoxy ethane product, as carbene-carbene coupling has been used extensively in carbon-carbon bond formation reactions[28]. The mechanism is anticipated to be via a four-membered ring intermediate as used in the first two proposals. This also emphasizes the dilemma of having oxy instead of alkoxy substituents in the final product.

Ways of generating carbonyl units are shown in **Fig. 2.13c**. In **(i)**, the metallate favours the charge on the metal, which facilitates a carbonyl insertion reaction. Attack of a second lithiated bithienyl on the bonded carbonyl with the elimination of the metal fragment affords **5**. In **(ii)**, the reverse reaction of the well-known metal (instead of the oxygen) alkylation reaction is suggested. This implies that the ethyl of the ethoxy substituent migrates to the metal. Dialkyl complexes of this type are very reactive and various possibilities for both inter- and intra-molecular reductive coupling reactions exist. **5** represents one of three possible organic products.

---

[28] a) K.H. Dötz, *Angew. Chem. Int. Ed. Engl.*, 23, **1984**, 587.
b) S.T. Nguyen, L.K. Johnson, R.H. Grubbs, *J. Am. Chem. Soc.*, 114, **1992**, 3974.
c) E.O. Fischer, B. Heckl, K.H. Dötz, J. Müller, H. Werner, *J. Organomet. Chem.*, 16, **1969**, P29.
d) E.O. Fischer, D. Plabst, *Chem. Ber.*, 107, **1974**, 3326.
e) C.P. Casey, R.L. Anderson, *J. Chem. Soc. Chem. Commun.*, **1975**, 895.
f) E.O. Fischer, A. Maasböl, *J. Organomet. Chem.*, 12, **1968**, P15.
g) M. Brookhart, G.O. Nelson, *J. Am. Chem. Soc.*, 99, **1977**, 6099.

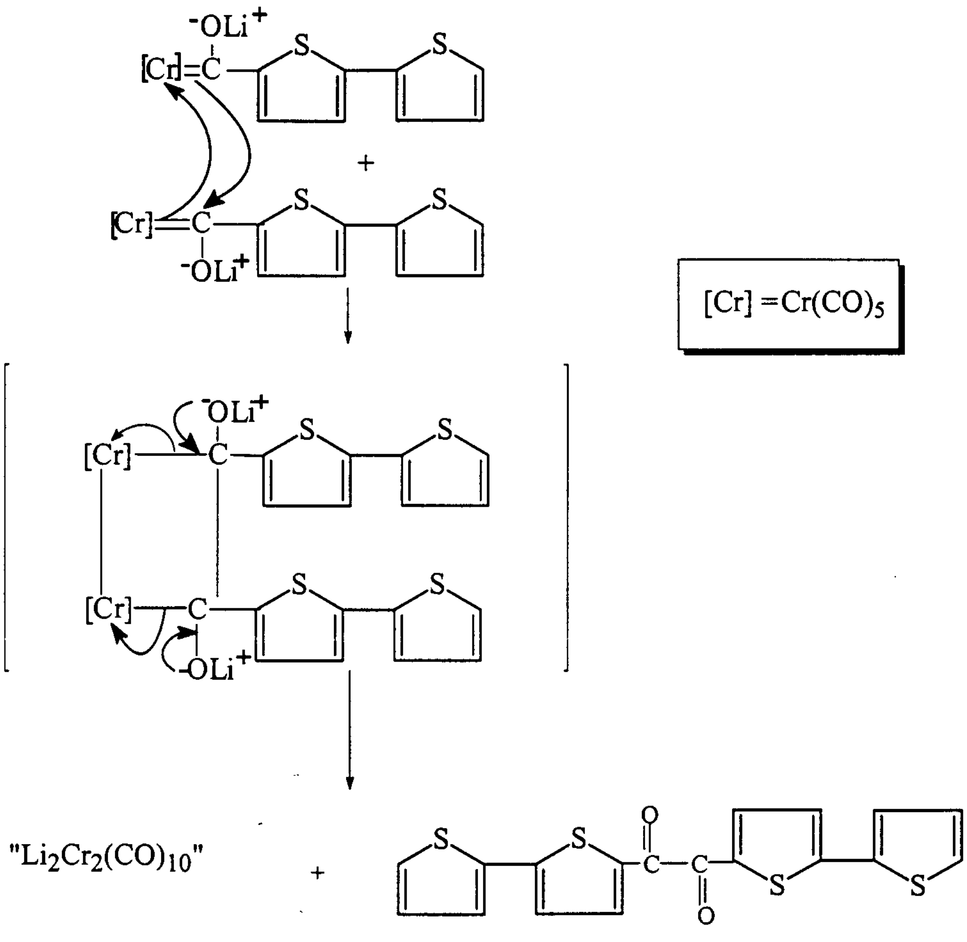

5

FIG. 2.13a: Coupling of two metal acylate units.

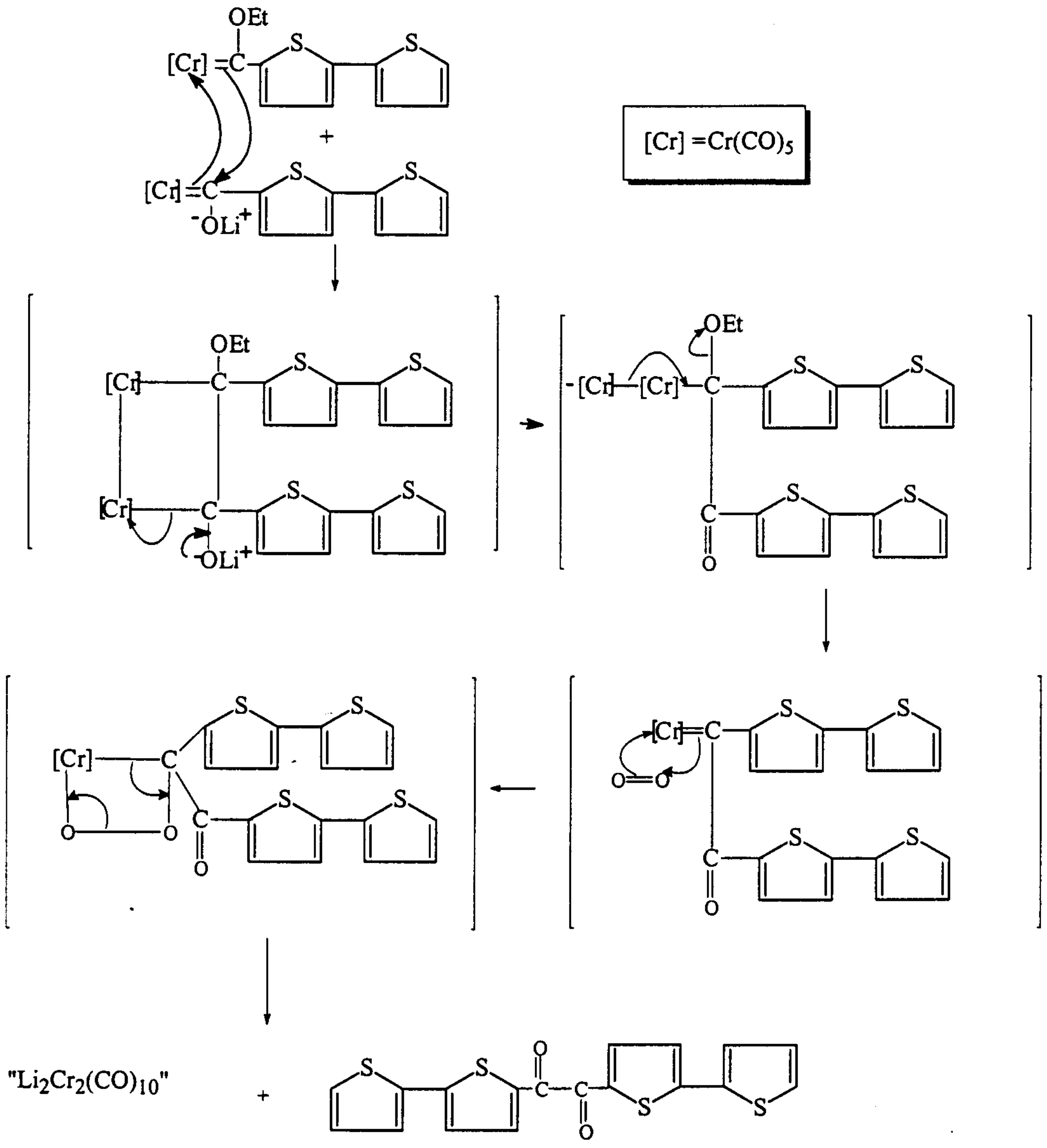

5

FIG. 2.13b: **Coupling of the alkylated monocarbene with an acylate unit.**

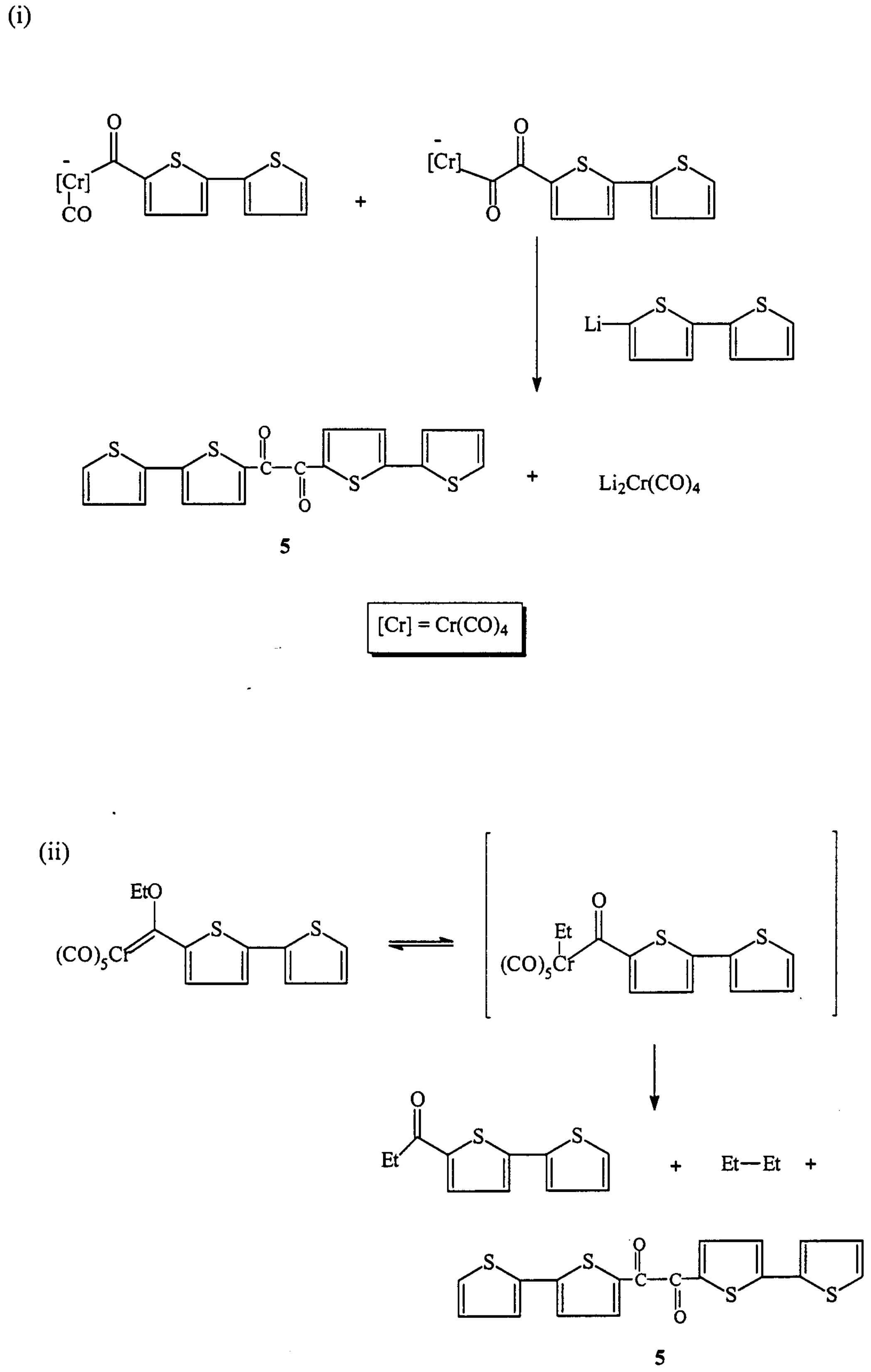

FIG. 2.13c: **Intermolecular mechanism or radical mechanism*.**

*After this thesis was submitted, it came to our attention that diketones were obtained[29] from the reaction of carbene acylates and R-X substrates via carbonyl insertion. If applied in our studies this would mean that 5 formed according to Fig. 2.13c(i).

2.4.2 Characterization of 5 by X-ray crystallography

The molecular structure of **5** was confirmed by a single crystal X-ray diffraction study. White, pillar-shaped crystals of **5** were formed in a 1:1 mixture of hexane:dichloromethane. **Fig. 2.14** shows a perspective view of the structure. Crystallographic data, acquisition and refinement details used in the study are summarized in **Appendix A**. **Fig. 2.15** shows the unit cell content of **5**.

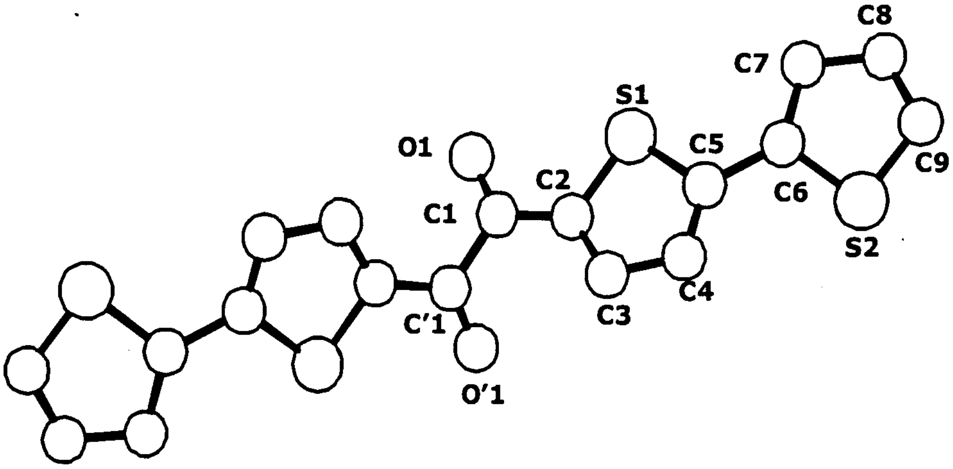

FIG. 2.14: A perspective view of 5 without H-atoms.

---

[29] H. Sakurai, K. Tanabe, K. Narasaka, *Chem. Lett. 2000*, 2, **2000**, 168.

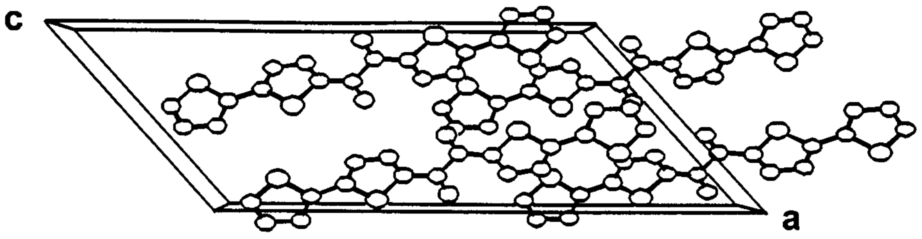

FIG. 2.15: The unit cell for 5.

The crystal structure of free bithiophene was elucidated by Visser and co-workers[30], refer to **Fig. 1.11, Chapter 1**. The bond lengths were found to be: 1.72(2) Å for S-C(2), 1.37(3) Å for C(2)-C(3), 1.43(3) Å for C(3)-C(4), 1.37(3) Å for C(4)-C(5), 1.70(2) Å for C(5)-S and 1.49(3) Å for C(5)-C(6). The bond angles were found to be 91.5(8) ° for C(2)-S-C(5), 110.0(8) ° for S-C(2)-C(3), 116.0(2) ° for C(2)-C(3)-C(4), 107.1(2) ° for C(3)-C(4)-C(5), 114.2(8) ° for C(4)-C(5)-S, 120.8(8) ° for S-C(5)-C(6) and 124.8(2) ° for C(4)-C(5)-C(6). Selected bond lengths and bond angles for **5** are listed in **Table 2.5**. The large ESD values of the free bithiophene data make any significant comparison between **5** and the free ligand impossible.

C(2)-S is 1.723(7) Å for the first ring of **5**, but the equivalent bond, C(9)-S(2) is 1.681(8) Å in the second ring of the complex and is slightly shorter. C(2)-C(3), C(3)-C(4), C(4)-C(5) have values of 1.353(10) Å, 1.400(9) Å, and 1.338(9) Å respectively. The corresponding bonds in the second ring of the compound, C(8)-C(9), C(7)-C(8) and C(6)-C(7) measured 1.320(11) Å, 1.409(10) Å and 1.422(9) Å respectively.

---

[30] G.J. Visser, G.J. Heeres, J. Wolters, A.Vos, *Acta Cryst.*, B24, **1968**, 467.

Table 2.5: Selected bond lengths and bond angles for 5

	Bond Length/Å		Bond Angle/°
O(1)-C(1)	1.223(8)	O(1)-C(1)-C(2)	123.3(7)
C(1)-C(1')	1.527(13)	C(1)-C(2)-S(1)	119.3(6)
C(1)-C(2)	1.445(9)	C(1)-C(2)-C(3)	128.7(7)
C(2)-C(3)	1.353(10)	C(3)-C(2)-S(1)	112.0(6)
C(2)-S(1)	1.723(7)	C(2)-C(3)-C(4)	113.1(7)
C(3)-C(4)	1.400(9)	C(3)-C(4)-C(5)	112.3(7)
C(4)-C(5)	1.338(9)	C(4)-C(5)-S(1)	112.8(5)
C(5)-S(1)	1.729(7)	C(4)-C(5)-C(6)	130.6(7)
C(5)-C(6)	1.520(9)	S(1)-C(5)-C(6)	116.4(5)
C(6)-C(7)	1.422(9)	C(2)-S(1)-C(5)	89.8(4)
C(6)-S(2)	1.732(7)	C(5)-C(6)-C(7)	130.8(6)
C(7)-C(8)	1.409(10)	C(5)-C(6)-S(2)	114.8(6)
C(8)-C(9)	1.320(11)	C(7)-C(6)-S(2)	114.4(5)
C(9)-S(2)	1.681(8)	C(6)-C(7)-C(8)	105.8(7)
		C(7)-C(8)-C(9)	116.3(8)
		C(8)-C(9)-S(2)	114.5(7)
		C(6)-S(2)-C(9)	88.9(4)

The bonds C(5)-S(1) and its counterpart in the second ring in **5**, C(6)-S(2), measure 1.729(7) Å and 1.732(7) Å respectively. The bond length of a typical C-C single bond between two double bonds is given by Bent[31] as 1.46 Å. The C(1)-C(2) and C(3)-C(4) bonds are slightly shorter (1.445(9) Å and 1.400(9) Å respectively) than this, due to delocalization of electron density - as shown in **Fig. 2.16**.

---

[31] H.A. Bent, *Chem. Rev.*, 61, **1961**, 275.

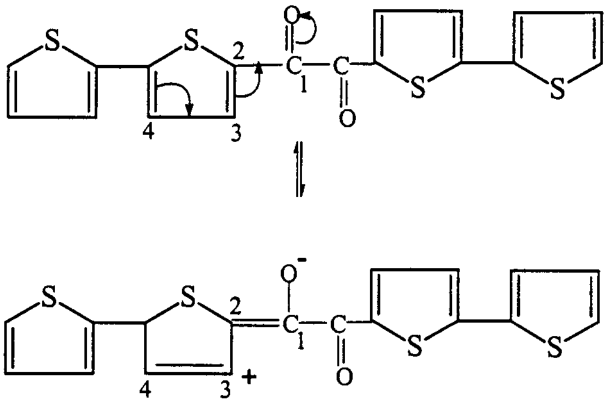

FIG. 2.16: The delocalization of electrons in 5.

Selected torsion angles of 5 are listed in **Table 2.6**.

Table 2.6: Selected torsion angles for 5.

Atoms involved	**Torsion Angle/^{O}**
O(1)-C(1)-C(2)-C(3)	173.754(1)
O(1)-C(1)-C(2)-S(1)	-5.867(1)
C(2)-C(3)-C(4)-C(5)	-0.608(1)
S(1)-C(2)-C(3)-C(4)	-0.092(1)
C(4)-C(5)-S(1)-C(2)	-0.913(1)
C(2)-C(4)-C(5)-S(1)	0.697(1)
S(2)-C(6)-C(7)-C(8)	-2.712(1)
C(8)-C(9)-S(2)-C(6)	-1.328(1)
S(1)-C(5)-C(6)-S(2)	-170.478(1)
C(4)-C(5)-C(6)-C(7)	-176.322(1)
S(1)-C(5)-C(6)-C(7)	7.847(1)
C(7)-C(8)-C(9)-S(2)	-0.038(1)
C(8)-C(9)-S(2)-C(6)	-1.328(1)

The torsion angles S(1)-C(2)-C(3)-C(4) and C(4)-C(5)-S(1)-C(2) have values of -0.092(1) ° and -0.913(1) ° respectively, thus indicating that the ring is planar. Similarly, the second ring can also be said to be planar, due to the values of the torsion angles S(2)-C(6)-C(7)-C(8) and C(8)-C(9)-S(2)-C(6) (i.e. -2.712(1) ° and -1.328(1) ° respectively).

The torsion angle S(1)-C(5)-C(6)-S(2) measures -170.478(1) ° and the torsion angle C(4)-C(5)-C(6)-C(7) has a value of -176.322(1) °. This indicates that the rings are both in the same plane and that they are in the *trans* conformation with respect to the sulfur atoms. From these and other torsion angles tabulated above, it is clear that the molecule is completely flat with all rings and atoms more or less co-planar. For two planes - one passing through C(2), C(3), C(4), C(5), S(1) and the other passing through C(6), C(7), C(8), C(9) and S(2) - the dihedral angle was found to be 7.973(3) °, which further confirms that the molecule is planar. This has important implications for the use of such molecules in conducting polymers and non-linear optical materials, as planarity is important for electron transfer processes in such materials.

3 TUNGSTEN CARBENE COMPLEXES OF BITHIOPHENE

3.1 Introduction

Aoki *et al*[1] produced the first tungsten thienyl carbene in 1992, using a method in which the carbene complex is temporarily protected towards nucleophilic attack through anion formation adjacent to the carbene carbon (**Fig. 3.1**). This approach enabled them to prepare a wide variety of alphatic carbene complexes with many elements of stereochemistry and functional groups, as well as the preparation of several functionalized heteroaromatic carbene complexes with the oxygen anion. Tungsten is also used extensively in the hydrodesufurization of thiophenes and other heteroaromatic compounds found in fossil fuels. Aluminium-supported tungsten and molybdenum promoted by cobalt or nickel are used as catalysts for most HDS reactions.

Caldwell and co-workers[2] reported that tungsten should be used as a promoter for palladium catalysts in the HDS of thiophene.

The idea of using carbene complexes in olefin metathesis has been mentioned in **Chapter 1**, but at this point it is interesting to note that tungsten carbene complexes have been used frequently in this area of research.

---

[1] S. Aoki, T. Fujimura, E. Nakamura, *J. Am. Chem. Soc.*, 114, 1992, 2985.

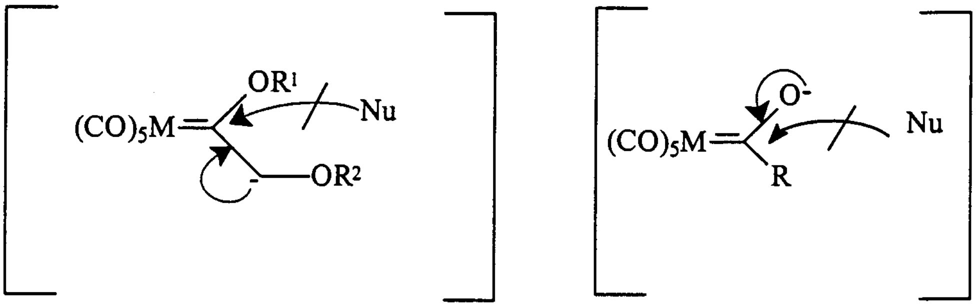

A) Use of the Carbon Anion as a protective group

B) Use of the oxygen anion as a protective group

FIG. 3.1: **Protection of the carbene against nucleophilic attack.**

Casey[3] demonstrated the reactivity of tungsten carbene complexes towards a variety of alkenes to yield metathesis products and cyclopropanes. He outlined a reaction scheme[4] in which these reactions took place via a metallacyclobutane intermediate and a carbene alkene intermediate (**Fig. 3.2**).

Katz[5] discovered, using diphenylcarbenepentacarbonyltungsten(0), that Fischer carbene complexes are reactive catalysts for acetylene polymerisation and postulated that this too occurred via the metallacyclobutane intermediate.

Dötz[6] points out that such intermediates catalyze the metathesis of cycloalkenes to yield polymers and that an induction of cycloalkene metathesis by acetylene is thus possible.

Shrock type carbene complexes, which have nucleophilic carbene carbon atoms, may also be used to catalyze the metathesis of alkenes.

---

[2] T.E. Caldwell, D.P. Land, *Polyhedron*, 16, **1997**, 3197.

[3] C.P. Casey, T.I. Burkhardt, *J. Am. Chem. Soc.*, 96, **1974**, 7808.

[4] C.P. Casey, H.E. Tunistra, M.C. Soleman, *J. Am. Chem. Soc.*, 98, **1976**, 608.

[5] T. I. Katz, S.I. Lee, *J. Am. Chem. Soc.*, 102, **1980**, 422.

[6] K.H. Dötz, H. Fischer, P. Hofmann, F.R. Kreissl, U. Schubert, K. Weiss, *Transition Metal Carbene Complexes*, Verlag Chemie, Weinheim, **1983**, 240.

Shrock[7] isolated a 5-coordinate tungsten-oxo-alkylidene complex which catalyzes olefin metathesis. He postulated that alkylidene complexes of tantalum and tungsten, which have "hard" ligands (such as oxo or alkoxo groups), are metathesis catalysts while those having "soft" ligands such as chloride, bromide or cyclopentadienyl groups, have no activity. The metallacyclobutane of the latter complexes rearranges into an olefin complex when they react with alkenes.

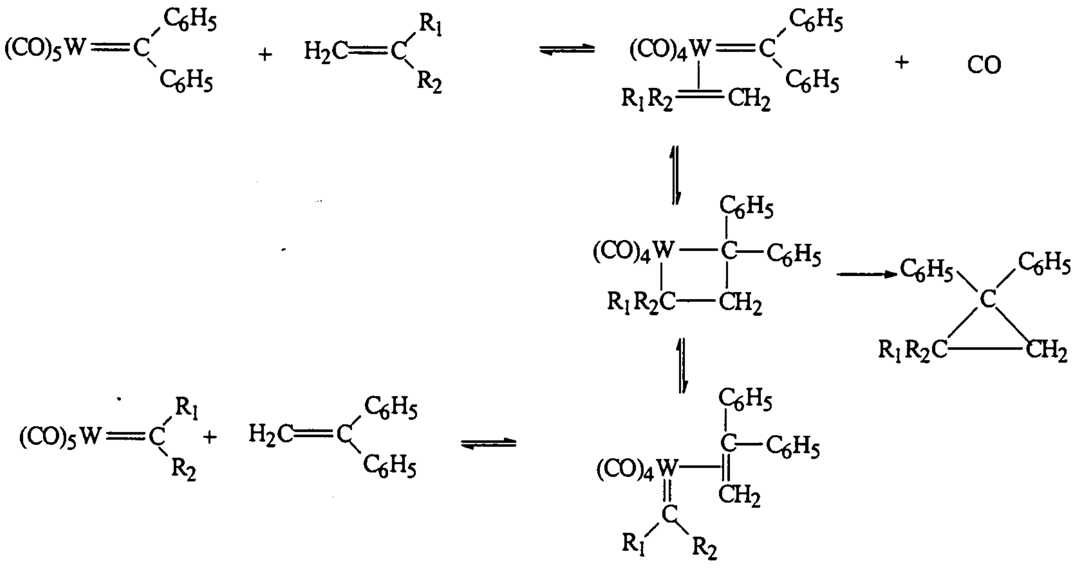

FIG. 3.2: **Reaction scheme of tungsten carbene complexes with alkenes.**

Cotton[8] describes tungsten carbene complexes as being more stable than those of chromium and this is borne out by Fischer[9]. We therefore turned our attention to investigating the formation and decomposition of tungsten carbene complexes of

---

[7] I.A. Wengrovius, R.R. Shrock, M.R. Churchill, I.R. Missert, W.I. Youngs, *J. Am. Chem. Soc.*, 102, **1980**, 4515.

[8] F.A. Cotton, C.M. Lukehart, *Prog. Inorg. Chem.*, 16, **1972**, 487.

[9] E.O. Fischer, *Angew. Chem., Int. Ed. Engl.*, 86, **1974**, 651.

bithiophene. A comparison could then be drawn between these and chromium carbene complexes of bithiophene.

3.2 Synthesis of tungsten bithiophene biscarbene complexes

The mono- and biscarbene tungsten complexes of bithiophene were synthesized according to the classical Fischer method, using THF as solvent. Again the butyllithium:TMEDA complex was able to abstract both the 5- and 5′-protons from the bithiophene rings, at low temperatures, when two equivalents of the base was reacted with one equivalent of bithiophene. The metal carbonyl was added, at which point nucleophilic attack by the dianion of the bithienylene occurs at the carbonyl carbons of two metal carbonyls to form the dilithium diacylmetallated product. The lithium salt is quenched with $Et_3O^+BF_4^-$ to afford the desired biscarbene complex. In addition to the biscarbene complex, the monocarbene complex and another complex were produced. **Fig. 3.3** shows the reaction scheme.

The red monocarbene complex, **6**, and the purple biscarbene complex, **7**, were isolated and characterized by ^1H and ^{13}C NMR spetroscopies, as well as infrared spectroscopy and mass spectrometry. Complex **8** was also isolated and characterized spectroscopically. The reaction mechanism for the reaction of **7** with oxygen to yield **8** is similar to that shown in **Fig. 2.8** in **Chapter 2** for the formation of **3** and will therefore not be repeated here.

The bisester, **4**, which was characterized previously in **Chapter 2** was also produced in this reaction, as a result of the further reaction of **8** with oxygen. The spectroscopic data and mechanism of formation for this product was discussed in

Chapter 2 and will not be dealt with again in this chapter. No other products, (such as **5**) resulting from the coupling of two thienyl ligands or olefin formation from the two monocarbene complexes, were formed in the case of tungsten, supporting literature's claims that these carbenes are more stable than those of chromium.

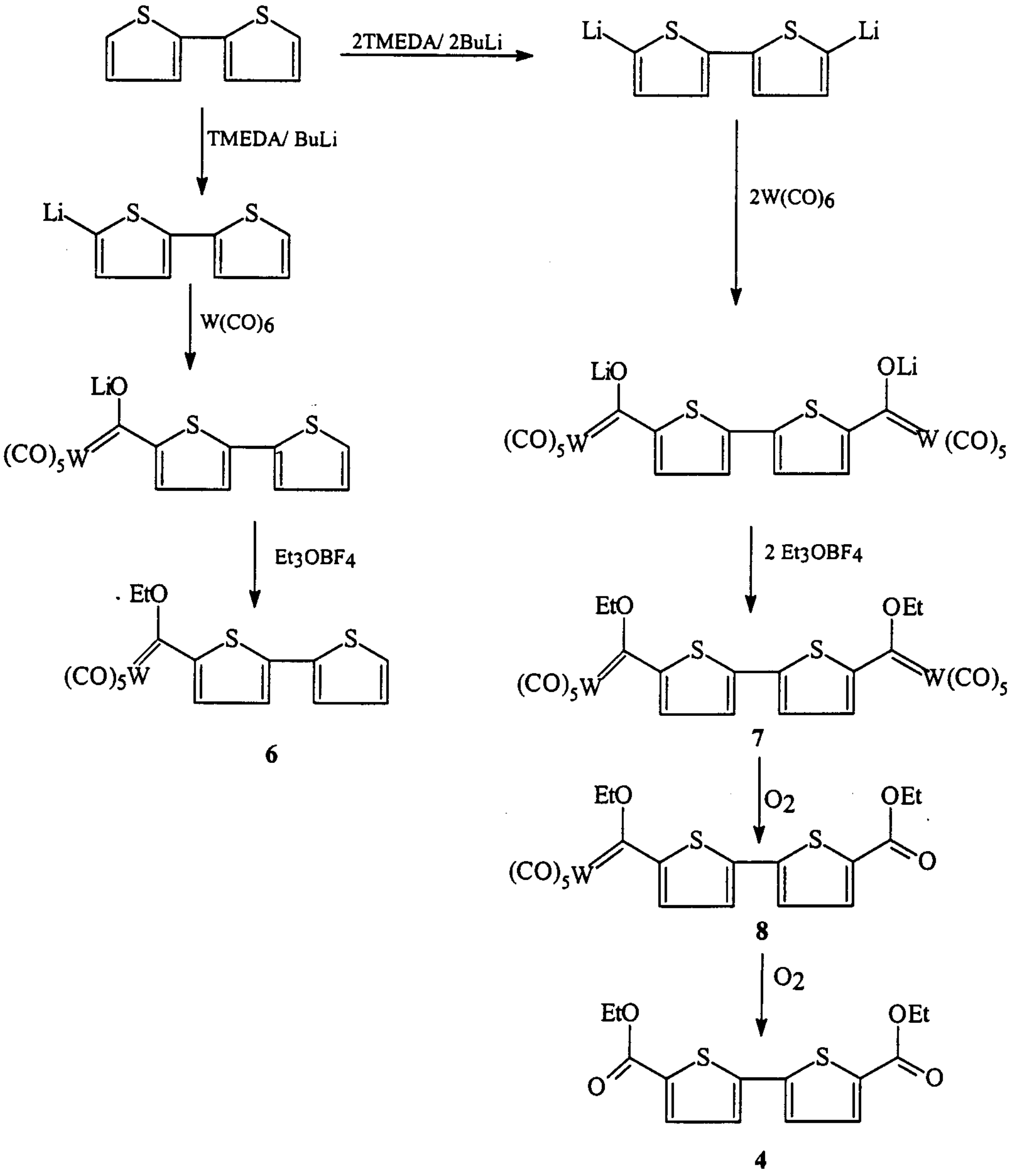

FIG. 3.3: The reaction scheme for the formation of 6, 7, and 8.

3.3 Spectroscopic characterization of tungsten bithiophene carbene complexes.

3.3.1 ^{1}H NMR spectroscopy

The ^{1}H NMR data are represented in **Table 3.1.**

Table 3.1: ^{1}H NMR data for Complexes 6, 7 and 8.

Proton	**Chemical Shifts (δ, ppm) & Coupling Constants (J, Hz)**					
	6		**7**		**8**	
	δ	**J**	**δ**	**J**	**δ**	**J**
H_3	8.09(d)	4.3	8.07(d)	4.4	8.08(d)	4.3
H_4	7.28(d)	4.3	7.46(d)	4.3	7.35(d)	4.3
H_7	7.39(d)	5.7	7.46(d)	4.3	7.35(d)	4.3
H_8	7.06(dd)	3.7, 5.0	8.07(d)	4.4	7.71(d)	4.0
H_9	7.41(d)	3.5	-	-	-	-
$O\mathbf{CH_2}CH_3$-M	4.96(q)	7.0	4.97(q)	7.1	4.97(q)	6.9
$O\mathbf{CH_2}CH_3$-O	-	-	-	-	4.35(q)	7.1
$OCH_2\mathbf{CH_3}$-M	1.64(t)	7.0	1.68(t)	7.1	1.65(t)	10.3
$OCH_2\mathbf{CH_3}$-O	-	-	-	-	1.38(t)	10.3

All NMR spectra were recorded in deuterated chloroform as solvent. The data support the proposed structures for the complexes. The effect of the electron-withdrawing nature of the carbene is evident from the fact that all the signals for **6**, **7** and **8** are further downfield than the corresponding signals in free bithiophene. The chemical shifts of **6** are similar to those of **1**, with only $\mathbf{H_3}$ being slightly further upfield in the tungsten complex (8.09 ppm for **6** compared to 8.16 ppm for **1**), and $\mathbf{H_9}$

and **H_7** slightly downfield of their corresponding values for **1** (complex **6**: 7.41 ppm (**H_9**) and 7.39 ppm (**H_7**) and complex **1**: 7.39 ppm (**H_9**) and 7.36 ppm (**H_7**)).

In **6**, the signal for **H_3** appears further downfield (8.09 ppm) than that for **H_4** (7.28 ppm) since **H_4** is less affected by the electron-withdrawing properties of the carbene moiety as shown in **Chapter 2** (**Fig. 2.10**).

The signal for **H_9** is shifted downfield of the signal for free bithiophene to a lesser degree than **H_3**, as **H_9** is not as deshielded as **H_3**. Resonance effects, similar to those shown in **Chapter 2** (**Fig. 2.10**) for **1** are responsible for the deshielding of **H_9**.

The signal for **H_8** is a doublet of doublets because of coupling to **H_7** and **H_9**. **Fig. 3.5** shows a portion of the spectrum in which the splitting of the peaks at 7.06 ppm can be clearly seen. The fact that the coupling constants were different for the couplings **H_8-H_7** and **H_8-H_9** enabled us to use these as well as the chemical shifts in assigning the peaks.

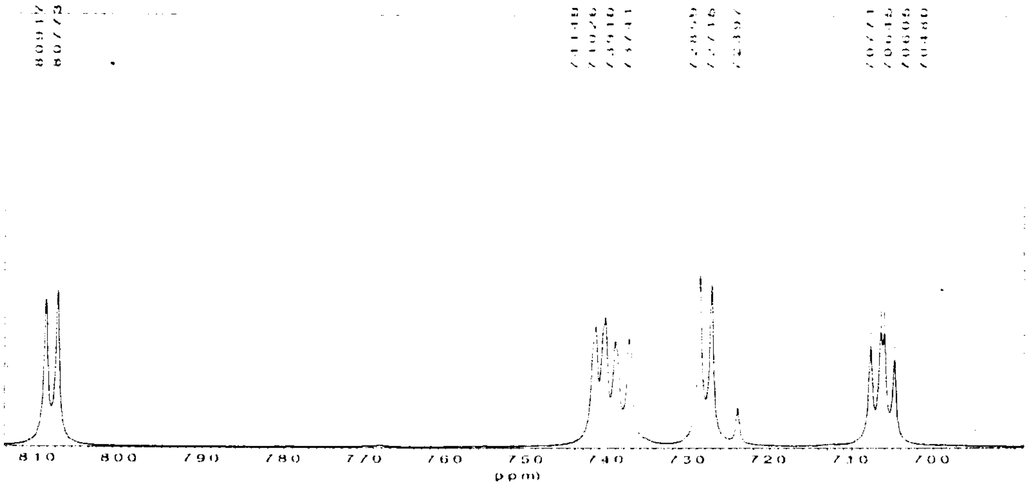

FIG. 3.4: **The thienyl portion of the ^{1}H NMR spectrum of 6**

Signals for the protons of **7** are similar to those of **2** with the exception of the signal for **H_3** (and the equivalent **H_8**) which arises slightly upfield in **6** (8.07 ppm) of the signal (8.16 ppm) for the corresponding protons in the chromium complex.

The effect of two carbene groups is evident, as the chemical shifts of the protons in 7 all appear downfield of those in **6**. This is because of the same type of draining of electrons from the ring system by two carbene moieties as described in **Chapter 2** (**Fig. 2.11**) for **2**. Two carbene groups draw electron density away from the rings more than one carbene group does, so the signals for the biscarbene complex lie further downfield than those of the monocarbene complex.

The signals for **8** also occur further upfield than those for the corresponding complex, **3**. Chemical shifts for **8** appear downfield of those for **6**, but upfield of those for 7. This can be rationalized by the fact that the deshielding of the protons is greatest with two carbene groups, next greatest with one carbene and an ester group and least with one carbene group only. This is because ester groups are electrophilic; although not as electrophilic as carbene moieties.

The quartet at 4.35 ppm and the triplet at 1.38 ppm which appear in the spectrum of **8** indicate that one of the metal fragments of 7 has fallen away due to reaction with oxygen and was modified to an ester functionality.

The metal-bound ethoxy groups of **6**, 7 and **8** show very similar chemical shifts as these complexes are derived from each other. The chemical shifts of the **CH_2** protons of the metal-bound ethoxy groups of **6**, 7 and **8** are much further upfield than those of the corresponding chromium complexes (4.96 ppm, 4.97 ppm and 4.97 ppm versus 5.14 ppm, 5.17 ppm and 5.17 ppm respectively).

3.3.2 ^{13}C NMR spectroscopy

The ^{13}C NMR data for **6**, 7 and **8** are shown in **Table 3.2**. **Fig. 3.5** shows the full ^{13}C NMR spectrum of **6**.

Comparing the chemical shifts of **6**, **7** and **8** with those of free bithiophene, it is clear that bonding to the metal fragment causes the chemical shifts to appear further downfield. The carbene chemical shifts of **6**, **7** and **8** do not, however, appear as far downfield as those of **1**, **2** and **3**. In **6**, **C_2** appears furthest downfield as it is most deshielded – being closest to the carbene substituent.

Table 3.2: ^{13}C NMR data for 6, 7 and 8.

Carbon	**Chemical Shifts (δ, ppm)**		
	6	**7**	**8**
Carbene	286.8	295.9	292.0
C_2	155.3	157.5	154.2
C_3	143.6	142.6	142.9
C_4	125.2	127.0	128.5
C_5, C_6 [a]	148.0, 136.4	145.2	126.2
C_7	127.6	127.0	130.0
C_8	128.5	142.6	134.6
C_9	126.4	157.5	145.9
OCH_2CH_3-M	78.1	78.3	78.4
OCH_2CH_3-O	-	-	61.6
OCH_2CH_3-M	15.0	15.0	15.0
OCH_2CH_3-O	-	-	14.3
$OCOCH_2CH_3$-O	-	-	177.0
M(CO)$_5$	202.5 (*trans*) 197.7 (*cis*)	202.6 (*trans*) 197.3 (*cis*)	207.3 (*trans*) 197.5 (*cis*)

[a] Cannot discriminate between resonances of **C_5** and **C_6**.

A HETCOR spectrum was used to assign the signals of the ^{13}C NMR spectrum by cross-referencing with the relevant hydrogen signals. **Fig. 3.6** shows the HETCOR spectrum of **6** in the thienyl region. The HETCOR spectrum shows that **C_3** is furthest downfield of all the hydrogen-carrying carbons, followed by **C_8**, **C_7**, **C_9** and then **C_4**. The remaining signals belong to **C_5** and **C_6**, but these cannot be assigned individually as they have no attached hydrogens and there is no way of knowing which will appear furthest downfield.

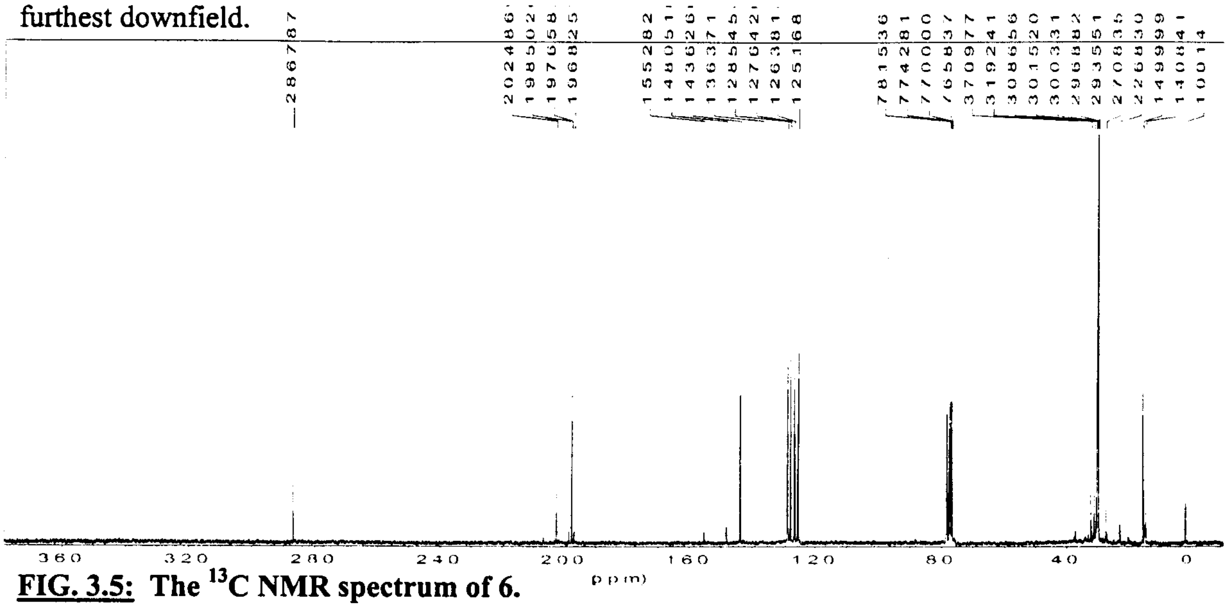

FIG. 3.5: **The ^{13}C NMR spectrum of 6.**

The signal for the carbene moiety in **7** appears at 295.9 ppm - further downfield than that of **8** (292.0 ppm) and **6** (286.8 ppm). This occurs because the carbene carbon atom is more deshielded in the biscarbene complex than in the decomposition product which, in turn, is more deshielded than the carbene carbon of the monocarbene complex.

Shielding of the terminal metal-carbonyl group in tungsten complexes is less than that of the chromium complexes due to the increased atomic number of tungsten over chromium as explained in **Chapter 2**. As a result chemical shifts for both the *cis* and *trans* configurations of complexes **6**, **7** and **8** are all upfield of the corresponding chromium complex chemical shifts. All other signals for the tungsten complexes are similar to those of the chromium complexes except the signal for C_2 of **6** which appears much further upfield than the corresponding signal for **1** (155.3 ppm and 166.5 ppm respectively). The signals for carbons C_5 and C_6 are shifted upfield for the decomposition products of both tungsten and chromium relative to their signals in the mono- and biscarbene complexes of the two metals.

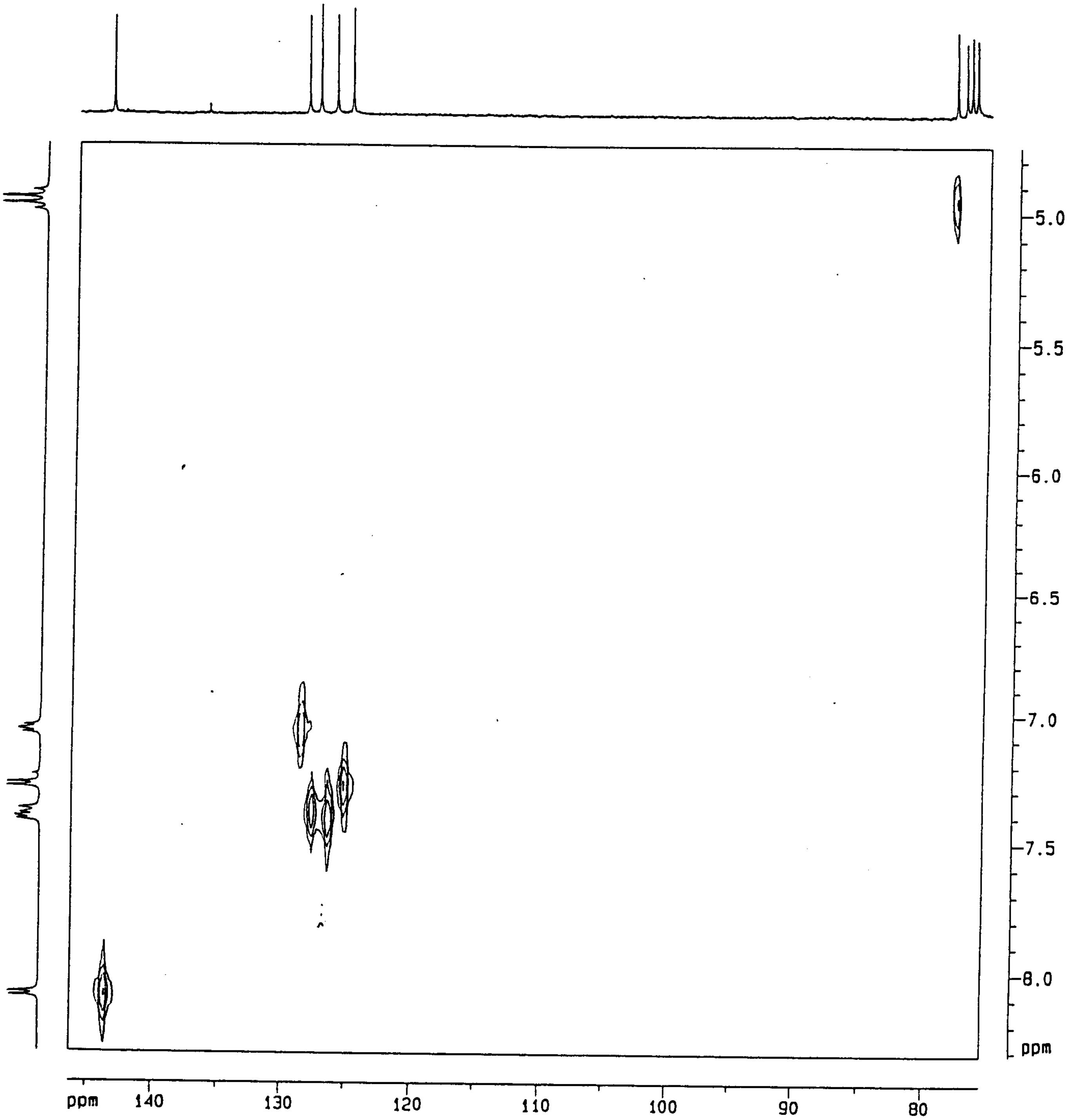

FIG. 3.6: The HETCOR spectrum of 6.

3.3.3 Infrared spectroscopy

Table 3.3: Infrared data for 6, 7 and 8.

Band	**Stretching Vibrational Frequency, ν_{CO}, cm^{-1}**		
	6	**7**	**8**
$A_1^{(1)}$	2065(m)	2062(m)	2065(m)
B	1978(w)	1975(w)	1976(w)
$A_1^{(2)}$	1950(w)	1938	1953(w)
E	1943(vs)	1938	1944(vs)

Infrared data were collected using hexane as a solvent for **6** and **8** and dichloromethane as a solvent in the case of **7**.

Characteristic ν_{CO} stretching vibrational frequencies, $A_1^{(1)}$, B, $A_1^{(2)}$ and E, can be identified for all three complexes. The $A_1^{(1)}$ bands for the tungsten complexes appear at higher frequencies than those of the corresponding chromium complexes. The B band appears at lower frequencies in the tungsten complexes than it does in the chromium complexes. Once again, when dichoromethane is used as a solvent the $A_1^{(2)}$ and E bands overlap.

3.3.4 Mass spectrometry

Table 3.4 shows the fragmentation data collected by mass spectrometry for **6** and **8**. The results listed are based on the W^{183}-isotope. Each of these complexes loses its carbonyl ligands first and then the COEt group, as was the case in the chromium complexes. The **M$^+$** peak was observed for **6** and **8**, but could not be found for the biscarbene complex. Even after repeated measurements, fragment ions containing the metal could only be detected in a few instances for dinuclear complexes of this type. In this case, no relevant fragments were observed for **7**.

Table 3.4: Fragmentation data for 6 and 8.

Fragment	**6**		**8**	
	m/z	I/%	*m/z*	I/%
M^+	546.2	22.8	618.1	31.7
M^+-OEt	-	-	-	-
M^+-CO	518.2	14.9	590.1	15.8
M^+-2OEt	-	-	-	-
M^+-2CO	490.1	27.2	561.2	31.7
M^+-3CO	460.0	3.0	533.1	4.7
M^+-4CO	435.0	30.0	505.1	65.0
$N^+ = M^+$-5CO	408.0	58.6	478.1	91.9
N^+-COEt	351.0	79.4	421.0	41.2
N^+-OCOEt	-	-	348.0	15.8

3.3.5 X-Ray crystallography

A single crystal X-ray diffraction study was conducted on crystals of **6**. The crystals were red in colour and needle-like in shape and were formed from a solution of 1:1 hexane: dichlorormethane. From this study it became clear that there were two molecules in the asymmetric unit of the crystal structure. **Fig. 3.7** and **Fig. 3.8** show perspective plots of the structures of the two molecules indicating the numbering of the non-hydrogen atoms. Molecule **A**, depicted in **Fig. 3.7**, is one rotational isomer while molecule **B**, depicted in **Fig. 3.8**, is another rotational isomer of **6**. Crystallographic data, acquisition and refinement details used in the study are summarized in **Appendix B**. **Fig. 3.9** shows the unit cell diagram for **6**.

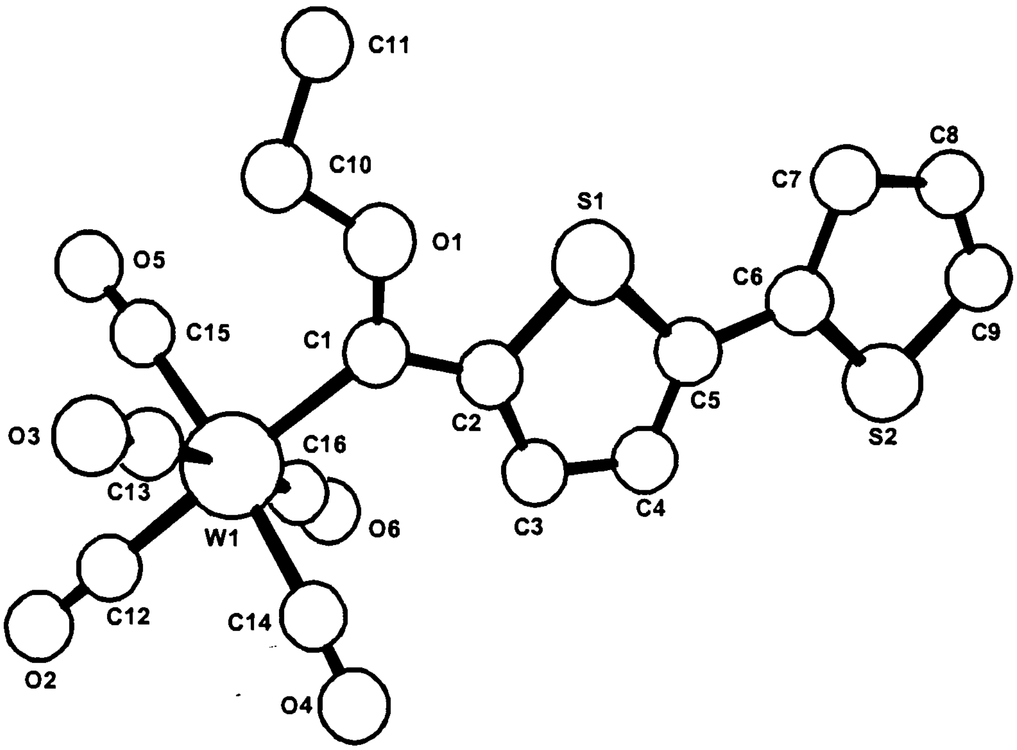

FIG. 3.7: **Perspective drawing of 6 (molecule A)**

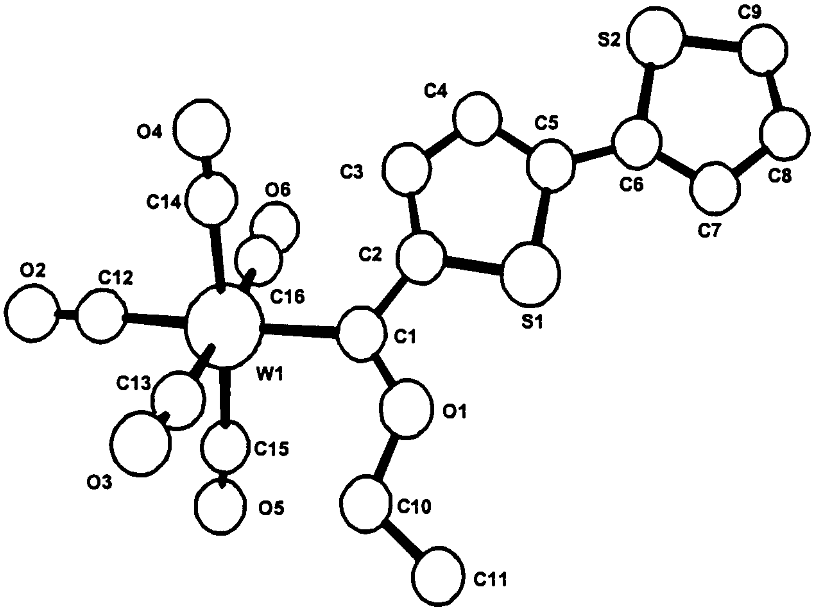

FIG. 3.8: **Perspective drawing of 6 (molecule B)**

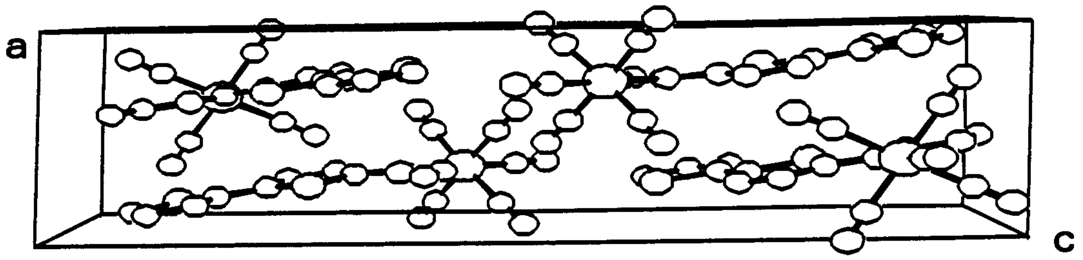

FIG. 3.9: Perspective drawing of the unit cell contents of 6.

Selected bond lengths and bond angles for **6** are listed in **Table 3.5**.

The bond lengths and bond angles of free bithiophene are listed in **Chapter 2, page73**. A diagram can be found in **Chapter 1** (Refer **Fig. 1.11**). Once again it must be noted that the ESD's of the measurements for the free ligand are so large that no meaningful comparisons can be made.

The C(2)-C(3), C(2)-S(1) and C(5)-S(1) bonds measure 1.388(11) Å, 1.737(8) Å, and 1.722(9) Å respectively for molecule **A** and 1.362(12) Å, 1.740(9) Å and 1.694(9) Å respectively for molecule **B**. C(3)-C(4) measures 1.400(11) Å for molecule **A** and 1.377(12) Å for molecule **B** and C(4)-C(5) measures 1.383(12) Å for molecule **A** and 1.388(11) Å for molecule **B**. C(6)-S(2) measures 1.701(10) Å for molecule **A** and 1.749(1) Å for molecule **B**. C(9)-S(2) measures 1.680(12) Å for molecule **A** and 1.749(1) Å for molecule **B**. These bonds are shorter than the corresponding bonds in the ring attached to the carbene. Some distortion (from the influence of the carbene moeity) is carried over to the second ring.

Table 3.5: Selected bond lengths and bond angles for 6

	Bond Length/Å			**Bond Angle/°**	
	Molecule A	Molecule B		Molecule A	Molecule B
W(1)-C(1)	2.182(9)	2.199(9)	W(1)-C(1)-O(1)	129.1(6)	128.1(7)
C(1)-O(1)	1.338(9)	1.328(9)	W(1)-C(1)C(2)	126.5(6)	124.8(6)
C(1)-C(2)	1.444(11)	1.444(12)	O(1)-C(1)-C(2)	104.3(7)	107.1(8)
C(2)-C(3)	1.388(11)	1.362(12)	C(1)-C(2)-C(3)	130.1(8)	130.0(9)
C(2)-S(1)	1.737(8)	1.740(9)	C(1)-C(2)-S(1)	120.7(6)	120.8(7)
C(3)-C(4)	1.40(11)	1.377(12)	C(3)-C(2)-S(1)	109.2(7)	109.2(7)
C(4)-C(5)	1.383(12)	1.388(11)	C(2)-C(3)-C(4)	115.0(8)	114.4(9)
C(5)-C(6)	1.483(12)	1.420(1)	C(3)-C(4)-C(5)	111.5(9)	113.3(9)
C(5)-S(1)	1.722(9)	1.694(9)	C(4)-C(5)-S(1)	111.9(7)	110.2(6)
C(6)-C(7)	1.479(13)	1.420(1)	C(4)-C(5)-C(6)	129.9(9)	133.9(8)
C(6)-S(2)	1.701(10)	1.749(1)	S(1)-C(5)-C(6)	118.2(8)	115.9(6)
C(7)-C(8)	1.45(2)	1.419(1)	C(2)-S(1)-C(5)	92.5(5)	92.9(4)
C(8)-C(9)	1.29(2)	1.419(1)	C(5)-C(6)-C(7)	126.9(9)	133.8(6)
C(9)-S(2)	1.680(12)	1.749(1)	C(5)-C(6)-S(2)	117.8(8)	116.1(5)
			C(7)-C(6)-S(2)	115.3(8)	110.0(6)
			C(6)-C(7)-C(8)	100.4(10)	111.9(9)
			C(7)-C(8)-C(9)	121(2)	115.7(11)
			C(8)-C(9)-S(2)	112.1(13)	108.0(8)
			C(6)-S(2)-C(9)	90.9(7)	94.3(5)

The C(5)-C(6) bond linking the two rings in the complex (which was extended in **5**) is shorter in length in **6** (1.483(12) Å in molecule **A** and 1.420(1) Å in molecule **B**). Selected torsion angles of **6** are listed in **Table 3.6**.

Table 3.6: Selected torsion angles for 6.

Atoms involved	Torsion Angle/°	
	Molecule A	**Molecule B**
C(12)-W(1)-C(1)-O(1)	159.6(7)	132.8(1)
C(12)-W(1)-C(1)-C(2)	-17.6 (7)	-49.3(1)
O(1)-C(1)-C(2)-S(1)	-9.5 (1)	5.9(1)
O(1)-C(1)-C(2)-C(3)	172.7(1)	-173.4(1)
S(1)-C(2)-C(3)-C(4)	-1.8(1)	0.8(1)
C(4)-C(5)-S(1)-C(2)	-1.4(1)	1.4(1)
C(2)-C(3)-C(4)-C(5)	0.7(1)	0.2(1)
C(4)-C(5)-C(6)-S(2)	3.9(1)	-4.3(1)
S(1)-C(5)-C(6)-C(7)	2.8(1)	-5.7(1)
S(1)-C(5)-C(6)-S(2)	-175.8(1)	176.4(1)
C(5)-C(6)-C(7)-C(8)	-176.7(1)	-177.4(1)
C(6)-C(7)-C(8)-C(9)	-5.1(2)	-1.9(1)
C(8)-C(9)-S(2)-C(6)	-3.6(1)	-1.5(1)
S(2)-C(6)-C(7)-C(8)	1.9(1)	0.6(1)
C(1)-W(1)-C(16)-O(6)	138.9(3)	141.8(11)

The torsion angles, S(1)-C(2)-C(3)-C(4) and C(4)-C(5)-S(1)-C(2) have values of -1.8(1) ° and -1.4(1) ° respectively for molecule **A** and, 0.8(1) ° and 1.4(1) ° respectively for molecule **B**, which indicates that the rings are planar in both molecules. Similarily, the second ring in both molecules is also planar as S(2)-C(6)-C(7)-C(8) and C(8)-C(9)-S(2)-C(6) have values of 1.9(1) °(molecule **A**) and 0.6(1) ° (molecule **B**) and -3.6(1) ° (molecule **A**) and -1.5(1) ° (molecule **B**) respectively. The rotation angles S(1)-C(5)-C(6)-S(2) of -175.8(1) ° for molecule **A** and 176.4(1) ° for molecule **B**, show that the two molecules are rotational isomers with the rings lying in opposite directions. The rings are in the same plane and are in the *trans* conformation with respect to the sulfur atoms in both molecules.

Looking at these and other torsion angles in the table it is clear that, with the exception of the area around the tungsten atom, the molecule is completely flat. The ethoxy group is twisted slighlty out of the plane of the rest of the molecule - as shown by the angle C(12)-W(1)-C(1)-O(1) being 159.6(1) ° for molecule **A** and a greater twist of 132.8(1) ° for molecule **B**.

The ligand environment around the metal closely resembles an octahedron, but there is some distortion as shown by the angle C(1)-W(1)-C(16)-O(6) (138.9(1) ° and 141.8(1) ° for molecule **A** and molecule **B** respectively) which deviate from 180 °.

For molecule **A**, two planes were selected. These consisted of a plane containing atoms C(2), C(3), C(4), C(5), S(1) and a second plane containing atoms C(6), C(7), C(8), C(9), S(2). The dihedral angle between these two planes was found to be 4.3(6) ° which indicates that the molecule is planar in this area. The corresponding two planes were selected for molecule **B** and, in this case, the dihedral angle was found to be 3.0(5) ° which indicates that this molecule is also planar. Dihedral angles between the planes of the two molecules are all small indicating that both molecules are in the same plane as well. Experimental errors in the measurements are quite large due to the lability of the ligand during X-ray studies and it is therefore not possible to draw definite conclusions on possible ring allocations.

4 MANGANESE CARBENE COMPLEXES OF BITHIOPHENE

4.1 Introduction

In order to make a meaningful comparison between the bithiophene carbene complexes of the transition metals, manganese bithiophene carbene complexes were included in this study because: i) manganese exhibits superior stability in complexes over chromium or tungsten with thiophene substrates; and ii) manganese belongs to a different group (VII) of transition metals and hence has a different electronic environment.

Mention has been made of manganese carbene complexes and their development in the previous chapters. One recent study, which bears mentioning, is that of Terblans[1] *et al* who synthesized and characterized thienylene bridged dinuclear biscarbene complexes of manganese and chromium. They also refluxed these in carbon disulfide and acetone and discovered that in the case of manganese this resulted in the formation of the thieno ester compounds: $[Mn(\eta^5\text{-}C_5H_4R)(CO)_2\{C(OEt)\text{-}C_4H_2SC(S)OEt\}]$ (R = H or Me) in addition to the mononuclear products: $[Mn(\eta^5\text{-}C_5H_4R)(CO)_2\{C(OEt)C_4H_2SC(O)OEt\}]$ (R = H or Me).

---

[1] Y.M. Terblans, H.M. Roos, S. Lotz, *J. Organomet. Chem.*, 566, **1998**, 133.

4.2 Synthesis of manganese bithiophene biscarbene complexes

The mono- and biscarbene manganese complexes of bithiophene were synthesized according to the classical Fischer method, using THF as solvent.

The butyllithium: TMEDA complex was used to abstract both the 5- and 5′-protons from the bithiophene rings, at low temperatures, and two equivalents of the base reacted smoothly with one equivalent of bithiophene.

The methylcyclopentadienyl manganese tricarbonyl precursor was added, at which point nucleophilic attack by the dianion of the bithienylene occurs at the carbonyl carbons to form the dinuclear dilithium diacylmetallated product.

The lithium salt is quenched with $Et_3O^+BF_4^-$ to afford the desired biscarbene complex. **Fig. 4.1** shows the reaction scheme. The orange-red monocarbene complex, **9**, and the purple biscarbene complex, **10** were the only isolatable products. These were isolated and characterized by NMR spectroscopy, as well as infrared spectroscopy and mass spectrometry.

The manganese complexes are much more stable than those of chromium or tungsten, thus no decomposition products were formed in isolatable amounts.

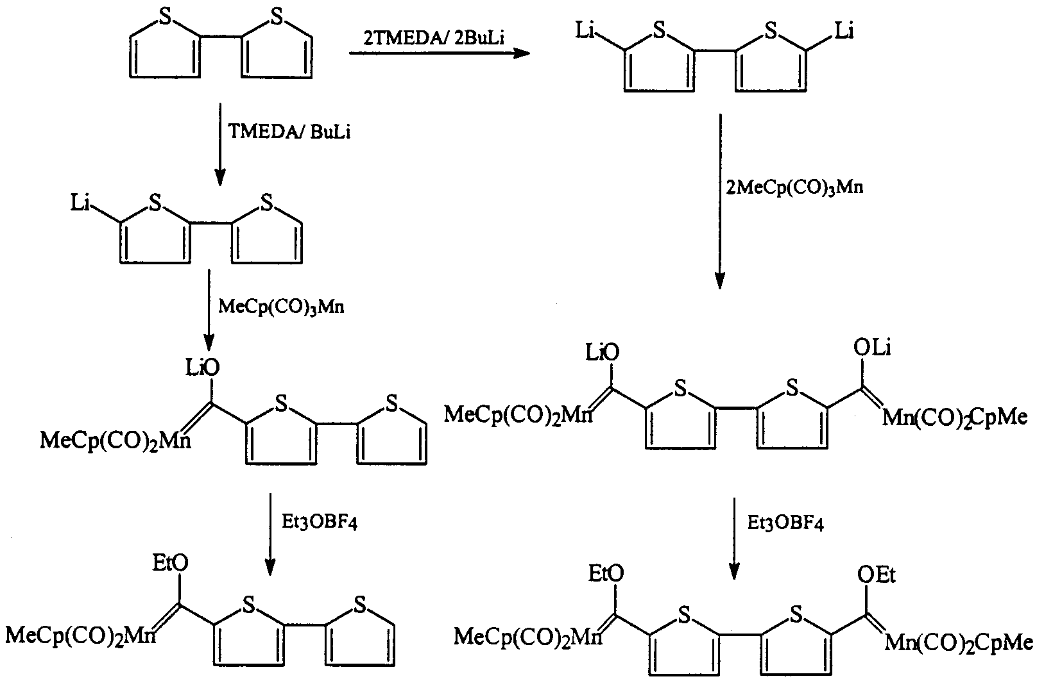

9

10

FIG. 4.1: Reaction scheme for the formation of 9 and 10

4.3 Spectroscopic characterization of manganese bithiophene carbene complexes.

4.3.1 ^{1}H NMR spectroscopy

All NMR spectra were recorded in deuterated chloroform as solvent. The ^{1}H NMR data are represented in **Table 4.1**.

The resolution for manganese carbene spectra is not as good as for the spectra of tungsten and chromium (due to the paramagnetic nature of manganese) and therefore coupling constants could not be determined in many cases.

The data support the proposed molecular structures of the complexes. The influence of bonding to the metal fragment on the chemical shifts of the protons is obvious when comparing the values for free bithiophene with those in **Table 4.1**.

Table 4.1: ^{1}H NMR data for 9 and 10.

Proton	**Chemical Shifts (δ, ppm) and Coupling Constants (J, Hz)**			
	9		**10**	
	δ	**J**	**δ**	**J**
H_3	7.81 (s) (br)	-	7.85 (s) (br)	-
H_4	7.16(s) (br)	-	7.23 (s) (br)	-
H_7	7.24 (s) (br)	-	7.23 (s) (br)	-
H_8	7.02 (s) (br)	-	7.85 (s) (br)	-
H_9	7.29(s) (br)	-	-	-
O**CH_2**CH_3-M	5.02 (q)	6.7	5.02 (s) (br)	-
OCH_2**CH_3**-M	1.58 (t)	6.5	1.58 (s) (br)	-
C_5H_4 CH_3	4.46 (s) (br) 4.34 (s) (br)	-	4.57(s) (br) 4.45 (s) (br)	-
C_5H_4**CH_3**	1.78 (s) (br)	-	1.78 (s) (br)	-

All values for the manganese complexes are shifted downfield of those for the free bithiophene ligand. This is due to the electrophilic nature of the adjacent carbene moiety, which causes draining of electron density from the rings. The protons in the complexes are, therefore, more deshielded than those of the uncoordinated ligand and appear further downfield.

The signals for **9** are generally found upfield of those for the chromium or tungsten complexes (e.g. $\mathbf{H_3}$ 7.81 ppm for **9**, 8.16 ppm for **1** and 8.18 ppm for **6**). The signal for $\mathbf{H_3}$ appears downfield of that for $\mathbf{H_4}$ due to electron draining effects described in **Chapter 2** (**Fig. 2.10**). The protons closest to the carbene component, are more deshielded and therefore appear furthest downfield in the spectrum. The other carbons were assigned accordingly. The signal for $\mathbf{H_9}$ appears further downfield than those of $\mathbf{H_4}$, $\mathbf{H_7}$ and $\mathbf{H_8}$ due to deshielding similar to that shown in **Chapter 2** (**Fig. 2.10**).

Signals for the biscarbene complex are also, in general, further upfield than those of the tungsten and chromium biscarbene complexes. $\mathbf{H_3}$ and $\mathbf{H_8}$ are equivalent and more deshielded than $\mathbf{H_4}$ and its equivalent $\mathbf{H_7}$ and, therefore, appear further downfield.

All the signals for **10** are further downfield than those for the corresponding protons in **9**. This is due to the presence of two carbene ligands in **10** as opposed to only one carbene ligand in **9**. The combined effect causes greater withdrawal of electron density from the rings (and hence greater deshielding) in **10** than in **9**. The electron-withdrawal in manganese complexes occurs similarly to that shown in **Chapter 2** (**Fig. 2.11**). Both complexes have ethoxy groups of similar electronic environment to the methylene and methyl group and, therefore, display the same resonances.

The signals at around 4.5 ppm indicate the presence of the cyclopentadienyl ring attached to the metal and the signal at 1.78 ppm indicates the presence of the methyl group attached to the Cp ring.

4.3.2 ^{13}C NMR spectroscopy

The ^{13}C NMR data for complexes are shown in **Table 4.2.**

Table 4.2: ^{13}C NMR data for 9 and 10.

Carbon	**Chemical Shifts (δ, ppm)**	
	9	**10**
Carbene	319.0	320.0
C_2	156.6	n.o.[a]
C_3	142.5	134.4
C_4	124.3	128.9
C_5, C_6	149.5, 137.5	149.6
C_7	126.1	128.9
C_8	128.1	134.4
C_9	125.0	n.o.
$\mathbf{O}CH_2CH_3$-M	73.7	74.0
OCH_2CH_3-M	15.3	15.0
$M(CO)_2$	231.0	232.0
$\mathbf{C_5H_4}CH_3$	83.4, 82.3	85.2, 83.3
$C_5H_4\mathbf{CH_3}$	13.5	14.1

[a] n.o. = not observed.

Some of the quaternary carbons of the biscarbene complex were not observed.

The chemical shifts of carbons in **9** and **10** appear further downfield than those of the free bithiophene ligand, indicating that the carbene carbon has an effect on the deshielding of these carbons.

The signal for the carbene carbon in these complexes appears much further downfield than that for chromium or tungsten (320.0 ppm for **10**, 319.0 ppm for **9**, 292.0 ppm for **8**, 295.9 for **7**, 286.8 ppm for **6**, 313.7 ppm for **3**, 314.3 ppm for **2** and 312.1 ppm for **1**). This is a result of the nature of the metal.

The carbene carbon in **9** appears much further upfield of the corresponding signal in **10**, since the carbene carbon displays greater deshielding in **10** due to the presence of two carbene groups in **10** as opposed to only one in **9**.

In addition to the nature of the metal, the carbonyl signals in **9** and **10** are different from those of the tungsten and chromium complexes as there are only two carbonyl groups on the metal.

The signals at 83-85 ppm indicate the presence of the cyclopentadienyl ring attached to the metal and the signals at 13-14 ppm indicate the presence of the methyl group attached to the Cp ring.

4.3.3 Infrared spectroscopy

The infrared data for complexes are summarized in **Table 4.3**.

Table 2.3: Infrared Data for 9 and 10.

Band	**Stretching Vibrational Frequency, ν_{CO}, cm^{-1}**	
	9	**10**
A	1945	1945
A'	1889	1890

The carbonyl ligands have the same vibrational frequencies in 9 and 10, indicating that the role of the metal fragment is constant in stabilizing the electrophilic carbene carbon. From the ^{1}H NMR and infrared data, it is clear that the bithiophene substituents are responsible for alleviating electronic differences in **9** and **10**. Terblans *et al*[1] measured dinuclear thienylene complexes of manganese and found that for the cyclopentadienyl manganese biscarbene complex, **A** appeared at 1948 cm^{-1} and **A'** appeared at 1896 cm^{-1}, while for the methylcyclopentadienyl manganese biscarbene complex, **A** appeared at 1944 cm^{-1} and **A'** appeared at 1893 cm^{-1}. Comparing the values for **9** and **10** with those measured by Terblans it is clear that the nature of the carbonyl is similar for thiophene and bithiophene complexes.

4.3.4 Mass spectrometry

Fragmentation data for complexes are summarized in **Table 4.4**. The data shows a general fragmentation pattern, in which the carbonyls are lost initially, followed by the loss of the COEt fragment energies.

Table 4.4: Fragmentation data for 9 and 10.

Fragment	**9**		**10**	
	m/z	I/%	*m/z*	I/%
M$^+$	412	11.7	658.2	13.9
M$^+$-2CO	356	81.1	602.1	44.9
M$^+$-4CO	-	-	546.0	100.0
M$^+$-COEt	299	100.0	489.0	39.8
M$^+$-2COEt	-	-	431.9	38.7

The fragmentation pattern deduced from the fragment ions observed for **9** and **10** follows the same sequence as those of the chromium and tungsten complexes. In the case of the monocarbene complex, both CO ligands are lost simultaneously. This is followed by the loss of a COEt fragment. Thereafter, no more identifiable fragments were observed.

For the biscarbene complex, the initial loss of two CO ligands is followed by the loss of a second pair of CO ligands. A COEt fragment is then lost followed by the loss of the other COEt fragment. Thereafter, no further identifiable fragments were observed.

The quality of the manganese biscarbene mass spectrum is much better than those of chromium or tungsten. This could possibly be ascribed to the fact that the manganese complexes are more volatile.

5 IRON BITHIENYL COMPLEXES

5.1 Introduction

For the sake of comparison between the bithiophene biscarbene complexes of the transition metals and bithienylene complexes it was necessary to use a transition metal, known to readily form alkyl bonds. Iron provides a convenient example. Several types of neutral iron carbene complexes have been prepared[1] which can be represented in general terms by: $[Cp^*(CO)XFe{=}C(ER)_2]$, $[Cp^*(^2D)_2Fe{=}CR(ER)]$, $[Cp^*(CO)XFe{=}CR(ER)]$, $[Cp^*(CO)(^2D)Fe{=}CR(ER)]$, $[Cp^*(CO)_2Fe{=}C(ER)_2]$, $[Cp^*(CO)RFe{=}C(ER)_2]$. At least two neutral 19-electron carbene complexes of iron are known with $Cp^* = C_5Me_5$. E represents a heteroatom such as N, O, S, and R represents a set of organic groups to achieve a rare gas shell in which the second or third iron atom is part of the carbene ligand (parts of the general groups R or ER). ^2D is either CO or $PCH_3(C_6H_5)_2$.

Iron has readily interchangeable Fe^{2+}- Fe^{3+} oxidation states, which make it particularly useful in the formation of molecular "wires" when bonded to aromatic rings and their polymers.

---

[1] J. Faust, W. Petz, J. Füssel, *Iron-carbene Complexes*, Springer-Verlag, Berlin, 1993.

Lapinte *et al*[2] have made a study of organometallic molecular wires based on the organoiron synthon (dppe)Cp*Fe (dppe = 1,2-bis(diphenylphosphino)ethane). They found the rich redox chemistry of iron to be especially useful in the synthesis of terminally capped molecular wires as it allowed the production of complexes with terminals possessing different redox states and facilitated the measurement and monitoring of metal-to-metal communication. Amongst other aromatic ligands, they chose thiophene and its oligomers for use as spacer units as these molecules fit the requirements for inter-molecular electron transfer because of their extensive delocalized π-systems.

Weyland *et al*[3] prepared bi- and tri- nuclear iron(III) complexes using $[Cp^*(dppe)Fe-]^+$ units bridged through 1,3-diethynylbenzene and 1,3,5-triethynylbenzene spacers to investigate ferromagnetic metal-metal exchange interactions. They discovered robust organometallic bi- and triradicals have a ferromagnetic coupling, with a magnetic interaction of significant strength, at nanoscale distances when using the phenyl ethynyl bridge between the two metal centres. Further study[4] of these complexes by Mössbauer spectroscopy, as well as ESR and UV-vis spectrometry, indicated that they contained localized Fe(II) and Fe(III) sites which facilitated electron transfer through these molecules.

Non-linear optics is another field in which these compounds find application. Weyland[5] also reported the production of a mixed valence Fe(II)/Fe(III) complex (with a phenyl ethynyl spacer) and investigated its usefulness in this application. The complex was shown to be one of the few known complexes to have fully reversible

---

[2] F. Paul, C. Lapinte, *Coord. Chem. Rev.*, 178-180, **1998**, 431.

[3] T. Weyland, K. Costuas, A. Mari, J.F. Halet, C.Lapinte, *Organometallics*, 17, **1998**, 5569.

[4] T. Weyland, K. Costuas, L. Toupet, J.F. Halet, C. Lapinte, *Organometallics*, 19, **2000**, 4228.

[5] T. Weyland, I. Ledoux, S. Brasselet, J. Zyss, C. Lapinte, *Organometallics*, 19, **2000**, 5235.

redox systems, which can be controlled by a one-electron redox process making it suitable for use as a reversible electronic switch of the molecular non-linear optical response.

Kiesewetter *et al*[6] pointed out that the preparation of complexes with hydrocarbons having sp^2 and sp- carbons bonded to iron is not straightforward, they therefore investigated methods for making iron-hydrocarbon complexes which have potential use in the field of molecular conductors. Amongst other such complexes they produced the dinuclear bis(acyl) complex $[Fe_2(Cp)_2(CO)_4\{\mu\text{- }C(O)C_4H_2SC(O)\}]$ by reacting $[Fe\ Cp(CO)_3]PF_6$ with dilithiated thiophene in the presence of TMEDA (**Fig. 5.1**).

Le Stang *et al*[7] also synthesized mixed valence complexes of iron, of the type [Cp*(dppe)Fe-C C-X-C C-Fe(dppe)Cp*][PF$_6$]. They compared the properties of the thiophene (X = 2,5-C_4H_2S) bridged complex with those of the all carbon bridged complex, without the thienylene spacer unit, and discovered that the introduction of the thiophene fragment constituted an attractive means of extending the size of molecular wires due to greatly facilitated synthesis with no noticeable negative impact on the electron conduction. Furthermore, the thiophene spacer appeared to provide more appropriate molecular arrangements in the solid state for efficient intramolecular electron transfer.

The iron precursor $[Fe(CpI)(CO)_2CH_3]$ and 2,5-bis[(trimethylstannyl)ethynyl]-thiophene were reacted by Buttinelli *et al*[8] in the presence of palladium in the first

---

[6] J. Kiesewetter, G. Poignant, V. Guerchais, *J. Organomet. Chem.*, 595, **2000**, 81.
[7] S. Le Stang, F. Paul, C. Lapinte, *Organometallics.*, 19, **2000**, 1035.
[8] A. Buttinelli, E. Viola, E. Antonelli, C. Lo Sterzo, *Organometallics*, 17, **1998**, 2574.

step of a polymerization reaction to form polymetalla-acetylides. These compounds also have found valuable application in the field of molecular conductors.

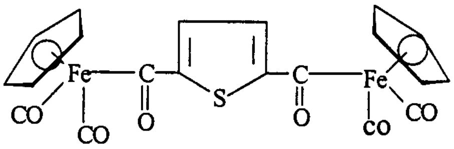

FIG. 5.1: **Dinuclear iron complex with thiophene spacer.**

5.2 Synthesis of dinuclear bisiron bithiophene bisalkyl complexes

The mono- and bisbithiophene iron complexes with a bithiophene spacer were synthesized according to the method described before for the synthesis of biscarbene complexes. The butyllithium:TMEDA complex was used to abstract both the 5- and 5′-protons from the bithiophene rings, at low temperatures, when two equivalents of the base was reacted with one equivalent of bithiophene. Cyclopentadienyl iron dicarbonyl iodide[9] was added, at which point nucleophilic attack by the dianion of the bithienylene occurs at the metal site by displacing the iodide ions. **Fig. 5.2** shows the reaction scheme.

The yellow monobithienyl complex, **11**, and the orange-red bisbithienyl complex, **12**, were the only isolable products. These were purified and subsequently characterized by NMR spectroscopy, as well as infrared spectroscopy and mass spectrometry. The dinuclear

iron bithienylene complex is much more stable than the corresponding dinuclear

---

[9] R. B. King, F.G.A. Stone, *Inorg. Synth.*, 7, **1963**, 110.

biscarbene complexes of chromium or tungsten, hence no further reactions were observed.

Notably no carbonyl insertion reactions occurred to stabilize the Fe-C alkyl bond..

These are usually common for iron alkyl bonds in coordinating solvents[10]

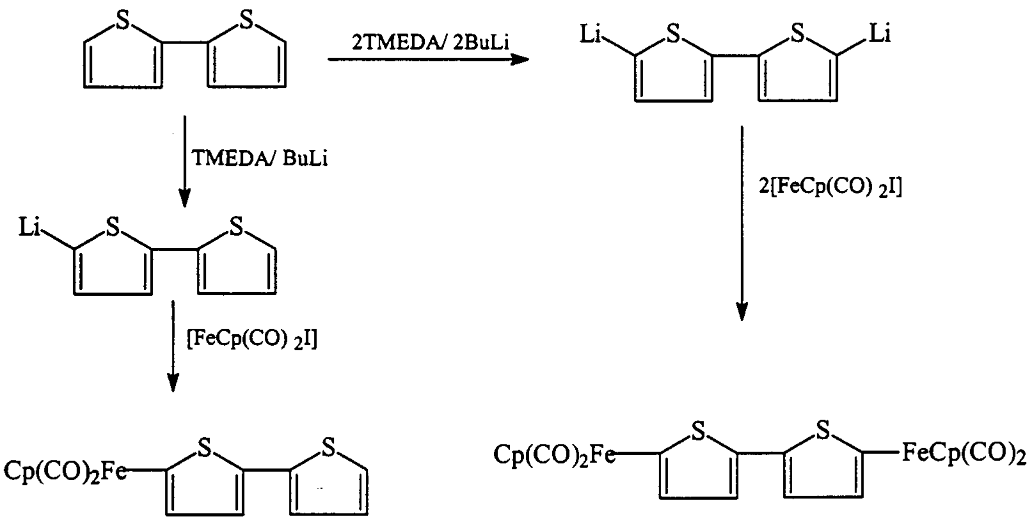

11 12

FIG. 5.2: Reaction scheme for the formation of 11 and 12.

5.3 Spectroscopic characterization of iron bithiophene complexes.

5.3.1 ^{1}H NMR spectroscopy

.The ^{1}H NMR data are represented in **Table 5.1.**

---

[10] J.P. Collman, R.G. Finke, J.N. Cawse, J.I. Brauman, *J. Am. Chem. Soc.*, 100, **1978**, 4766.

Table 5.1: ^{1}H NMR data for 11 and 12.

Proton	Chemical Shifts (δ, ppm) and Coupling Constants (J, Hz)			
	11		12	
	δ	J	δ	J
H_3	7.24 (s) (br)	-	6.96 (d)	1.8
H_4	6.98 (s) (br)	-	6.64 (d)	2.3
H_7	7.05 (m)	4.4	6.64 (d)	2.3
H_8	6.93 (m)	3.9	6.96 (d)	1.8
H_9	7.11 (s) (br)		-	-
C_4H_5	4.98 (s)	-	4.96 (s)	-

All NMR spectra were recorded in deuterated chloroform as solvent. The data support the molecular structures proposed for these complexes.

Despite repeated attempts, it was not possible to obtain a good spectrum for **11** as it decomposed quickly in solution compared with **12**, which was stable both in solution and in the solid state. Only broad singlets for **H_3**, **H_4** and **H_9** and multiplets for **H_7** and **H_8**, in which the coupling could not clearly be elucidated, could be observed. These signals appear upfield of the signals for chromium, tungsten and manganese and, in some cases, upfield of the signal for the free ligand. This can be ascribed to the lack of the electron-withdrawing carbene moiety in these complexes. There is, however, some influence from the metal in terms of the order in which the hydrogen signals appear in the spectrum. This mimics the order of appearance of signals in the spectra of chromium, tungsten and manganese.

The hydrogen closest to the metal appears furthest downfield due to coordination to the iron resulting in slight deshielding of this proton. The signal for **H_9** appears next due to similar electronic effects as shown in **Fig. 2.10** in **Chapter 2**.

The presence of the Cp ring is indicated by the signal at 4.98 ppm in **11** and 4.96 ppm in **12**.

5.3.2 ^{13}C NMR spectroscopy

The ^{13}C NMR data for complexes are shown in **Table 5.2**.

The data support the molecular structures proposed for these complexes.

The quaternary carbons, **C_2**, **C_5**, **C_6** and, in the case of the dinuclear thienylene complex, **C_9** were not detected. The signals are all upfield of those for the chromium, tungsten and manganese complexes and are close to those for free bithiophene.

Table 5.2: ^{13}C NMR data for 11 and 12.

Carbon	**Chemical Shifts (δ, ppm)**	
	11	**12**
C_2	n.o.[a]	n.o.
C_3	138.2	139.3
C_4	120.7	124.5
C_5	n.o.	n.o.
C_6	n.o.	n.o.
C_7	124.8	124.5
C_8	126.5	138.3
C_9	121.4	n.o.
C_5H_5	84.7	86.1
$M(CO)_2$	213.2	214.8

[a] n.o. = not observed.

The order of appearance of the signals is the same as that for the chromium, tungsten and manganese complexes. There is only one signal for the two carbonyl ligands.

These signals appear downfield of those for the tungsten complexes, but upfield of those for the manganese and chromium complexes. Landman[11] prepared and characterized several iron complexes with thienyl and thienothienyl spacers. The 2,5-$\{FeCp(CO)_2\}_2$thiophene complex and the mono- and diiron complexes of 3,6-dimethylthieno[3,2-b]thiophene are of particular interest. Landman recorded chemical shifts of 215.2, 214.4 and 214.2 ppm respectively for the $M(CO)_2$ signals of these complexes. Comparing these values with those for the $M(CO)_2$ signals of **11** and **12** (213.2 ppm and 214.8 ppm) it is clear that the chemical environments of the metal carbonyls is similar for all these complexes.

5.3.3 Infrared Spectroscopy

The Infrared data for complexes are summarized in **Table 5.3**.

Table 5.3: Infrared Data for 11and 12.

Band	Stretching Vibrational Frequency, ν_{CO}, cm^{-1}	
	11	**12**
A	2034(m)	2028(m)
A'	1987(m)	1976(m)

The ν_{CO} values for the **A** and **A'** bands of $CpFe(CO)_2Me$ were recorded by Piper *et al*[12] at 2010 and 1955 cm^{-1} respectively, considerably lower than those of $CpFe(CO)_2Ph$, which they reported at 2020 and 1960 cm^{-1}.

---

[11] M. Landman, *Synthesis of Metal complexes with Thiophene Ligands*, University of Pretoria, **2000**.

[12] T. S. Piper, G. Wilkinson, *J. Inorg. Nucl. Chem.*, 3, **1956**, 104.

Landman[11] reported values of 2025 and 1972 cm^{-1} for the 2,5-{FeCp(CO)$_2$}$_2$thiophene complex and the 2026 and 1974 cm^{-1} for the monoiron complex of 3,6-dimethylthieno[3,2-b]thiophene and signals at 2023 and 1972 cm^{-1} for the diiron complex of 3,6-dimethylthieno[3,2-b]thiophene. Comparing these values with those obtained for **11** and **12**, it seems that the signals shift to higher frequencies as the ligand changes from Me < Ph < thiophene < thienothiophene < bithiophene.

5.3.4 Mass spectrometry

Fragmentation data for complexes are summarized in **Table 5.4**.

Table 5.4: Fragmentation patterns for 11 and 12.

Fragment	11		12	
	m/z	I/%	*m/z*	I/%
M^+-CO	314.0	28.7	490.0	5.8
M^+-2CO	285.9	94.1	462.0	75.9
M^+-4CO	-	-	406.0	100.0
M^+-Cp-2CO	219.2	24.7	340.0	4.9
M^+-2Cp-4CO	-	-	274.0	2.1
M^+-$FeC_8H_6S_2^+$	-	-	221.0	0.8
M^+-$C_8H_6S_2^+$	166.0	100.0	166.0	15.58

From the table a general fragmentation pattern in which the carbonyls are lost initially followed by the loss of the Cp fragments emerges. The **m/z** values for the bithiophene ion and, for **12**, the iron-bithienyl ion were observed on the mass spectra.

5.3.5 Conclusion

The synthesis from metallated bithiophene and iron halide precursors was successful in affording binuclear complexes in high yields. It represents an alternative route for metal-carbon coupling reactions involving troublesome tin precursors and palladium catalysts[8]. Even though the bisiron complexes were poorly soluble, spectroscopic measurements were possible in polar solvents, and the complex was fully characterized. The greater stability displayed by the bisiron complexes, compared to the monoiron complexes (which is directly opposite to the case for the mono- and biscarbene complexes) was an unexpected result. In fact, the high stability in air and at room temperature of the diiron complex, **12**, is of great importance for planning future projects when the high instability of the corresponding thienylene complexes[11] is taken into account. Also, LaPinte[2,5,7] used acetylide fragments between the iron metals and the thiophene carbons to stabilize their complexes. Hence, further studies with oligothiophene spacers are essential and the relationship between thiophene chain length and stability needs to be investigated. Unfortunately, the bisiron complex crystallizes to form very flat, sheet-like crystals, which made single crystal structure determinations impossible. Structural studies should involve bisiron complexes where the carbonyl ligands are displaced by bulky phospine ligands. The latter is also important for electrochemical studies.

6 CONCLUSION

The mono- and biscarbene complexes of chromium, tungsten and manganese with a bithiophene spacer were synthesized and characterized. These complexes showed slightly increased stability over those prepared by Terblans *et al*[1] using a thiophene spacer and over those prepared by Landman[2] who used a thienothiophene spacer. This is evident from the fact that, with the exception of chromium, fewer decomposition products were formed for the bithiophene complexes than reported for the other spacer ligands. The chromium complexes were less stable than those of tungsten, which in turn were less stable than the manganese complexes. The latter were most stable of all, exhibiting no decomposition products at all. From this comparison of stabilities, it appears that moving across groups in the periodic table, the stability of the complexes increases.

The mono- and dinuclear bithienylene complexes of iron were also produced and characterized. These were more stable than those produced with a thienylene spacer by Landman[2], who could only isolate the diiron complex as the monothienyl complex was too unstable to purify. The bithienylene diiron complex prepared in this study was found to be very stable. In its solid state, (as flat orange crystals) it showed no visible decomposition even after long (several days) exposure to air. Unfortunately, the solubility of the diiron bithieylene complex was poor. The monobithienyl iron

---

[1] Y.M Terblans, *Thiophene Bimetallic Carbene Complexes*, University of Pretoria, Pretoria, **1996.**
[2] M. Landman, *Synthesis of Metal complexes with Thiophene Ligands*, University of Pretoria, **2000.**

complex was less stable, but could be isolated and analyzed. The monobithienyl complex decomposed quickly in solution however.

The relative stabilities of the mono- and diiron complex represented the exact opposite of those for the carbene complexes, in which the monocarbene complexes showed greater stability than the biscarbene complexes.

The collection of crystallographic data was made difficult because bithiophene decomposes under X-ray radiation[3], but the structures we were able to determine showed clearly that adding substituents to the rings causes the rings to align in the same plane. This has important implications for electron transfer through the rings and the use of such materials in the construction of molecular wires[4].

During the reaction of the chromium metal fragment, with bithiophene a novel organic by-product **5** was discovered and characterized by X-ray crystallography. The question of the origin of this product remains unanswered and will be further investigated. In this product, the rings were coupled via carbonyls, which can find application in the design of new synthetic reaction routes in metal carbonyl chemistry. The sequence, carbonyl to carbene to carbon-carbon coupled product via metallacyclic intermediates is questionable in this instance. Was the carbene step by-passed or does the reaction represent new insights into "carbene chemistry"?

The crystallographic data showed that the molecule is completely flat which would facilitate electron flow through the molecule. This is interesting as it is anticipated that the conjugation will be sidetracked to the very electronegative oxygens of the carbonyl units.

---

[3] G.J. Visser, G.J. Heeres, J. Wolters, A.Vos, *Acta Cryst.*, B24, **1968**, 467.

[4] J. Roncali, *Chem.Rev.*, 97, **1997**, 173.

7 EXPERIMENTAL

7.1 Standard operating procedures

All syntheses and characterization procedures were carried out under an inert atmosphere of nitrogen or argon gas, using standard Schlenk methods[1]. Solvents were dried under an inert atmosphere of nitrogen gas in accordance with the conventional laboratory methods[2]. Unless specified, all other chemicals were used as received, without further purification. Kieselgel 60 (particle size 0.0063 - 0.200 mm) was used in all column chromatography. The columns were cooled by circulating cold (-30 ^{0}C) iso-propanol through the column jacket. Characterization of complexes was done under inert atmosphere where possible.

7.2 Characterization techniques

7.2.1 Infrared spectroscopy

Infrared spectra were recorded on a BOMEM Michelson - 100 FT spectrophotometer,

---

[1] D.F. Shriver, M.A. Drezdon in *The Manipulation of Air-Sensitive Compounds,* 2nd edition, John Wiley and Sons, New York, **1986.**

[2] D.D. Perrin, W.L.F. Armarego, D.R. Perrin in *Purification of Laboratory Chemicals,* 2nd edition, Pergamon, New York, **1980.**

using either dichloromethane or hexane as a solvent. Only the vibrational bands in the carbonyl stretching region (ca. 1500 - 2200 cm^{-1}) are reported.

7.2.2 Nuclear magnetic resonance spectroscopy

NMR spectra were recorded on a Brüker AC-300 spectrometer. ^{1}H NMR spectra were recorded at 300.135 MHz and ^{13}C NMR spectra were recorded at 75.469 MHz. The signal of the deuterated solvent was used as a reference, e.g. for ^{1}H NMR the signal of deuterated chloroform is at 7.24 ppm and for ^{13}C NMR the signal for deuterated chloroform is at 77.0 ppm.

7.2.3 Mass spectrometry

Mass spectra were measured by the electron impact method and were all recorded on a Finnegan 8200 mass spectrometer at ca 70eV.

7.2.4 Melting point determinations

Only those melting points, which could be measured without decomposition of the products, were recorded. These were measured using a Gallenkamp Melting Point Apparatus.

7.2.5 X-ray crystallography

Crystallographic data for complexes **5** and **6**, measured at 296 K with an Enraf Nonius CAD4 diffractometer using graphite-monochromated Mo-radiation, are listed in Tables A1 and B1. Unit cell dimensions were obtained by the least squares method, fitting the setting angles of 25 high order reflections for each crystal. During data collection, the orientation of the crystals was verified every 400 reflections and three standard reflections were measured every hour, for each crystal, to check crystal stability. Optimum values for scan angles and aperture settings were determined experimentally. The data sets were corrected for absorption (empirical, based on azimuthal scans of nine reflections for each crystal) as well as for Lorentz-polarization effects.

The structures were solved by conventional direct methods and Fourier techniques using SHELX86[3], and were refined using $\sigma^{-2}(F_o)$ weights and full matrix methods with SHELX76[4]. All the non-hydrogen atoms were refined anisotropically, and the hydrogen atoms were placed in calculated positions and were refined (using a riding model) with common isotropic thermal parameters that converged as indicated in Tables **A1** and **B1**. Atomic scattering factors were taken from the literature[5]. Some disorder existed in one of the thiophene rings of one of the two molecules in the asymmetric unit in **6**, but a satisfactory solution was obtained by fixing the bond distances to standard values.

Both crystals of **5** and **6** were of relatively poor diffraction quality and this fact influenced the quality of the solutions. It was not possible to obtain any better crystals

---

[3] G. M. Sheldrick, SHELX86. *A program for the solution of crystal structures*. University of Göttingen, **1986**.

[4] G. M. Sheldrick, SHELX76. *Program for crystal structure determination*. University of Cambridge, **1976**.

[5] International Tables for X-Ray Crystallography, Kynoch press. Birmingham, **1974**, Volume IV. D. T. Cromer and D. Liberman, *J. Chem. Phys.*,4, **1970**, 1891.

using a wide variety of solvents and different crystallization techniques. It was suspected that a higher symmetry space group for **6** could exist, but this could not be observed with the quality of the crystals available.

7.3 Synthesis of organometallic compounds

7.3.1 Preparation of precursors

The following compounds were prepared according to known literature methods: Cyclopentadienyliron dicarbonyl iodide[6], and triethyl oxonium tetrafluoroborate[7].

7.3.2 Lithiation of bithiophene

In each case, the first step of the synthesis involved the dilithiation of bithiophene. Bithiophene (0.83 g, 5 mmol) was weighed out and dissolved in 50 ml of tetrahydrofuran (THF) at -90 ^{0}C under Argon gas. The clear solution was stirred continuously. 1.50 ml, (10 mmol) of tetramethylethylenediamine (TMEDA) was added, followed by 6.4 ml (10 mmol) of n-BuLi (which was added drop wise). The solution was stirred for 5 minutes after the additions and then allowed to warm up slightly to -50 ^{0}C. It was stirred for another 15 minutes at this temperature, during which the solution changed colour from clear to milky (in some cases a slight yellow coloration was also observed). Reaction of this lithiated product with the relevant transition metal complex followed immediately.

---

[6] R.B. King, F.G.A. Stone, *Inorg. Synth.*, 7, **1963**, 110.

[7] H. Meerwein, *Org. Synth.*, 46, **1966**, 113.

7.3.3 The synthesis of bithiophene chromium complexes

The solution of lithiated bithiophene was cooled to -80 ^{0}C and stirred. [Cr(CO)$_6$], (2.2 g, 10 mmol) was added and the mixture turned bright yellow. This was stirred at -80 ^{0}C for 1 hour and then allowed to warm to room temperature (20 ^{0}C) and stirred for another hour during which it turned bright red. The THF was removed under reduced pressure and replaced with 50 ml of dichloromethane. The solution was then cooled to -30 ^{0}C and 1.9 g (10 mmol) Et$_3$OBF$_4$ was added. This was stirred for 1 hour at -30 ^{0}C and then allowed to heat up to room temperature (20 ^{0}C) and stirred for a further 1 hour during which it turned dark purple.

The solvent was removed under reduced pressure and the reaction mixture purified by column chromatograhy. The first fraction collected was the known yellow butyl carbene complex, [Cr{C(OEt)Bu}(CO)$_5$] and was discarded. The second fraction eluted with pure hexane and was identified as the red, monocarbene complex, [Cr{C(OEt)C$_4$H$_2$S-C$_4$H$_3$S}(CO)$_5$], 0.890 g (43 %). The third fraction was eluted using 1:1 hexane:dichloromethane as the eluent and was found to be the deep purple biscarbene complex, [(CO)$_5$Cr{C(OEt)C$_4$H$_2$S-C$_4$H$_2$SC(OEt)}Cr(CO)$_5$], 1.5 g (45 %). The fourth fraction was removed using pure dichloromethane and identified as the decomposition product, [Cr{C(OEt)C$_4$H$_2$S-C$_4$H$_2$SC(O)OEt}(CO)$_5$], 0.243 g (10 %). It was deep pink in colour. The monocarbene complex was found to yield another product upon crystallization: [C$_4$H$_3$S-C$_4$ H$_2$SC(O)C(O) C$_4$H$_2$S-C$_4$H$_3$S].

7.3.4 The synthesis of bithiophene tungsten complexes

These were produced by a single reaction of an excess of [W(CO)$_6$] with the lithiation product formed according to the method above. The solution of lithiated bithiophene was cooled to -80 ^{0}C and stirred during the addition of [W(CO)$_6$] (3.5 g, 10 mmol). The reaction mixture was stirred continuously for 1 hour after the addition during which time it changed colour to a milky yellow-green. The mixture was then allowed to warm up to room temperature (20 ^{0}C) and was stirred for a further 1 hour. The colour changed again to yield a bright red milky solution. The THF was then removed under reduced pressure and the contents of the Schlenk tube were re-dissolved in dichloromethane (50 ml). The solution was cooled to -30 ^{0}C and 1.9 g (10 mmol) of triethyloxonium tetrafluoroborate (Et_3OBF_4) was added while the solution was stirred. The mixture was stirred for an hour at -30 ^{0}C and then allowed to warm up to room temperature (20 ^{0}C). It was stirred for another 1 hour during which it turned bright red. The solvent was removed under reduced pressure. The products were isolated from a chromatography column using dichloromethane and hexane as eluents. The first fraction was a yellow product, identified as the known butyl carbene complex, [W{C(OEt)Bu}(CO)$_5$]. It was present in a very small amount, and was discarded. The next was a red product identified as the mono-carbene complex [W{C(OEt)C_4H_2S-C_4H_3S}(CO)$_5$]. It was eluted with pure hexane and the yield was 0.606 g (28 %). The third fraction was dark purple in colour and was eluted with a 1:1 hexane:dichloromethane mixture. It was identified as the biscarbene product, [(CO)$_5$W{C(OEt)C_4H_2S-C_4H_2SC(OEt)}W(CO)$_5$], yield 1.72 g (49 %). A fourth fraction was also collected using 1:1 hexane:dichloromethane as eluent. It was dark red in colour and identified as the decomposition product [W{C(OEt)C_4H_2S-C_4H_2SC(O)OEt}$(CO)_5$], yield 0.278 g (11 %).

7.3.5 The synthesis of bithiophene manganese complexes

The lithiated solution prepared according to **7.3.2** above was cooled to -80 ^{0}C and stirred while 1.59 ml (2.19 g, 10 mmol) [MnCpMe$(CO)_3$] was added. The mixture was stirred for 1 hour at -80 ^{0}C and then allowed to warm up to room temperature (20 ^{0}C). It was stirred at room temperature for an hour. The solvent was removed under reduced pressure and replaced by 50 ml of dichloromethane. The solution was then cooled to -30 ^{0}C and 1.9 g (10 mmol) Et_3OBF_4 was added. The mixture was stirred for one hour and then allowed to warm to room temperature. It was then stirred for another hour during which the solution turned dark red. The solvent was removed under reduced pressure and the products purified by column chromatography. In this case the first fraction was an organic one and was discarded, the second fraction removed with hexane as an eluent was the yellow dimanagenese complex, [$Mn_2(CO)_{10}$] (yield about 2 %). This was discarded, as it was not present in sufficient amount for analysis. The third fraction was dark purple and identified as the biscarbene complex [MeCp$(CO)_2$Mn{C(OEt)(C_4H_2S-C_4H_2SC(OEt)}Mn$(CO)_2$CpMe]. It was eluted using a 1:1 mixture of hexane:dichloromethane at a yield of 1.81 g (55 %). The Mn monocarbene complex [MnCpMe{$(CO)_2$C(OEt)C_4H_2S-C_4H_3S}] was removed using pure dichloromethane and was orange-red in colour (yield : 0.743 g, 35 %).

7.3.6 The synthesis of bithiophene iron complexes

The solution of lithiated bithiophene prepared as in **8.3.1** above was cooled to -80 ^{0}C and stirred while cyclopentadienyl iron dicarbonyl iodide [$FeCp(CO)_2I$] (3.0 g, 10 mmol) was added. The mixture was stirred for 1 hour at -80^{0}C and then allowed to warm up to room temperature and stirred for another hour. The solution turned bright red. The solvent was then removed under reduced pressure and replaced with 50ml of dichloromethane. The reaction mixture was filtered through a silica gel filter using dichloromethane. This resulted in a thick layer of orange solid forming on the top of the filter. More of this orange product was recovered by washing the filtrate with hexane - as the orange product showed only very slight solubility in hexane and the rest of the reaction products could easily be dissolved in hexane. The orange product was identified as the diiron bithienylene complex: [$Cp(CO)_2Fe\{C_4H_2S\text{-}C_4H_2S\}Fe(CO)_2Cp$] with a yield of 2.31 g (88.9%). It readily formed crystals out of 1:1 dichloromethane:hexane. The crystals were flat, orange and air stable; however, they were too thin for crystallographic studies to be carried out on them successfully.

The remainder of the product mixture was separated by column chromatography. The first fraction to be removed with pure hexane was a yellow-green oil in too small a quantity for analysis (about 2%). It was discarded. The second fraction was removed using a 1:1 hexane:dichloromethane mixture as eluent. This was identified as the yellow monocarbene complex, [$FeCp\{C(OEt)C_4H_2S\text{-}C_4H_3S\}(CO)_2$], with a yield of 0.129 g, 7.5%. It was very unstable and decomposed rapidly in solution as well as when solvent was removed under reduced pressure. The decomposition of this product gave a brown product, which could not be dissolved and therefore could not be analyzed.

APPENDIX A

Table A1: Crystallographic data for 5.

Empirical formula	$C_{18}H_{10}O_2S_4$
fw	386.54
Space group	C2/c (no. 15)
a, Å	21.982 (8)
b, Å	7.422 (3)
c, Å	12.248 (6)
α, °	90
β, °	123.42 (4)
γ °	90
V, $Å^3$	1668 (1)
Z	4
$F(000)$	792.00
D_c, g cm^{-3}	1.54
Crystal size, mm/colour	0.16 x 0.19 x 0.23, white
μ(Mo-K_α), cm^{-1}	5.12
Scan type (ω:2θ)	1:1
Scan range (θ °)	$3<\theta°<30$
Zone collected: h; k; l	(-30, +30); (0, +10); (0, +17)
Max scan speed (deg.min^{-1})	4.12
Max. Scan time, sec.	60
Scan angle (ω+ 0.34tanθ) °	0.61
Aperture size (mm)	1.3 x 4.0
No. Reflections measured	2709
Decay, %(uncorrected)	1.3 %
EAC correction factor: max, min, av.	1.000, 0.830, 0.902
No. unique reflections ($I>3\sigma(I)$)	1423
R_{int}	0.017
Parameters refined	110
Max. Positional shift/esd	<0.01
Res. elect. dens. ($eÅ^{-3}$): max, min	1.061, -0.954
Residuals: R^a, R_w^b	0.106, 0.081

^{a} $R = \sum[|F_o| - |F_c|]/\ \sum|F_o|$. ^{b} $R_w = \sum[w(|F_o| - |F_c|)^2/\ \sum w|F_o|]^{½}$; $w^{-1} = \sigma^2(F_o)$

Table A2: Fractional atomic coordinates (x10^4) and equivalent thermal parameters (x 10^3 Å^2) for 5.

	x_a	y_b	z_c	U_{eq}
O(1)	4530(3)	1388(9)	897(5)	68(2)
C(1)	4616(3)	696(12)	1879(7)	50(2)
C(2)	4024(3)	-1(12)	1946(7)	48(2)
C(3)	4056(4)	-926(12)	2928(8)	53(2)
C(4)	3368(4)	-1398(12)	2651(7)	51(2)
C(5)	2827(4)	-813(11)	1474(7)	45(2)
S(1)	3139(1)	315(3)	639(2)	50(1)
C(6)	2005(4)	-888(11)	814(8)	51(2)
C(7)	1428(3)	-352(11)	-416(7)	37(2)
C(8)	779(5)	-767(14)	-542(9)	81(3)
C(9)	853(4)	-1457(14)	519(9)	75(3)
S(2)	1722(1)	-1717(5)	1786(3)	91(1)

Table A3: Fractional coordinates of the hydrogen atoms (x10^4) and isotropic thermal parameters (x 10^3 Å^2) for 5.

	x_a	y_b	z_c	U_{iso}
H(3)	4560(4)	-1281(12)	3827(8)	76(11)
H(4)	3287(4)	-2162(12)	3311(7)	76(11)
H(7)	1482(3)	243(11)	-1209(7)	76(11)
H(8)	248(5)	-558(14)	-1427(9)	76(11)
H(9)	399(4)	-1811(14)	586(9)	76(11)

Table A4: Anisotropic thermal parameters (x10^3 °A^2) for 5.

	U(11)	U(22)	U(33)	U(23)	U(13)	U(12)
O(1)	36(3)	114(6)	68(4)	16(4)	37(3)	1(4)
C(1)	36(4)	73(7)	48(5)	8(5)	28(4)	6(4)
C(2)	30(4)	73(7)	45(4)	3(5)	24(3)	1(4)
C(3)	33(4)	73(7)	55(5)	3(5)	26(4)	6(4)
C(4)	41(4)	63(6)	60(5)	12(5)	34(4)	3(4)
C(5)	43(4)	55(6)	50(5)	1(4)	35(4)	-5(4)
S(1)	33(1)	73(2)	49(1)	5(1)	27(1)	-1(1)
C(6)	59(5)	48(6)	82(6)	-6(5)	61(5)	-13(4)
C(7)	14(3)	57(5)	46(4)	5(4)	21(3)	-3(4)
C(8)	58(6)	109(10)	69(7)	21(7)	30(5)	5(6)
C(9)	30(4)	94(8)	104(8)	-13(7)	39(5)	-10(5)
S(2)	68(2)	130(3)	98(2)	5(2)	59(2)	-11(2)

Table A5: Bond lengths and bond angles for 5

	Bond Length/Å		Bond Angle/^{O}
O(1)-C(1)	1.223(8)	O(1)-C(1)-C(2)	123.3(7)
C(1)-C(1')	1.527(13)	C(1)-C(2)-S(1)	119.3(6)
C(1)-C(2)	1.445(9)	C(1)-C(2)-C(3)	128.7(7)
C(2)-C(3)	1.353(10)	C(3)-C(2)-S(1)	112.0(6)
C(2)-S(1)	1.723(7)	C(2)-C(3)-C(4)	113.1(7)
C(3)-C(4)	1.400(9)	C(3)-C(4)-C(5)	112.3(7)
C(4)-C(5)	1.338(9)	C(4)-C(5)-S(1)	112.8(5)
C(5)-S(1)	1.729(7)	C(4)-C(5)-C(6)	130.6(7)
C(5)-C(6)	1.520(9)	S(1)-C(5)-C(6)	116.4(5)
C(6)-C(7)	1.422(9)	C(2)-S(1)-C(5)	89.8(4)
C(6)-S(2)	1.732(7)	C(5)-C(6)-C(7)	130.8(6)
C(7)-C(8)	1.409(10)	C(5)-C(6)-S(2)	114.8(6)
C(8)-C(9)	1.320(11)	C(7)-C(6)-S(2)	114.4(5)
C(9)-S(2)	1.681(8)	C(6)-C(7)-C(8)	105.8(7)
		C(7)-C(8)-C(9)	116.3(8)
		C(8)-C(9)-S(2)	114.5(7)
		C(6)-S(2)-C(9)	88.9(4)

Table A6: Selected torsion angles for 5.

Atoms involved	Torsion Angle/$^{\circ}$
O(1)-C(1)-C(2)-C(3)	173.7(1)
O(1)-C(1)-C(2)-S(1)	-5.8(1)
C(1)-C(2)-C(3)-C(4)	-179.7(1)
S(1)-C(2)-C(3)-C(4)	-0.1(1)
C(1)-C(2)-S(1)-C(5)	-179.7(1)
C(3)-C(2)-S(1)-C(5)	0.5(1)
C(2)-C(3)-C(4)-C(5)	-0.6(1)
C(3)-C(4)-C(5)-S(1)	1.0(1)
C(3)-C(4)-C(5)-C(6)	-174.9(1)
C(4)-C(5)-S(1)-C(2)	-0.9(1)
C(6)-C(5)-S(1)-C(2)	175.6(1)
C(4)-C(5)-C(6)-C(7)	-176.3(1)
C(4)-C(5)-C(6)-S(2)	5.3(1)
S(1)-C(5)-C(6)-C(7)	7.8(1)
S(1)-C(5)-C(6)-S(2)	-170.4(1)
C(5)-C(6)-C(7)-C(8)	178.9(1)
S(2)-C(6)-C(7)-C(8)	-2.7(1)
C(5)-C(6)-S(2)-C(9)	-176.0(1)
C(7)-C(6)-S(2)-C(9)	2.3(1)
C(8)-C(6)-S(2)-C(9)	0.7(1)
C(6)-C(7)-C(8)-C(9)	1.7(1)
C(7)-C(8)-C(9)-S(2)	-0.0(1)
C(8)-C(9)-S(2)-C(6)	-1.3(1)

APPENDIX B

Table B1: Crystallographic data for 6

Empirical formula	$C_{16}H_{10}O_6S_2W$
fw	546.23
Space group	P-1 (no. 2)
a, Å	7.605 (3)
b, Å	9.706 (1)
c, Å	25.272 (3)
α, °	91.35 (1)
β, °	91.65 (2)
γ, °	94.02 (2)
V, Å ^{3}	1859 (1)
Z	4
$F(000)$	1039.81
D_c, g cm^{-3}	1.95
Crystal size, mm/colour	0.21 x 0.25 x 0.31, red
μ(Mo-K$_\alpha$), cm^{-1}	61.75
Scan type (ω:2θ)	1:1
Scan range (θ °)	$3<\theta^\circ<30$
Zone collected: h; k; l	(-10, +10); (-13, +13); (0, +35)
Max scan speed (deg.min^{-1})	5.49
Max. Scan time, sec.	60
Scan angle (ω + 0.34tanθ) °	0.47
Aperture size (mm)	1.3 x 4.0
No. reflections measured	11030
Decay, %(corrected)	3.5 %
EAC correction factor: max, min, av.	1.000, 0.878, 0.951
No. unique reflections (I>3σ(I))	6483
R_{int}	0.00
Parameters refined	458
Max. Positional shift/esd	<0.08
Res. elect. dens. (eÅ^{-3}): max, min	1.521, -0.923
Residuals: R^a, R_w^b	0.052, 0.038

${}^a R = \sum[|F_o| - |F_c|] / \sum|F_o|$. ${}^b R_w = \sum[w(|F_o| - |F_c|)^2 / \sum w|F_o|]^{½}$; $w^{-1} = \sigma^2(F_o)$

Table B2: Fractional atomic coordinates ($x10^4$) and equivalent thermal factors ($x\ 10^3$ Å^2) for 6.

	x_a		y_b		z_c		U_{eq}	
	Molecule A	Molecule B	Molecule A	Molecule B	Molecule A	Molecule B	Molecule A	Molecule B
W(1)	7350(1)	3843(1)	80137(1)	11103(1)	4237(1)	1325(1)	48(1)	65(1)
C(1)	7390(10)	3626(13)	6677(8)	8869(9)	3568(2)	1461(4)	59(2)	61(3)
O(1)	7304(8)	3882(10)	5296(6)	7846(6)	3568(2)	1120(3)	59(2)	74(2)
C(2)	7595(11)	3218(12)	7016(8)	8249(9)	3019(3)	1961(4)	45(2)	54(2)
C(3)	7576(12)	2697(13)	8281(9)	8837(10)	2775(4)	2420(4)	56(2)	63(3)
C(4)	7928(12)	2425(12)	8251(10)	7927(10)	2233(4)	2824(4)	60(3)	62(3)
C(5)	8203(11)	2743(12)	6929(10)	6578(8)	2053(4)	2684(3)	58(3)	60(3)
S(1)	8001(3)	3335(3)	5750(3)	6483(2)	2550(1)	2044(1)	58(1)	60(1)
C(6)	8635(13)	2659(13)	6423(12)	5314(7)	1517(4)	2957(2)	71(3)	101(4)
C(7)	8845(13)	2840(13)	4976(11)	3918(6)	1349(3)	2802(3)	63(3)	42(2)
C(8)	9355(22)	2563(20)	5170(17)	3009(12)	804(7)	3228(4)	139(6)	203(8)
C(9)	9375(20)	2221(15)	6367(17)	3645(6)	596(5)	3722(5)	128(6)	130(5)
S(2)	8973(6)	2175(6)	7613(5)	5422(5)	1041(2)	3629(2)	143(2)	159(2)
C(10)	7167(14)	4257(17)	4494(9)	8076(10)	4043(4)	566(4)	67(3)	89(4)
C(11)	7247(14)	4441(18)	3011(8)	6698(10)	3870(4)	296(4)	72(3)	96(4)
C(12)	7363(12)	1444(16)	9527(10)	11328(11)	4822(4)	1682(4)	63(3)	79(3)
O(2)	7359(10)	181(11)	10336(8)	11482(9)	5170(3)	1867(4)	94(3)	119(3)
C(13)	5407(15)	6236(16)	7035(10)	11058(11)	4607(4)	947(5)	68(3)	81(4)
O(3)	4307(10)	7502(12)	6475(8)	1134(9)	4835(3)	746(4)	94(3)	120(3)
C(14)	5539(13)	2495(18)	9260(9)	10940(12)	3859(4)	621(5)	55(2)	85(4)
O(4)	4564(9)	1741(13)	9942(7)	10985(10)	3674(3)	229(3)	79(2)	115(3)
C(15)	9132(15)	5259(17)	7150(10)	11396(12)	4672(4)	2032(5)	67(3)	80(4)
O(5)	10152(10)	6016(12)	6665(8)	11560(9)	4941(3)	2415(3)	103(3)	106(3)
C(16)	9329(14)	4052(19)	9365(10)	13140(12)	3905(4)	1227(5)	62(3)	105(4)
O(6)	10358(10)	4198(16)	10091(8)	14287(8)	3733(3)	1159(4)	90(2)	163(4)

Table B3: Fractional coordinates of the hydrogen atoms (x10^4) and isotropic thermal parameters (x 10^3 Å^2) for 6.

	x_a		y_b		z_c		U_{iso}	
	Molecule A	Molecule B	Molecule A	Molecule B	Molecule A	Molecule B	Molecule A	Molecule B
H(3)	7311(12)	2513(13)	9220(9)	9927(10)	2987(4)	2463(4)	114(9)	114(9)
H(4)	7977(12)	2006(12)	9147(10)	8233(10)	1987(4)	3212(4)	114(9)	114(9)
H(7)	8668(13)	3154(13)	4038(11)	3588(6)	1568(3)	2407(3)	114(9)	114(9)
H(8)	9724(22)	2603(20)	4296(17)	1904(12)	571(7)	3178(4)	114(9)	114(9)
H(9)	9620(20)	2027(15)	6551(17)	3124(6)	184(5)	4091(5)	114(9)	114(9)
H(10A)	8248(14)	3189(17)	4799(9)	8580(10)	4317(4)	380(4)	114(9)	114(9)
H(10B)	5932(14)	5469(17)	4641(9)	8717(10)	4230(4)	538(4)	114(9)	114(9)
H(11A)	6979(14)	4791(18)	2539(8)	6954(10)	4245(4)	-102(4)	114(9)	114(9)
H(11B)	8606(14)	3273(18)	2901(8)	5996(10)	3774(4)	285(4)	114(9)	114(9)
H(11C)	6392(14)	5515(18)	2509(8)	6213(10)	3564(4)	489(4)	114(9)	114(9)

Table B4: Anisotropic thermal factors ($\times 10^3$ Å^2) for 6.

	U(11)		U(22)		U(33)		U(23)		U(13)		U(12)	
	*A	B	A	B	A	B	A	B	A	B	A	B
W(1)	49(1)	80(1)	51(1)	49(1)	45(1)	67(1)	1(1)	3(1)	5(1)	11(1)	6(1)	9(1)
C(1)	38(5)	64(7)	45(5)	52(5)	58(6)	67(7)	14(4)	-14(5)	4(4)	5(5)	3(4)	10(5)
O(1)	77(5)	117(6)	57(4)	46(4)	45(4)	61(5)	4(3)	1(3)	11(3)	24(4)	8(3)	15(4)
C(2)	47(5)	58(6)	48(5)	53(5)	42(5)	54(6)	-5(4)	-1(5)	5(4)	7(5)	8(4)	9(4)
C(3)	60(6)	69(7)	57(6)	56(6)	51(6)	65(7)	0(5)	-1(5)	7(5)	5(6)	9(5)	3(5)
C(4)	52(6)	56(6)	70(6)	66(6)	57(6)	62(7)	8(5)	3(5)	10(5)	2(5)	3(5)	-1(5)
C(5)	39(5)	41(6)	87(7)	94(8)	48(6)	44(6)	15(5)	3(5)	-2(5)	-1(5)	3(5)	0(5)
S(1)	60(2)	66(2)	63(1)	56(1)	52(1)	60(2)	-4(1)	1(1)	0(1)	11(1)	12(1)	8(1)
C(6)	55(7)	36(6)	119(9)	227(15)	41(6)	42(6)	18(6)	46(8)	-4(5)	1(5)	8(6)	4(8)
C(7)	74(7)	70(6)	85(7)	12(3)	31(5)	43(5)	-19(5)	11(3)	7(5)	12(4)	14(6)	4(3)
C(8)	145(15)	76(11)	154(16)	220(19)	122(16)	308(28)	-44(12)	-182(19)	-15(12)	-1(5)	70(14)	34(13)
C(9)	127(13)	76(9)	209(18)	83(9)	54(9)	231(19)	-39(11)	106(11)	22(9)	-29(11)	71(14)	-13(7)
S(2)	150(4)	125(4)	207(5)	219(5)	75(3)	134(4)	21(3)	22(4)	18(3)	5(3)	28(3)	17(4)
C(10)	96(9)	151(12)	52(6)	74(7)	55(6)	46(6)	12(5)	8(6)	7(6)	33(7)	10(5)	17(7)
C(11)	84(8)	162(13)	43(5)	69(7)	89(8)	57(7)	13(6)	-10(6)	8(7)	27(8)	0(5)	6(8)
C(12)	46(6)	93(10)	81(7)	80(8)	63(7)	66(8)	8(6)	-5(6)	5(5)	0(7)	6(5)	31(7)
O(2)	99(6)	88(7)	102(6)	134(8)	80(6)	144(9)	-36(5)	18(6)	0(5)	35(6)	9(5)	53(6)
C(13)	88(9)	90(10)	63(7)	69(7)	57(7)	85(9)	10(5)	-3(6)	18(6)	20(8)	21(6)	6(7)
O(3)	97(6)	89(7)	91(6)	140(8)	97(6)	130(9)	24(5)	-2(7)	46(5)	38(6)	7(5)	-10(6)
C(14)	79(7)	113(11)	52(6)	72(7)	45(6)	76(9)	-1(4)	12(7)	9(5)	34(8)	3(5)	29(7)
O(4)	74(5)	127(8)	77(5)	138(8)	87(6)	82(7)	7(4)	11(6)	-14(4)	-14(6)	23(4)	32(6)
C(15)	81(8)	97(10)	63(6)	73(8)	58(7)	71(8)	8(5)	-8(7)	-5(6)	16(7)	4(6)	7(7)
O(5)	96(7)	110(8)	99(6)	114(7)	114(7)	92(7)	35(5)	-20(6)	-35(6)	-7(6)	8(5)	12(6)
C(16)	66(7)	147(13)	64(6)	79(8)	56(6)	93(10)	-2(5)	-11(8)	-3(6)	49(9)	13(5)	26(9)
O(6)	72(6)	290(15)	91(6)	55(5)	105(7)	151(10)	14(5)	13(6)	26(5)	89(9)	-21(4)	20(7)

*A and B in this table refer to Molecule A and Molecule B respectively.

Table B5: Bond lengths and bond angles for 6

	Bond Length/Å			Bond Angle/°	
	Molecule A	Molecule B		Molecule A	Molecule B
W(1)-C(1)	2.182(9)	2.199(9)	C(1)-W(1)-C(12)	177.4(4)	90.9(4)
W(1)-C(12)	1.979(10)	2.081(12)	C(1)-W(1)-C(13)	94.4(3)	94.1(4)
W(1)-C(13)	2.026(11)	2.081(12)	C(12)-W(1)-C(13)	88.0(4)	174.9(4)
W(1)-C(14)	2.044(10)	2.024(13)	C(1)-W(1)-C(14)	92.2(3)	94.4(4)
W(1)-C(15)	2.028(11)	2.064(12)	C(12)-W(1)-C(14)	86.8(4)	87.6(5)
W(1)-C(16)	2.062(10)	1.995(12)	C(13)-W(1)-C(14)	90.9(4)	91.2(5)
C(1)-O(1)	1.338(9)	1.328(9)	C(1)-W(1)-C(15)	93.4(4)	89.1(4)
C(1)-C(2)	1.444(11)	1.444(12)	C(12)-W(1)-C(15)	87.7(4)	92.9(5)
O(1)-C(10)	1.450(9)	1.455(10)	C(13)-W(1)-C(15)	88.4(4)	88.0(5)
C(2)-C(3)	1.388(11)	1.362(12)	C(14)-W(1)-C(15)	174.5(4)	176.4(5)
C(2)-S(1)	1.737(8)	1.740(9)	C(1)-W(1)-C(16)	89.8(3)	178.1(5)
C(3)-C(4)	1.405(11)	1.377(12)	C(12)-W(1)-C(16)	87.7(4)	88.4(5)
C(4)-C(5)	1.383(12)	1.388(11)	C(13)-W(1)-C(16)	175.8(4)	86.6(5)
C(5)-C(6)	1.483(12)	1.420(1)	C(14)-W(1)-C(16)	88.9(4)	87.3(5)
C(5)-S(1)	1.722(9)	1.694(9)	C(15)-W(1)-C(16)	91.4(4)	89.2(5)
C(6)-C(7)	1.479(13)	1.420(1)	W(1)-C(1)-O(1)	129.1(6)	128.1(7)
C(6)-S(2)	1.701(10)	1.749(1)	W(1)-C(1)C(2)	126.5(6)	124.8(6)
C(7)-C(8)	1.45(2)	1.419(1)	O(1)-C(1)-C(2)	104.3(7)	107.1(8)
C(8)-C(9)	1.29(2)	1.419(1)	C(1)-O(1)-C(10)	123.7(7)	122.7(8)
C(9)-S(2)	1.680(12)	1.749(1)	C(1)-C(2)-C(3)	130.1(8)	130.0(9)
C(10)-C(11)	1.501(10)	1.504(11)	C(1)-C(2)-S(1)	120.7(6)	120.8(7)
C(12)-O(2)	1.165(10)	1.099(12)	C(3)-C(2)-S(1)	109.2(7)	109.2(7)
C(13)-O(3)	1.144(11)	1.100(12)	C(2)-C(3)-C(4)	115.0(8)	114.4(9)
C(14)-O(4)	1.126(10)	1.133(13)	C(3)-C(4)-C(5)	111.5(9)	113.3(9)
C(15)-O(5)	1.149(11)	1.114(12)	C(4)-C(5)-S(1)	111.9(7)	110.2(6)
C(16)-O(6)	1.121(10)	1.129(12)	C(4)-C(5)-C(6)	129.9(9)	133.9(8)
			S(1)-C(5)-C(6)	118.2(8)	115.9(6)
			C(2)-S(1)-C(5)	92.5(5)	92.9(4)

			C(5)-C(6)-C(7)	126.9(9)	133.8(6)
			C(5)-C(6)-S(2)	117.8(8)	116.1(5)
			C(7)-C(6)-S(2)	115.3(8)	110.0(6)
			C(6)-C(7)-C(8)	100.4(10)	111.9(9)
			C(7)-C(8)-C(9)	121(2)	115.7(11)
			C(8)-C(9)-S(2)	112.1(13)	108.0(8)
			C(6)-S(2)-C(9)	90.9(7)	94.3(5)
			O(1)-C(10)-C(11)	106.3(8)	108.4(8)
			W(1)-C(12)-O(2)	179.3(9)	178.2(11)
			W(1)-C(13)-O(3)	176.1(9)	175.0(11)
			W(1)-C(14)-O(4)	175.7(8)	173.4(12)
			W(1)-C(15)-O(5)	175.5(10)	179.5(10)
			W(1)-C(16)-O(6)	176.3(9)	177.9(11)

Table B6: Selected torsion angles for 6.

Atoms involved	Torsion Angle/^{O}	
	Molecule A	**Molecule B**
C(12)-W(1)-C(1)-O(1)	159.6(7)	132.8(1)
C(12)-W(1)-C(1)-C(2)	-17.6 (7)	-49.2(1)
C(13)-W(1)-C(1)-O(1)	-42.4(1)	-46.3(1)
C(13)-W(1)-C(1)-C(2)	140.3(1)	131.5(1)
C(14)-W(1)-C(1)-O(1)	-133.5(1)	45.1(1)
C(14)-W(1)-C(1)-C(2)	49.2(1)	-136.9(1)
C(15)-W(1)-C(1)-O(1)	46.2(1)	-134.2(1)
C(15)-W(1)-C(1)-C(2)	-130.9(1)	43.6(1)
C(16)-W(1)-C(1)-O(1)	137.5(1)	-157.7(12)
C(16)-W(1)-C(1)-C(2)	-39.6(1)	20.2(12)
C(7)-C(8)-C(9)-S(2)	6.0(2)	2.2(1)
C(8)-C(9)-S(2)-C(6)	-3.6(1)	-1.5(1)
C(1)-W(1)-C(12)-O(2)	169.4(6)	-175.6(6)
C(13)-W(1)-C(12)-O(2)	11.4(8)	-4.8(10)

C(14)-W(1)-C(12)-O(2)	102.4(8)	-81.2(6)
C(15)-W(1)-C(12)-O(2)	-77.0(8)	95.3(6)
C(16)-W(1)-C(12)-O(2)	-168.4(8)	6.2(6)
C(1)-W(1)-C(13)-O(3)	-172.0(3)	-175.8(3)
C(12)-W(1)-C(13)-O(3)	6.9(4)	13.4(8)
C(14)-W(1)-C(13)-O(3)	-79.8(4)	89.6(4)
C(15)-W(1)-C(13)-O(3)	94.6(4)	-86.9(4)
C(16)-W(1)-C(13)-O(3)	7.3(8)	2.4(4)
C(1)-W(1)-C(14)-O(4)	-167.4(3)	170.9(3)
C(12)-W(1)-C(14)-O(4)	10.1(3)	80.2(3)
C(13)-W(1)-C(14)-O(4)	98.1(3)	-94.9(3)
C(15)-W(1)-C(14)-O(4)	14.9(6)	-19.1(10)
C(16)-W(1)-C(14)-O(4)	-77.6(3)	-8.4(4)
C(1)-W(1)-C(15)-O(5)	167.3(3)	-126.7(12).
C(12)-W(1)-C(15)-O(5)	-10.2(4)	-35.9(12)
C(13)-W(1)-C(15)-O(5)	-98.3(3)	139.1(12)
C(14)-W(1)-C(15)-O(5)	-15.0(7)	63.3(16)
C(16)-W(1)-C(15)-O(5)	77.4(4)	52.5(12)
C(1)-W(1)-C(16)-O(6)	138.9(3)	141.8(11)
C(12)-W(1)-C(16)-O(6)	-40.0(4)	-148.7(6)
C(13)-W(1)-C(16)-O(6)	-40.4(8)	30.3(7)
C(14)-W(1)-C(16)-O(6)	46.7(4)	-60.9(7)
C(15)-W(1)-C(16)-O(6)	-127.6(3)	118.3(6)
W(1)-C(1)-O(1)-C(10)	-0.2(1)	-4.2(1)
C(2)-C(1)-O(1)-C(10)	177.4(1)	177.6(1)
W(1)-C(1)-C(2)-C(3)	-9.5(1)	8.3(1)
W(1)-C(1)-C(2)-S(1)	168.1(1)	-172.3(0)
O(1)-C(1)-C(2)-C(3)	172.6(1)	-173.4(1)
O(1)-C(1)-C(2)-S(1)	-9.5(1)	5.9(1)
C(1)-O(1)-C(10)-C(11)	-175.7(1)	-179.0(1)
C(1)-C(2)-C(3)-C(4)	176.1(1)	-179.8(1)

S(1)-C(2)-C(3)-C(4)	-1.7(1)	0.8(1)
C(1)-C(2)-S(1)-C(5)	-176.3(1)	179.3(1)
C(3)-C(2)-S(1)-C(5)	1.7(1)	-1.2(1)
C(2)-C(3)-C(4)-C(5)	0.7(1)	0.2(1)
C(3)-C(4)-C(5)-S(1)	0.6(1)	-1.2(1)
C(3)-C(4)-C(5)-C(6)	-179.0(1)	179.4(1)
C(4)-C(5)-S(1)-C(2)	-1.4(1)	1.4(1)
C(6)-C(5)-S(1)-C(2)	178.3(1)	-179.1(1)
C(4)-C(5)-C(6)-C(7)	-177.4(1)	173.6(1)
C(4)-C(5)-C(6)-S(2)	3.9(1)	-4.3(1)
S(1)-C(5)-C(6)-C(7)	2.8(2)	-5.7(1)
S(1)-C(5)-C(6)-S(2)	-175.7(1)	176.4(0)
C(5)-C(6)-C(7)-C(8)	-176.6(1)	-177.4(1)
S(2)-C(6)-C(7)-C(8)	1.9(1)	0.6(1)
C(5)-C(6)-S(2)-C(9)	179.4(1)	178.9(1)
C(7)-C(6)-S(2)-C(9)	0.6(1)	0.6(1)
C(6)-C(7)-C(8)-C(9)	-5.0(2)	-1.9(1)